Late-Cenozoic Topographic Evolution of the Cascade Range, Washington State, USA

Sara Gran Mitchell

A dissertation submitted in partial fulfillment of the
requirements for the degree of

Doctor of Philosophy

University of Washington

2006

Program Authorized to Offer Degree:
Department of Earth and Space Sciences

University of Washington
Graduate School

This is to certify that I have examined this copy of a doctoral dissertation by

Sara Gran Mitchell

and have found that it is complete and satisfactory in all respects,
and that any and all revisions required by the final
examining committee have been made.

Chair of the Supervisory Committee:

_____
David R. Montgomery

Reading Committee:

_____
David R. Montgomery

_____
Stephen C. Porter

_____
John O. Stone

Date: _____

In presenting this thesis in partial fulfillment of the requirements for the doctoral degree at the University of Washington, I agree that the Library shall make its copies freely available for inspection. I further agree that extensive photocopying of the dissertation is allowable only for scholarly purposes, consistent with "fair use" as prescribed in the U.S. Copyright Law. Requests for copying or reproduction of this dissertation may be referred to ProQuest Information and Learning, 300 North Zeeb Road, Ann Arbor, MI 48106-1346, 1-800-521-0600, to whom the author has granted "the right to reproduce and sell (a) copies of the manuscript in microform and/or (b) printed copies of the manuscript made from microform."

Signature _____

Date _____

University of Washington

Abstract

Late-Cenozoic Topographic Evolution of the Cascade Range, Washington State, USA

Sara Gran Mitchell

Chair of the Supervisory Committee:
Professor David R. Montgomery
Department of Earth and Space Sciences

The topography of the Cascade Range in Washington State reflects its long geologic, tectonic, erosion, and climatic history. This dissertation utilizes exhumation rate, paleoclimate, and geologic data, in addition to topographic analyses to evaluate hypotheses regarding the physiographic evolution of the range. Spatial relationships between topography, exhumation rate, climate, and erosion potential are analyzed to explore the influence of glacial erosion on the height and morphology of the Cascades. Finally, I constrain the extent to which isostatic compensation from valley incision affects peak altitude trends across the range.

A "triangulation" approach using many lines of evidence indicates that the Cascade Range has a polygenetic topographic history; in northern Washington the range likely had significant relief during the late Miocene, while in southern Washington it had modest relief. Both regions were subsequently uplifted and modified by erosion. In the central Cascades, non-volcanic summits rise ~600 m above the average Quaternary glacial equilibrium line altitude (ELA) despite a ten-fold variation in exhumation rate. This evidence, along with hypsometric analysis and erosion modeling, suggests that glaciers limit the altitude of Cascade peaks by eroding most intensely and for the longest duration at the average Quaternary ELA, creating cirques at that altitude and steepening the slopes above cirques to the degree that they fail. This limiting of summit altitudes across the transition zone between the northern and southern Cascades created a landscape that was misinterpreted as an uplifted erosion surface and erased topographic differences that once existed due to the two regions' different

physiographic histories. Independent constraints suggest that the flexural rigidity of the crust is > 10^{23} N m and thus the effective elastic thickness is > 24 km. This constraint limits the maximum effect differential erosion can have on Cascade Range relief to 700 and 300 m in the northern and southern areas of the range, respectively. Therefore, the remaining differences in altitude between the northern and southern Cascades in Washington must be due to differences in the geology or tectonics.

TABLE OF CONTENTS

LIST OF FIGURES

LIST OF TABLES

Table Number Page

ACKNOWLEDGEMENTS

This research was funded by the Department of Earth and Space Sciences at the University of Washington, the Washington NASA Space Grant Consortium, a National Science Foundation Graduate Research Fellowship, and National Science Foundation research grant EAR-0087413. This research on the Cascades grew out of a collaboration that included Peter Reiners (Yale University) and Todd Ehlers (University of Michigan). Harvey Greenberg provided extensive help with the GIS analyses; many of the complex GIS analyses featured in this dissertation could not have been done without his assistance.

Much gratitude goes to my advisor David Montgomery, whose enthusiasm and endless capacity for draft revisions helped push this research along. I also thank Stephen Porter and John Stone of dissertation reading committee for their edits and comments. I greatly appreciated the generous support and encouragement I received from committee member Richard Stewart, who passed away in April, 2006. I am also grateful for the many helpful discussions I had with other Earth and Space Sciences faculty members and my fellow grad students regarding this research.

This work would not have been possible without the support of my family. My parents Dick Gran and Gloria Gran have encouraged me to pursue science since I first showed an interest in it. My brother Rik Gran has been an infinite source of information about academia in general and physics in particular. Finally, I thank my husband David Mitchell for his unwavering encouragement, support, and patience while I pursued this degree.

CHAPTER 1

Introduction

The topography of a mountain range reflects the synthesis of the tectonic, geologic, erosion, and climate history of its location. As such, one might approach studying the linkages between tectonics, climate, erosional processes, and topography by asking, "what can the modern topography tell us about the geologic, tectonic, erosional, and climatic history of this mountain range?" Another approach might be to ask, "based on our understanding of them, how have these processes influenced the topography of this region?" In this dissertation, I use these questions to frame studies of the geomorphic evolution and topographic controls of the Cascade Range in Washington State (Figure 1.1).

It is notoriously difficult to "date" topography. While previous generations used terminology such as "youthful," and "mature," to describe landscapes with certain morphological attributes, our modern understanding is that mountainous topography is constantly adjusting to the dynamic forces of erosion and tectonics. As a result, a large but seemingly singular physiographic feature such as a mountain range may have a topographic history that is complex in both time and space. Determining the topographic evolution of a mountain range necessitates a multi-disciplinary approach.

The form and height of a mountain range are influenced by erosion processes such as glacial erosion and valley incision. The degree to which, and mechanisms by which, each of these processes influence the height of mountains are topics of much current interest in the field of Earth surface processes. For example, whether alpine glacial erosion increases or decreases the relief of mountain ranges is still debated. Do glaciers preferentially erode high, glaciated terrain and thus decrease relief (e.g., Brozovic et al., 1997; Whipple et al., 1999)? Or does glacial erosion preferentially deepen and widen valleys, triggering an isostatic uplift response, and thus potentially increase relief, local or regional (e.g., Molnar and England, 1990)? Furthermore, how do the relative influences of glacial erosion and isostatic response compare with the

influence of geology and tectonics on the topography? Finally, are erosional processes effective enough to mask significant differences in topographic development related to tectonics and geology?

This dissertation utilizes exhumation rate, paleoclimate, and geologic data in addition to quantitative analysis of the topography to constrain and evaluate models of the physiographic development of the Cascade Range in Washington. I also analyze spatial relationships between topography, exhumation rate, climate, and erosion potential to investigate the influence of glacial erosion on the height and morphology of the range. Finally, this dissertation constrains the degree to which isostatic uplift resulting from valley incision contributes to north-south trends in relief in the Cascades.

The Cascade Range of Washington State

The Cascade Range in Washington State is an ideal setting to investigate the evolution of mountain topography (Figure 1.2). First, the physiography and "age" of the range have been studied from a multitude of approaches for over a century, providing a number of hypotheses to test. Depending on the analysis and specific study area, the Cascades in Washington have been proposed to: A) predate the late Miocene (e.g., Reidel et al., 1989), B) postdate the late Miocene (e.g., Chaney, 1938; Cheney, 1997; Takeuchi and Larson, 2005), or C) pre- or postdate the late Miocene depending on location (Mackin and Cary, 1965). Mountain-building analyses of the Cascades also benefit from the presence of a structural and topographic datum: the Columbia River Basalt flows deposited between 15.5 and 10 My ago. These immense basalt flows erupted in eastern Washington and spread in vast sheets, inundating the middle Miocene landscape. Because the original surfaces of these flows are assumed to have been essentially horizontal, deformation of preserved basalt surfaces records the uplift of both the ground surface and the rock itself since their solidification.

In addition, the Cascades are an excellent field area to investigate the influences of glacial erosion on topography. While the range was extensively glaciated during the Pleistocene, today glaciers are limited to the highest peaks. Thus I can study the effect

of glaciation on a landscape without needing to "see through" existing ice. Furthermore, the extent and history of glaciations in the Cascade Range of Washington are well-constrained by previous studies (Waitt and Thorson, 1983; Booth et al., 2004; Kaufman et al., 2004). Finally, steep, long-lived precipitation gradients have resulted in gradients in glacier equilibrium line altitudes that can be compared with the observed topography (Porter, 1977; 1989).

Furthermore, the Cascade Range is a good location to study the effects of crustal strength and isostatic compensation due to mass removal resulting from valley incision on range-scale topographic patterns. The role of isostasy in controlling the relief differences between the high, rugged crystalline core of the northern Cascades and the lower volcanic terrain of the southern Cascades has been an unanswered but intriguing question. Using constraints on the crustal rigidity in the Cascade region (Lowry, 2000; James et al, 2000; Fluck et al., 2003), I determine the degree to which the difference in peak altitude between the northern and southern Cascades is due simply to the greater extent of valley incision in the north.

Summary of Previous Work

The topographic history and evolution of the Cascade Range specifically and the role of glacial erosion and valley incision on mountain topography in general have been the focus of many previous investigations. In the early 1900s, the Cascade Range was thought to be the result of the post-Miocene uplift and incision of a low-relief erosion surface (Russell, 1900; Smith, 1903; Willis, 1903). The interpretation of an uplifted plateau was based on the presence of inferred erosion surfaces on the eastern flank of the range and a remarkable concordance of peak altitudes on the western flank; the timing of uplift was based on the deformation of the Columbia River Basalts, which were already known to be Miocene in age. Later, paleobotanical and isotopic evidence was used to show that the strong orographic rainshadow now present in Washington State developed sometime after ~16 My, implying the absence of an orographic barrier before that time (Chaney, 1938; Chaney 1959; Smiley, 1968; Leopold and Denton,

1987; Takeuchi and Larson, 2005). This paleoclimatic argument that the Cascades are younger than 16 My has been referred to in subsequent studies discussing the age of the range (e.g., Reiners et al., 2002, 2003). Conversely, other research has suggested that the Cascade Range stood as a topographic high during the emplacement of the Columbia River Basalt flows, acting as a barrier to the westward flow of the basalts (Reidel et al., 1989; Beeson and Tolan, 1989) and creating east-dipping topographic gradients for sediment transport (Schminke, 1964; Smith et al., 1988, 1989). A hybrid argument was put forward by Mackin and Cary (1965), who suggested in an obscure essay, written for general audiences, that the Cascade Range in northern Washington stood in significant relief during the late Miocene, blocking the basalt flows, while southern Washington had low to modest relief, and thus did not act as much of a barrier to either rainfall from the west or the basalt flows from the east. Geologic mapping shows that basalt flows did cross the axis of the Cascades through the Columbia River Valley at the southern border of Washington State.

The role of glacial erosion on the topography of mountain ranges has long been a topic of study. Questions regarding alpine glacial erosion still include the following: A) how fast do glaciers erode (e.g., Harbor and Warburton, 1993; Hallet et al., 1996; Burbank, 2002), B) how does glacial erosion of bedrock create classic erosional landforms such as cirques and U-shaped valleys (e.g., Harbor, 1992; Matsuoka and Sakai, 1999; Bennett et al., 1999; Oskin and Burbank, 2005), and C) does glacial erosion increase or decrease the relief of mountainous topography (Molnar and England, 1990; Whipple et al., 1999; Montgomery, 2002). The “glacial buzzsaw” theory specifically addresses the question of whether or not alpine glacial erosion is fast enough to keep pace with bedrock uplift rates and occurs predominantly at high altitudes, thus limiting the altitude to which mountains can rise in glaciated conditions (Brozovic et al., 1997).

Similarly, the role of isostasy in determining peak altitudes has long been recognized in the scientific literature. As early as the mid 1900s, Wager (1933) and Holmes (1945) suggested that mass removed from high-relief terrain such as the

Himalaya would be replaced from below by mantle flow, triggering rock uplift and further adding to the altitude of a mountain range. Later, the ability to use digital topographic data in 3-dimensional isostatic models allowed researchers to constrain the magnitude of peak uplift due to valley incision (e.g., Montgomery, 1994; Gilchrist et al., 1994; Small and Anderson, 1995). Whereas Molnar and England (1990) hypothesized that increased valley excavation due to glacial erosion associated with global cooling in the Cenozoic could have triggered significant peak uplift, the more-recent studies have suggested that the effect may account for a only a few hundreds of meters at most of increased peak altitude, limited in part due to the rigidity of the crust (e.g., Small and Anderson, 1998; Montgomery and Greenberg, 2000; Stern et al., 2005).

Overview of Dissertation

This dissertation is organized into three main chapters, each of which was developed as a stand-alone paper. Chapter Two, entitled, "Polygenetic topography of the Cascade Range in Washington State," summarizes the history of geomorphic investigations of the Cascade Range and offers a solution to the century-long debate regarding the topographic origin of the range. Specifically, I evaluate three alternative models for the Cenozoic topographic evolution of the Cascade Range of Washington State by analyzing the topography, geology, and exhumation patterns across the range. The models for topographic evolution include: A) post-Miocene uplift of the range from initially low-relief topography, B) post-Miocene uplift of the range superimposed on pre-existing high-relief topography, and C) post-Miocene uplift of a high-relief Cascades in northern Washington and low-relief Cascades in southern Washington.

My analysis in Chapter Two shows that the third model—a polygenetic topographic history—is most consistent with the topographic data and the previously contradictory interpretations of geologic, paleontologic, and isotopic lines of evidence regarding the Cascades physiographic history. South of Snoqualmie Pass, the east-derived, ~15 My Columbia River Basalt (CRB) reaches nearly as far west as the modern drainage divide and is warped upward to the crest of the range. This relationship

between the basalt and the range requires that the relief on the east flank of the southern Cascades during the late Miocene was subdued. In the northern Cascades, the CRB does not extend into the range, CRB deformation only reflects 30-60% of the total relief, and the exhumation data are consistent with initially high relief. Thus, the northern Cascades were likely a topographic barrier to the west-flowing flood basalts. Moreover, a polygenetic topographic history appears most consistent with the geologic data and the paleobotanical and isotopic evidence for rainshadow formation during the middle Miocene. Despite significant differences in topographic history and rock hardness, the maximum and mean altitudes of the Cascade Range decrease smoothly from northern to southern Washington. I suggest that erosion, particularly glacial erosion, has reduced the topographic distinctions between the northern and southern Cascades, resulting in a single physiographic feature despite a polygenetic topographic history. This chapter is a significant advance on our current understanding of the morphological development of the Cascade Range and represents a methodological approach that may be useful in deciphering the physiographic evolution of other similarly complex ranges.

Chapter Three, entitled, "Influence of a glacial buzzsaw on the height and morphology of the Cascade Range, central Washington State," is a GIS-based analysis of the effects of glacial erosion on altitude trends in the Cascades of central Washington. Analyses of the climate, exhumation patterns, and topography of the Cascades indicate that glacial erosion limits the height and controls the morphology of this range. Erosion linked to long-term spatial gradients in the equilibrium line altitude (ELA) of glaciers created a tilted, planar zone of 373 cirques across the central part of the range; peaks and ridges now rise ≤ 600 m above this zone. Hypsometric analysis of the region shows that the proportion of land area above the cirques drops sharply, and mean slopes of > 30º indicate that the areas above the cirques may be at or near threshold steepness. The mean plus 1σ relief of cirque basins (570 m) is very similar to the ~600-m envelope above which few peaks rise. The summit altitudes are set by a combination of higher rates of glacial and paraglacial erosion above the ELA and enhanced hillslope processes due to the creation of steep topography. On the high-

precipitation western flank of the Cascades, the dominance of glacial and hillslope erosion at and above the ELA most likely explains the lack of a correspondence between stream-power erosion models and measured exhumation rates from apatite (U-Th/He) thermochronometry.

In Chapter Three, I show that by limiting peak altitudes based on climatic rather than geologic or tectonic controls, glaciers may have effectively smoothed any pre-existing topographic distinction between the northern and southern Cascades. Erosion rates derived from AHe thermochronometry are high enough on the western flank of the range to prevent the survival of an uplifted "peneplain" in this region. Rather, glacial erosion created the concordance of summit altitudes that led to the long-standing misinterpretation that the entire Cascade Range in Washington was a remnant peneplain, uplifted and incised after the middle Miocene. Thus, the "glacial buzzsaw" effectively masked the polygenetic topographic history of the range discussed in Chapter Two.

Chapter Four is entitled, "Contribution of isostatic response due to valley incision to altitude trends of the Cascade Range, Washington State." Peaks in the Cascade Range in northern Washington are on average ~ 1000 m higher than in southern Washington. The degree to which this difference in altitude is a result of: A) differential valley excavation, or B) variations in hillslope length and average slope, was tested using a 3-dimensional model for isostatic rock uplift and calculations of hillslope length and slope, respectively. The magnitude of potential rock uplift determined by the model is highly dependent on the flexural rigidity (D) and the related effective elastic thickness (T_e) of the crust of this region. The rigidity of the crust was constrained using published estimates and by estimating the depth of the seismogenic zone in the area ($D > 10^{23}$ Nm and $T_e > 24$ km).

The constraint on flexural rigidity thus places an upper limit on the potential for peak uplift in the Cascade Range due to isostatic effects. In the Cascades, the maximum possible peak uplift due to the incision of valleys is 700 m; the upper limit on superelevation averaged across the region range from < 200 m in the southern Cascades

to 575 m in the northern Cascades. This additional altitude is minor compared to the altitude of the highest peaks in those areas, ~1600 m to 2700 m, respectively. This effectively refutes the hypothesis that the incision and widening of valleys from glacial erosion triggered enough peak uplift to affect climate patterns for this region of the world. Furthermore, I show in Chapter Four that differences in peak altitudes due to isostatic compensation account for about 300 m, or <50% of the observed 800 m increase in peak altitudes towards the north. Steeper slopes in the north also contribute somewhat to higher altitudes, but valley spacing, and thus hillslope lengths, is indistinguishable between north and south. Thus, while differences in valley incision and slope angles contribute modestly to the differences in altitude between the Cascades of northern and southern Washington, additional non-geomorphic factors such as crustal thickness or tectonics are necessary to explain the full increase in both peak and mean altitudes towards the north.

Chapters Two, Three and Four all address the general themes of mountain building and erosional controls on topography through a specific examination of the topographic evolution and erosion processes of the Cascade Range in Washington. This region is a complex geologic and physiographic feature, and as such, no one line of evidence or evidence from a single location can be conclusive regarding its surface uplift history. This research shows the utility of a "triangulation" approach based on integrating multiple lines of evidence towards investigating the physiographic development of the Cascades and of mountain ranges in general. I also address the question of whether glacial erosion, and thus ultimately climatically controlled erosion processes, limits peak altitudes in the Cascade Range: topographic and exhumation-rate data show that it does. In addition, my research emphasizes how post-uplift erosion, particularly glacial erosion that selectively removes high topography, can complicate the interpretation of uplift histories. For example, the limitation of peak altitudes by glacial erosion in the central Cascades merged the long-standing high topography of the northern Cascades to the "younger" topography in southern Washington, creating a seamless landscape that could be (and was widely) misinterpreted as a feature with a

single topographic origin. Finally, my investigation into the role of uplift due to isostatic compensation from valley incision addresses the degree to which isostasy and valley incision play a role in altitude trends in the Cascades, and helps to isolate the degree to which differences in altitude are due to geomorphic factors such as valley spacing and incision compared to differences in tectonics and geology.

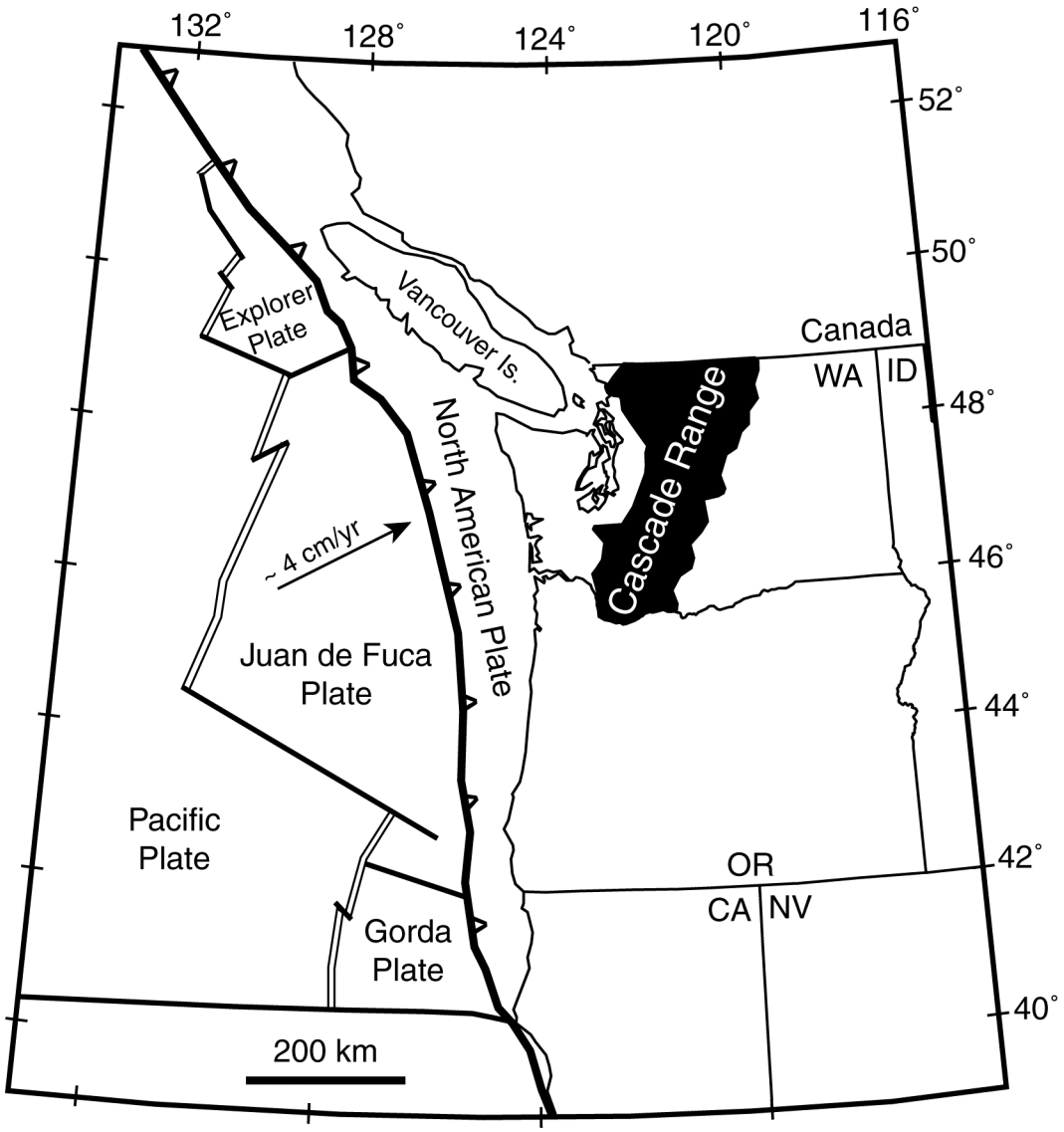

Figure 1.1: Location and tectonic setting of the Cascade Range, Washington State.

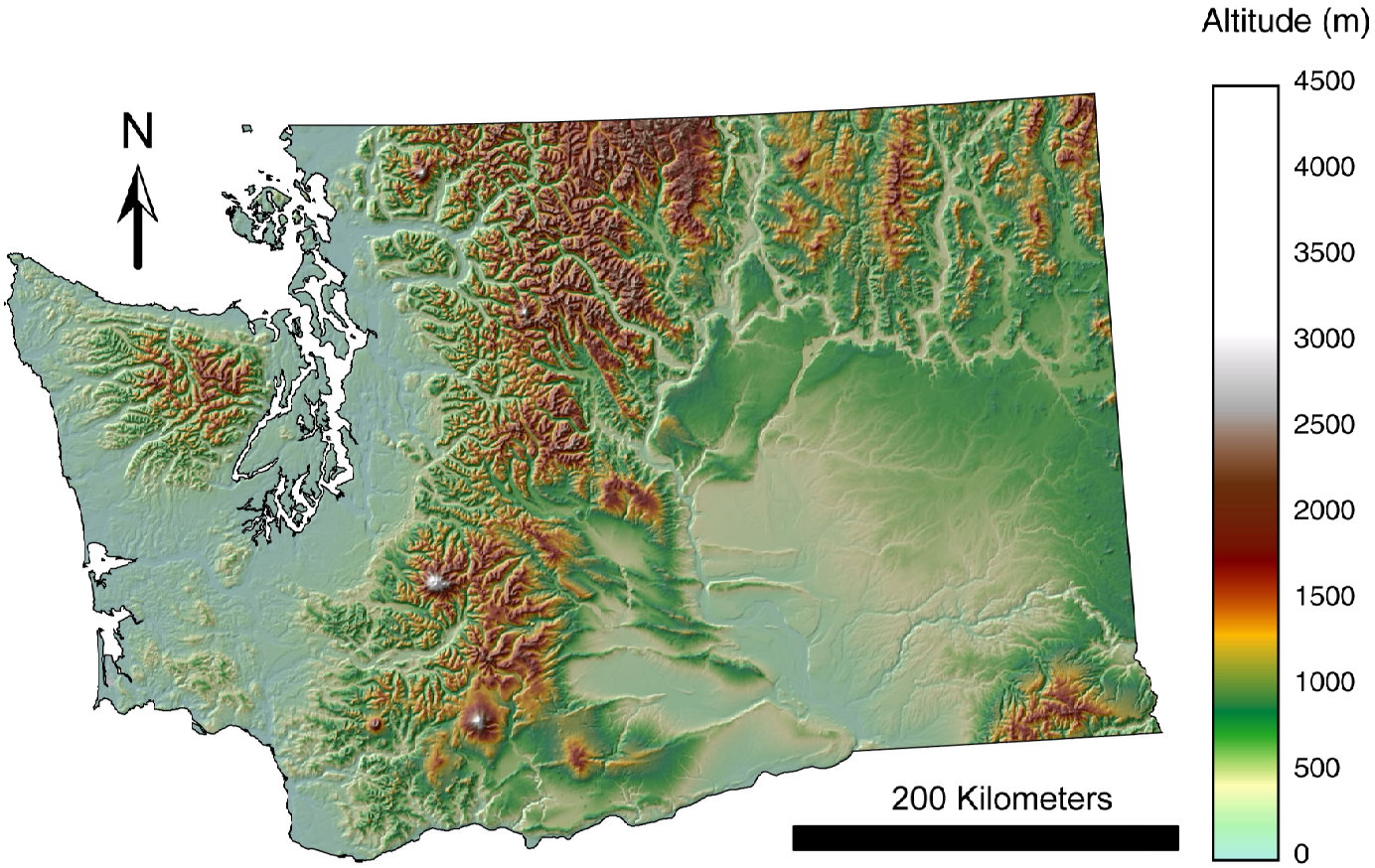

Figure 1.2: Topography of Washington State. Shaded relief, altitude indicated by color.

Notes to Chapter 1

Beeson, M.H., and Tolan, T.L., 1989, The Columbia River Basalt Group in the Cascade Range—a middle Miocene reference datum for structural analysis: *in* Muffler, L.J.P., Weaver, C.S., Blackwell, D.D. editors, Proceedings of workshop XLIV—Geological, geophysical and tectonic setting of the Cascade Range: US Geological Survey Open File Report 89-178, p. 257-290.

Bennett, M.R., Huddart, D., Glasser, N.F., 1999, Large-scale bedrock displacement by cirque glaciers: Arctic, Antarctic, and Alpine Research, v. 31, p. 99-107.

Booth, D.B., Troost, K.G., Clague, J.J., and Waitt, R.B., 2004, The Cordilleran Ice Sheet: In: Gillespie, A.R., Porter, S.C., and Atwater, B.F., eds., The Quaternary period in the United States, Developments in Quaternary Science v. 1, p. 17-43.

Brozovic, N., Burbank, D.W., and Meigs, A.J., 1997, Climatic limits on landscape development in the northwestern Himalaya: Science, v. 276, p. 571-574.

Burbank, D.W., 2002, Rates of erosion and their implications for exhumation: Mineralogical Magazine, v. 66, no. 1(434), p. 25-52.

Chaney, R.W., 1938, Paleoecological interpretations of Cenozoic plants in western North America: Botanical Review, v. 4, p. 371-396.

Chaney, R.W., 1959, Miocene floras of the Columbia Plateau—Part 1, Composition and interpretation: Carnegie Institution of Washington Publication, v. 617, p. 1-34.

Cheney, E.S., 1997, What is the age and extent of the Cascade magmatic arc?: Washington Geology, v. 25, no. 2, p. 28-32.

Fluck, P., Hyndman, R.D., and Lowe, C., 2003, Effective elastic thickness T_e of the lithosphere in western Canada: Journal of Geophysical Research, v. 108, no. B9, 2430, doi:10.1029/2002JB002201.

Gilchrist, A.R., Summerfield, M.A., and Cockburn, H.A.P., 1994, Landscape dissection, isostatic uplift, and the morphologic development of orogens: Geology, v. 22, p. 963-966.

Hallet, B., Hunter, L., and Bogen, L., 1996, Rates of erosion and sediment evacuation by glaciers; a review of field data and their implications: Global and Planetary Change, v. 12, p. 213-235.

Harbor, J.M., 1992, Numerical modeling of the development of U-shaped valleys by glacial erosion: Geological Society of America Bulletin, v. 104, p. 1364-1375.

Harbor, J.M. and Warburton, J., 1993, Relative rates of glacial and nonglacial erosion in alpine environments: Arctic and Alpine Research, v. 25, p. 1-7.

Haugerud, R.A., 2004, Cascadia—Physiography: USGS Miscellaneous Investigations Map I-2689.

Holmes, A., 1944, *Principles of Physical Geology*, Thomas Nelson and Sons, London, 532 p.

James, T.S., Clague, J.J., Wang, K., and Hutchinson, I. 2000, Postglacial rebound at the northern Cascadia subduction zone: Quaternary Science Reviews, v. 19, p. 1527-1541.

Kaufman , D.S., Porter, S.C., and Gillespie, A.R., 2004, Quaternary alpine glaciation in Alaska, the Pacific Northwest, Sierra Nevada, and Hawaii: in Gillespie, A.R., Porter, S.C., and Atwater, B.F., eds., *The Quaternary Period in the United States*: Amsterdam, Elsevier, p. 77-103.

Leopold, E.B., and Denton, M.F., 1987, Comparative age of grassland and steppe east and west of the northern Rocky Mountains: Annals of the Missouri Botanical Garden, v. 74, p. 841-867.

Lowry, A.R., Ribe, N.M., and Smith, R.B., 2000, Dynamic elevation of the Cordillera, western United States: Journal of Geophysical Research, v. 105, no B10, p. 23,371-23,390.

Mackin, J.H., and Cary, A.S., 1965, Origin of Cascade landscapes: Washington Division of Mines and Geology Information Circular 41, 35 p.

Molnar, P. and England, P.C., 1990. Late Cenozoic uplift of mountain ranges and global climate change: Chicken or egg?: Nature, v. 346, p. 29-34.

Montgomery, D.R., 2002, Valley formation by fluvial and glacial erosion: Geology, v. 30, no. 11, p. 1047-1050.

Montgomery, D.R. and Greenberg, H.M., 2000, Local relief and the height of Mt. Olympus: Earth Surface Processes and Landforms, v. 25, p. 385-396.

Matsuoka, N. and Sakai, H. 1999, Rockfall activity from an alpine cliff during thawing periods: Geomorphology, v. 28, p. 309-328.

Oskin, M., Burbank, D.W., 2005, Alpine landscape evolution dominated by cirque retreat: Geology, v. 33, no. 12, p. 933-936.

Porter, S.C., 1989, Some geological implications of average Quaternary glacial conditions: Quaternary Research, v. 32, p. 245-261.

Porter, S.C., 1977, Present and past glaciation threshold in the Cascade Range, Washington, U.S.A.: Topographic and climatic controls, and paleoclimate implications: Journal of Glaciology, v. 18, p. 101-116.

Reidel, S.P., Tolan, T.L., Hooper, P.R., Beeson, M.H., Fecht, K.R., Bentley, R.D., and Anderson, J.L., 1989, The Grande Ronde Basalt, Columbia River Basalt Group; Stratigraphic descriptions and correlations in Washington, Oregon, and Idaho, *in* Reidel, S. P.; Hooper, P. R., editors, Volcanism and tectonism in the Columbia River flood-basalt province: Geological Society of America Special Paper 239, p. 21-53.

Reiners, P.W., Ehlers, T.A., Mitchell, S.G., and Montgomery, D.R., 2003, Coupled spatial variations in precipitation and long-term erosion rates across the Washington Cascades: Nature, v. 426, p. 645-647.

Reiners, P.W., Ehlers, T.A., Garver, J.I., Mitchell, S.G., Montgomery, D.R., Vance, J.A., and Nicolescu, S., 2002, Late Miocene exhumation and uplift of the Washington Cascade Range: Geology v. 30, p. 767-770.

Russell, I.C., 1900, A preliminary paper on the geology of the Cascade Mountains in northern Washington: USGS Annual Report v. 20, pt. 2, 83-210.

Schmincke, H.U., ms, 1964, Petrology, paleocurrents, and stratigraphy of the Ellensburg Formation and interbedded Yakima Basalt flows, south-central Washington [Ph.D. thesis]: Baltimore, Johns Hopkins University, 426 p.

Small, E.E., Anderson, R.S., 1998, Pleistocene relief production in Laramide mountain ranges, western United States: Geology v. 26, no. 2, p. 123-126.

Small, E.E., Anderson, R.S., 1995, Geomorphically driven late Cenozoic rock uplift in the Sierra Nevada: Science, v. 270, no. 5234, p. 277-280.

Smiley, C.J., 1963, The Ellensburg flora of Washington: University of California Publications in Geological Sciences: v. 35, no. 3, p. 159-276.

Smith, G.O., 1903, Geology and Physiography of Central Washington: USGS Professional Paper v. 19, p. 1-46.

Smith, G.A., Bjornstad, B.N., and Fecht, K.R., 1989, Neogene terrestrial sedimentation on and adjacent to the Columbia Plateau; Washington, Oregon and Idaho, *in* Reidel, S. P. and Hooper, P. R., editors., Volcanism and tectonism in the Columbia River flood-basalt province: Geological Society of America, Special Paper 239, p. 187-198.

Smith, G.A., 1988, Neogene synvolcanic and syntectonic sedimentation in central Washington: Geological Society of America Bulletin, v. 100, no. 9, p. 1479-1492.

Stern, T.A., Baxter, A.K., and Barrett, P.J., 2005, Isostatic rebound due to glacial erosion within the Transantarctic Mountains: Geology, v. 33, no. 3, p. 221-224.

Takeuchi, A., and Larson, P.B., 2005, Oxygen isotope evidence for the last Cenozoic development of an orographic rain shadow in eastern Washington, USA: Geology, v. 33, no. 4, p. 313-316.

Wager, L.R., 1933, The rise of the Himalaya, Nature, v. 132, p. 28.

Waitt, R. B., Jr., 1975, Late Pleistocene alpine glaciers and the Cordilleran Ice Sheet at Washington Pass, north Cascade Range, Washington: Arctic and Alpine Research, v. 7, p. 25-32.

Waitt, R. B., Jr., and Thorson, R. M., 1983, The Cordilleran ice sheet in Washington, Idaho and Montana, *in* Porter, S.C., ed., Late Quaternary Environments of the United States: Minneapolis, University of Minnesota Press, p. 53-70.

Whipple, K.X., Kirby, E., and Brocklehurst, S.H., 1999, Geomorphic limits to climate-induced increases in topographic relief: Nature, v. 401, p. 39-43.

Willis, B., 1903, Physiography and deformation of the Wenatchee-Chelan district Cascade Range: USGS Professional Paper, v. 19, p. 47-97.

CHAPTER 2

Polygenetic Topography of the Cascade Range in Washington State

Summary

Three models were evaluated for the Cenozoic topographic evolution of the Cascade Range of Washington State by analyzing the topography, geology, and exhumation patterns across the range. The models for topographic evolution include: 1) post-Miocene uplift of the range from initially low-relief topography, 2) post-Miocene uplift of the range superimposed on pre-existing high-relief topography, and 3) post-Miocene uplift of a high-relief Cascades in northern Washington and low-relief Cascades in southern Washington. The third model—a polygenetic topographic history—is most consistent with the analysis of topographic data and the previously contradictory geologic, paleontologic, and isotopic lines of evidence regarding the Cascades physiographic history. South of Snoqualmie Pass and north of the Columbia River Gorge, the east-derived, ~15-10 My Columbia River Basalt (CRB) reaches nearly as far west as the modern drainage divide and is warped upward to the crest of the range. These features require subdued relief on the east flank of the southern Cascades during the late Miocene. In the northern Cascades, the CRB does not extend into the range, CRB deformation only reflects 30-60% of the total relief, and the exhumation data are consistent with long-lived high relief. Thus, the northern Cascades were likely already a topographic barrier to the west-flowing flood basalts. Moreover, a polygenetic topographic history appears most consistent with the geology and the paleontologic and isotopic evidence for rainshadow formation during the middle Miocene. Despite differences in topographic history and rock hardness, the maximum and mean altitudes of the Cascade Range decrease smoothly from northern to southern Washington. A possible explanation is that glacial erosion reduced the topographic distinctions between the northern and southern Cascades, resulting in a single mountain range with a polygenetic topographic history.

Introduction

The surface uplift and modern topography of a mountain range are usually interpreted as the result of a single, though perhaps complex, orographic event; a classic example is the rise of the Himalaya from the continental collision of the Indian Plate with Asia since ~50 My ago (Searle and Treloar, 1993). However, the long-term topographic history of mountainous regions is often obscured by deformation and/or erosion and by the problem that only indirect indications of paleo-elevation are typically available. Hence, separating exhumation from surface uplift is often problematic (England and Molnar, 1990). Here, I synthesize previous studies and present new analyses to show that whereas the Cascade Range in Washington State now has the topographic expression of a continuous mountain range, the modern landscape is the result of a mountain building history that is complex in both time and space. Specifically, I update, extend, and combine analyses of geologic, thermochronometric, and topographic data to evaluate the range of different models proposed for the Cenozoic topographic evolution of the Cascade Range in Washington.

Within Washington State, the Cascade Range extends approximately 150 km west to east and spans the state's 400 km north-to-south distance (Figure 2.1A). The range is located ~200 km inland from the Cascadia subduction zone, the active tectonic boundary that forms the border between the North American and Juan de Fuca plates (Figure 2.1B). Terrane accretion, collisional deformation, continental volcanic arc activity, erosion, and sedimentation within the past 200 My have all contributed to the geologic and topographic complexity of western Washington (e.g., Christiansen et al., 1992). The spectacular Quaternary volcanoes in the Cascades, including Mt. Rainier, Mount St. Helens, Mt. Adams, Glacier Peak, and Mount Baker, are arc volcanoes related to the ongoing subduction of the Juan de Fuca plate; however, these young volcanoes form relatively minor features on the broad antiform that supplies most of the relief of the range. My goals are to decipher the general altitude and relief patterns of the Cascades prior to the arching of the range, and to evaluate the paleotopography and the recent uplift in the context of the regional geologic setting. In this chapter, I follow

the terminology of Haugerud (2004) and use the terms “North Cascades,” or “North Cascade Range” to refer to the sector of the Cascade Range north of Snoqualmie Pass. I also refer to Haugerud’s (2004) High and Western Cascades south of Snoqualmie Pass but still within Washington State as the “southern Cascades,” or “southern Cascade Range,” although both the High and Western Cascades extend south into Oregon and California (Figure 1B). Similarly, when I refer to the “Cascades,” or, “Cascade Range,” I refer to the combined northern and southern portions of the range in Washington only.

Early geologic investigators of Washington State (e.g., Russell, 1900; Willis, 1903, Smith, 1903) pondered how and when the Cascade Range became the topographic feature observed today. Not surprisingly, models for the topographic development of the range evolved significantly over the past century. Due to the presence of a regionally widespread Miocene marker unit, the extensive Columbia River Basalt (CRB), much of the analysis of Cascade topographic history has focused on post-Miocene topographic evolution, as I do here. However, a wide range of conflicting interpretations has been offered to explain the topographic history of the Cascades. The earliest hypothesis proposed that the entire region forming the Cascade Range in Washington was a low-relief surface (peneplain) at the start of the Miocene that was subsequently uplifted to its current altitude in the past 10-15 My (Russell, 1900; Smith, 1903). A second hypothesis suggests that a mountain range already formed a topographic barrier along nearly the entire length of Washington in the middle Miocene. In this hypothesis, the Miocene Cascade Range funneled the Columbia River Basalt though the Columbia River gorge in the far southern part of the state, and sustained additional uplift after the emplacement of the basalt (e.g., Reidel et al., 1989). A third hypothesis combines elements of the previous two, suggesting that while the northern portion of the range stood in relatively high relief at the start of the Miocene, the low-relief southern part only became a “mountain range” after renewed post-Miocene uplift raised the entire region (Mackin and Cary, 1965). These conflicting interpretations of the topographic evolution of the range remain unresolved.

I further discuss and then evaluate the three hypotheses for the physiographic

development of the Cascade Range using several new data sets: 1) digital topographic data from a new 10-m grid digital elevation model (DEM), 2) digital 1:100,000 scale geologic maps, and 3) exhumation rate data from apatite (U-Th)/He (AHe) thermochronometry (Reiners et al., 2002, 2003). I then discuss how this new topographic analysis supports the hypothesis of polygenetic topography. Furthermore, I suggest how this hypothesis reconciles previous, contradictory interpretations based on regional observations. Finally, I propose a hypothesis for why the topographic differences between the North Cascades and southern Cascade Range are relatively subtle, given their disparate geologic and topographic histories.

Previous Work

The long-running discussion regarding the topographic evolution of the Cascade Range follows general trends in the development of geomorphic thinking. Early workers focused on the deformation of basalt flows and inferred erosion surfaces (Russell, 1900; Willis, 1903; Smith, 1903). Paleobotanical evidence of changing climate due to the development of an orographic barrier was also brought to bear on the question (Chaney, 1938, 1959; Smiley, 1963; Leopold and Denton, 1987). Geomorphologists who worked in the Cascades for years proposed scenarios that summarized decades worth of research and observations (Mackin and Cary, 1965). In the past couple decades, localized studies of deformation of sedimentary units (Swanson, 1997; Cheney, 1997) and isotopic evidence of climate change (Takeuchi and Larson, 2005; McDaniel et al., 1998) entered the debate. Most recently, apatite (U-Th)/He dating illuminated the Cenozoic exhumation history of the Cascades (Reiners et al., 2002, 2003). However, because many of these previous investigations were based on outcrop- or map-scale research focused on a relatively small region, or did not address surface uplift, there is currently no modern, comprehensive analysis on the Cenozoic topographic development of the Cascade Range in Washington State.

Evidence for Post-Miocene Uplift of a Low-Relief Initial Topography

Undisputed evidence for significant post-Miocene surface uplift of the Cascade Range is the deformation of the 17 to 15.5 My-old Grande Ronde member of the Columbia River Basalt (CRB) on the eastern flank of the range (e.g., Russell, 1900; Smith, 1903; Willis, 1903) (Figure 2.2A). The CRB is a thick sequence of flood basalts, the majority of which were deposited in extensive, horizontal sheets (Reidel et al., 1989). On some areas of the eastern flank of the range, these basalt flows now rise westward toward the crest of the range. These tilted basalts are so distinctive that before I.C. Russell began to map the geology of the Washington Cascades in the 1880s, the prevailing opinion was that the range consisted primarily of tilted basalt flows (Russell, 1900).

Russell's work on the topography and uplift of the Cascades focused on the tilting of the CRB, which were recognized as of Miocene age based on fossils found in interbedded sedimentary units (Russell, 1900), and on the intriguing concordance of peak heights across the range—many peaks rise to the same elevation as surrounding peaks, with only the young volcanoes extending above the general "surface" of peak elevations. Russell proposed that the surface formed by the summits (excluding the Quaternary volcanoes) represented the uplift of a low-relief erosion surface, or peneplain, into a broad, flat tableland that was subsequently dissected into the steep peaks seen today. In his view, the warping of the CRB on the eastern flank of the Cascades and the modern continuity of peak heights implied post-Miocene uplift from a low-relief erosion surface to a > 2000 m-high plateau subsequently incised to form the modern topography, with the current peaks defining the uplift and deformation of the original surface.

Russell's successor, George Otis Smith, also pondered the concordance of peak heights in the Cascade Range and commented that in the core of the range and to the west, the peaks are all very sharp, the concordance far from perfect, and there are no identifiable "erosion surface" remnants in the crest or western parts of the range as there are on the eastern flank. Smith also worked extensively in the basalts on the east side of

the Cascades. He too was interested in the timing and character of their deformation, and how that deformation related to the formation of the Cascades. Smith identified a series of flat, non-basalt surfaces he considered remnants of an erosion surface on the east side of the range. Tilted in a similar manner to the basalts, Smith interpreted these surfaces as further supporting the idea of an initial low-relief phase of topography prior to the most recent uplift (Smith, 1903). Smith noted that the deformation of both the low-relief surfaces and the basalt is complex; for example, east of the range, the basalt has been folded into a series of dramatic E-W- trending anticlines in addition to the broader warping on the Cascade flank. Much later, S.C. Porter (1976) suggested that Smith's non-basalt, beveled surfaces represented a pre-basalt erosion surface that was once covered, and perhaps protected, by basalt that was subsequently stripped off. Hammond (1988) also reported evidence for a beveled erosion surface, later uplifted to form the Cascade Range.

In addition to physiographic interpretation, paleobotanical evidence favoring the formation of a strong orographic barrier (rainshadow) during the Miocene also provides data for the timing and rate of topographic development of the range. Chaney (1938) noted the change from mesic to xeric flora during and after the Miocene in sedimentary deposits east of the Cascades in California, Oregon, and southern Washington. Early in the Cenozoic, moisture-dependent trees such as redwoods and sequoias grew throughout the Pacific Northwest, including regions now well east of the Cascade Range where post-Miocene formations lack fossils from moisture-loving ecosystems. Today, the sagebrush ecosystem east of the Washington Cascades is adapted to a continental climate with hot, dry summers and cold winters. Chaney (1938) attributed this climatic transition to the development of a regional rainshadow as a result of the uplift of the range.

As a student of Chaney, Smiley (1963) investigated paleoecological changes on the east side of the Cascade Range using plant fossils of the Ellensburg Formation, a deposit that forms a discontinuous sediment apron along the east side of the range in and south of the upper Yakima River valley (Figure 2.3). Smiley suggests that this

sediment apron formed during the relatively rapid surface uplift of the range. The source material for the Ellensburg appears to be a few isolated, high-volume volcanic centers located near what is now Snoqualmie Pass near the modern crest of range (Figure 2.1A) (Smiley, 1963; Smith, 1988; Smith et al., 1989). Fluvial and mass-wasting processes moved this volcanic debris eastward as the range was uplifted, and it was interfingered with the west-flowing CRBs. Plant fossils preserved in this subaerial depositional environment show a change in flora from moist conditions in the early Miocene to xeric conditions by the late Miocene. That the sedimentary deposits are finer grained in the early Miocene than in the later Miocene suggested to Smiley (1963) that the topography became steeper through time, enabling the rivers to move larger and larger sediment clasts. Later, Leopold and Denton (1987) also used paleobotanical evidence to show that the Columbia Plateau (the area east of the southern Cascade Range; Figure 2.1) remained "open" in a climatic sense to the west until ~ 8 My ago, at which time the uplift of the range and subsequent rainshadow caused a progressive change from a "mesic, summer-wet to xeric, summer-dry" flora (Leopold and Denton, 1987, p. 848).

More recently, isotopic evidence from eastern Washington further supported the hypothesis of rainshadow formation during the Miocene. Orographic barriers tend to cause depletion in precipitation $\delta^{18}O$ values on the leeward side of the range, as the water molecules containing the heavier isotope preferentially condense and precipitate on the windward side of the mountains, while lighter isotopes travel and precipitate farther downwind (Chamberlain and Poage, 2000). This change in the $\delta^{18}O$ content of precipitation can be preserved in soil minerals that incorporate the oxygen isotopes in their mineral structure. In eastern Washington, the change in the $\delta^{18}O$ of authigenic smectites (clay minerals associated with soil formation) taken from paleosols and tuffs dated from 16 My to the present records a depletion of approximately 4 ‰, the same depletion seen currently in precipitation falling on the east versus west side of the range (Takeuchi and Larson, 2005). This depletion of ^{18}O in eastern Washington precipitation began ca. 16 My ago and continued steadily to 4 My ago, indicating that the uplift of an

orographic barrier began at ca. 16 Ma. These recent isotopic data are thus consistent with the paleobotanical evidence for the development of a rainshadow during the middle Miocene.

Researchers have also investigated the uplift of the Cascade Range in Washington by studying structures and tilting in sedimentary deposits on the east side of the range. Swanson (1997) studied volcanic deposits along the Tieton River, an east-flowing river that drains part of the southern Washington Cascades, and found 3 My-old fluvial deposits that now have a significantly steeper dip than the modern river valley. Swanson concluded that this difference in dip indicates post-3 My-old tilting of the sediments, resulting from differential uplift in the center of the range. Cheney (1997) suggests that deformation of the 3 My-old Ringold Formation of central Washington, east of the range, also implies significant post-Pliocene uplift of the Cascade Range.

Finally, small exposures of ~15.6 My-old Grande Ronde Basalt (GRB) near the crest of the range hint at a once-greater, and possibly continuous, areal extent over southwestern Washington (Figure 2.2A). Hammond et al. (1992) describe Steamboat Mountain, a 1630-m-high promontory with 380 m of GRB at its top, located ~10 km west of Mt. Adams and about 1 km *west* of the modern drainage divide (Figure 2.3). Hammond et al. (1992) suggest that the basalt of Steamboat Mountain represents either an embayment of GRB into the pre-existing volcanic arc (which would have formed localized peaks), or an intravalley flow, extending east to west across much of the arc. In either case, this outcrop demonstrates that portions of the basalt flowed, at least locally, well into the Cascade arc and westward beyond the modern drainage divide.

Evidence for High Miocene Topography

Two main data sets have been used to argue for high topography in the Cascade Range during the Miocene: 1) the stratigraphy, structure, and extent of the CRB, and 2) the sedimentology of pre- and syn-CRB sedimentary deposits now also found on the southern east flank of the range. A central inference running through late 20th century CRB literature is that the basalt was “ponded” against a Miocene Cascade Range

(alternatively called the “Ancestral Cascades” or, in southern Washington, the Western Cascade Range), and flowed to the Pacific Ocean and other parts of western Washington through the 60-km-wide westward outlet of the Columbia River valley, a persistent structural trough between the Washington and Oregon Cascades (Beeson and Tolan, 1989; Reidel et al., 1989). The primary evidence that basalt ponded against the eastern flank of the range is the macro-scale thinning of the basalt against that flank and non-horizontal contacts of basalt with underlying rocks (Anderson and Vogt, 1987; Reidel et al., 1989). There is also a suggestion that basalts extending beyond the main margin were originally narrow valley deposits and now represent inverted topography (Hammond and others, 1992). In this view, the thinning of basalt flows towards the crest of the Cascades implies that the basalt was essentially “filling the bathtub” of the Columbia Basin, and that narrow tongues of CRB entered the range through deep valleys in a pre-existing southern Cascades (Campbell, 1988). These basalts, being more resistant to erosion than the surrounding rock, now form ridges. These interpretations imply that the current boundary of the basalt is depositional and forms the eastern edge of the Miocene Cascades.

Evidence for significant Miocene Cascade Range relief is also found in the Ellensburg Formation, a Miocene sedimentary unit that interfingers with and caps CRB flows on the east flank of the range. The Ellensburg Formation, as noted above, consists of a large volume of fluvially transported, primarily volcaniclastic sediment derived from the west (Smith et al., 1989, Schmincke, 1964). The center of volcanism appears to be near Lake Keechelus in the central Cascades, and this sediment must have traveled downslope to the Nile and Selah basins of eastern Washington (Smith, 1988; Figure 2.3). Formations stratigraphically and compositionally analogous to the Ellensburg, such as the coarse, fluvially deposited Mashel Formation, found over 50 km away on the west side of the Cascades, suggest that these volcanic centers could have been quite extensive and had significant relief. Relatively rare non-volcanic clasts have been attributed to two possible origins. Smiley (1963) suggested that these clasts, which appear to be more common in the younger layers of the Ellensburg, were transported

from the northwest and thus represent the progressive exhumation of the North Cascades. Alternatively, Schmincke (1964) suggested that these non-volcanic clasts were transported by an ancient Columbia River, which drained highlands in British Columbia, Idaho, and eastern Washington, as well as northern Washington. Either interpretation of provenance indicates that the crystalline core of northern Washington (now the North Cascades) was exposed and had enough relief to generate and then fluvially transport cobble-sized clasts toward the east.

Textures within the CRB flows also suggest pre-existing east-sloping topography in the Cascade region. Reports of palagonite, basalt deltas, and water-quenched pillow structures have been interpreted as indicating that the basalt flowed into standing water in some locations and to suggest that east-flowing rivers on east-dipping topography were blocked by the encroaching basalt sheets (e.g., Mackin and Cary, 1965; Summers, 1976). Mackin and Cary (1965) schematically show a series of basalt-dammed lakes located adjacent to the North Cascades during the Miocene.

Hypothesis of a Polygenetic Origin

The two models of physiographic development appear mutually exclusive; one invoking topography high enough to block the flows of CRB from the east at 17 My, the other indicating the lack of an orographic barrier (and thus no mountain range) until after that time. However, J. Hoover Mackin proposed a hybrid model in a retrospective essay written for a general audience (Mackin and Cary, 1965). According to Mackin and Cary (1965), the Cascade Range south of Mt. Rainier was a low-relief, low-elevation plain that was inundated and covered by the CRB, with isolated volcanoes located near the present Cascade Range axis supplying volcaniclastic debris to deposits such as the Ellensburg Formation. During this same time, however, the northern Cascades already stood as a "somewhat rougher landscape on granitic rocks," and were already at least a kilometer high when the basalts were erupted (Mackin and Cary, 1965). Both northern and southern Cascades were subsequently uplifted, tilting the basalts on the range flanks. As discussed further below, I argue that this view is most

consistent with the Miocene rainshadow development, the deformation of the basalts, the apparent deeper exhumation of rocks in the north Cascades, and the topographic analyses I present here.

Methods

This investigation focuses on DEM analyses using a new 10-m-grid DEM of Washington State and combining such analyses with geologic and exhumation rate data (Reiners et al., 2002, 2003). First, several geomorphic parameters were measured throughout the range to characterize the topography and constrain the differences in the morphologies of the northern and southern parts of the range. GIS and thermochonometric methods were then combined to investigate patterns of uplift and erosion that shaped the modern topography. Using GIS, I analyzed the extent and spatial pattern of uplift in the Grande Ronde member of the CRB. To determine the spatial variation in the proportion of the modern elevation of the range attributable to post-Miocene uplift, I evaluated latitudinal gradients in the local elevation maxima of the CRB and compared them to the elevation of the range as a whole. I also investigated the spatial relationship of the CRB relative to the eastern flank of the range and the modern drainage divide. In addition, Cenozoic exhumation rates estimated from apatite (U-Th)/He thermochronometric data were used to constrain the thickness of rock removed since Miocene times, and evaluated for consistency with uplift and the basalt outcrop patterns. These data were then combined to determine spatial patterns in surface uplift through the constraint of relative amounts of rock uplift and exhumation.

Topographic Analysis of the Cascades

A fundamental question behind this analysis of the topographic development of the Cascades is whether the topography of the North Cascades and southern Cascade Range in Washington State are now demonstrably distinct from each other, and if so, in what manner. Peaks in the North Cascades generally rise to higher altitudes (excluding Quaternary volcanoes) and have generally steeper slopes than the southern Cascade

Range, but to my knowledge no modern morphometric techniques based on analysis of digital elevation models (DEMs), have been employed to investigate or quantify such distinctions. I use the 10 x 10 m grid size DEM of the Cascades, constructed from 7.5-minute USGS topographic quadrangles, to investigate patterns in the mean and maximum elevations, slope, and relief of the range (Figure 2.2A). Because the underlying geology is a potential factor in determining topography, I divide the range into northern and southern regions based on the southern limit of the exposed crystalline core, which is approximately the latitude of Snoqualmie Pass (Figure 2.1). This division between North and southern Cascades corresponds to Haugerud's (2004) delineation of physiographic provinces. Due to orographic effects, the west side has considerably higher precipitation than the eastern side. Because precipitation is also a potential factor in controlling or modifying the topography of the range, I further divided the study area into regions east and west of the drainage divide (Figure 2.1, dashed line).

For my analyses of maximum and mean elevations, relief, and slope, I divided the area of the DEM indicated in Figure 1 into 10 km^2 cells (Figure 2.2B). Within each 10 km^2 analysis cell, I determined the maximum elevation, mean elevation, relief, and average slope. I then determined the means and standard deviations of each of these parameters across each 10 km-wide row. Because there appears to be a topographic distinction between the eastern and western sides of the Cascade Range, I also split each row at the drainage divide and then calculated the mean and standard deviation of each of the topographic parameters for the two sides of the range.

Spatial and Topographic Patterns of the Grande Ronde Basalt

One of the fundamental questions addressed in this study is whether the current boundaries of the CRB are depositional or erosional. A geologic map suggests that the ca. 17 to 15.5 Ma Grande Ronde Basalt (GRB), one of the earliest and most spatially extensive members of the CRB, covers ~150,000 km^2 of Washington, Oregon, and Idaho (Tolan and others, 1989). This basalt flowed outward in nearly horizontal sheets, hundreds of kilometers from source vents in eastern Washington, Idaho, and Oregon.

The presence of GRB indicates that an area had relief less than the thickness of the flow that now covers it. While I can confidently assert that all areas now covered by basalt were not what one would call a "mountain range" during the time that the basalt was emplaced, it is more difficult to be definitive about the paleorelief in areas where basalt is lacking. A lack of basalt could either be due to its erosional stripping from an originally low-relief surface, or because the area had enough relief to stand above the basalt flows. I circumvented this ambiguity by investigating the spatial and topographic trends of the basalt relative to the topography of the Cascade Range in Washington.

The GRB has four distinct units based on magnetic polarity; I use the youngest two members of the GRB, N2 and R2, as the marker formations for rock uplift because together they are the flows now found on the eastern flank of the southern Cascade Range in Washington. To analyze the topography of the modern basalt surfaces, I created a topographic coverage of these units of the GRB by clipping the 10-m DEM of the study area to the area mapped as this basalt on the 60-minute, 1:100,000 scale digital state geologic map series (Tabor et al., 1982; Frizzell et al., 1984; Walsh, 1986a; Walsh, 1986b; Korosec, 1987a; Korosec, 1987b; Phillips, 1987a; Phillips, 1987b; Phillips and Walsh, 1987; Schasse, 1987a; Tabor et al., 1987; Gulick and Korosec, 1990a; Gulick and Korosec, 1990b; Schuster, 1994a; Schuster, 1994b; Schuster, 1994c) (Figure 2.2 A). Using this new DEM of the GRB, I investigated its topography and the relationship of this topography to that of the Cascades as a whole. Specifically, I investigated west-east trends in GRB elevation within the Cascade Range, the spatial distribution of the modern basalt outcrop relative to the Cascade Range, and trends in the maximum elevation relative to the maximum elevation of the range at the same latitudes.

For several of these analyses, I divided the DEM of the range into nineteen, E-W trending, 20-km-wide rectangles, or "swaths," oriented orthogonally to the N-S trend of the range (Figure 2.2B). This division of the DEM allows the construction of a series of W-to-E-oriented topographic profiles and an investigation of different physiographic trends in the basalt. To construct the topographic profiles across each swath, I

calculated the maximum, mean, and minimum elevations at each 20 km by 10 m interval. I then repeated the calculation of maximum, mean, and minimum elevations for just the areas covered by basalt; note that there is no basalt in swaths north of swath 11 (Figure 2.2). These topographic profiles illustrate the deformation of the basalt and show its location and elevation relative to the non-basalt areas of the range. Assuming the surfaces of the basalt flows were originally horizontal, their topographic relief today constrains the differential rock uplift that occurred since the late Miocene.

I also compared the degree of overlap between basalt and the Cascade Range between the northern and southern regions of my study area to help determined the Miocene paleotopography. For this analysis, I identified the average UTM easting coordinate of the western basalt limit in each 20-km-wide swath, and compared it to the average UTM easting coordinates of the eastern limit of the Cascade physiographic province and the drainage divide within that swath (Haugerud, 2004), as defined using the DEM and shown in Figure 2.1.

I also analyzed how high the basalt has been uplifted relative to the overall altitude of the range. Areas that had low paleorelief near the axis of the range in Miocene time would allow the GRB to encroach close to that axis. When this area subsequently was uplifted, the basalt, if preserved, would be commensurately higher than the basalt covering areas farther from the axis. Conversely, if there were high paleorelief in the location of the uplift axis, then the basalt would be blocked by topography, and not approach the area of highest post-Miocene uplift—preserved basalt should not be found at high elevation. Within each of the 20 km swaths, I determined the maximum elevation for both the entire swath and for just the GRB, excluding the high volcanic peaks because they did not exist in their present location at the time of GRB eruption.

Paleotopography and Exhumation Constrained from Apatite (U-Th)/He Thermochronometry

The tilting of CRB on the eastern flank of the Cascade Range in Washington has long motivated the question of whether the basalt once covered more of the region

before Miocene uplift. There is a scenic viewpoint on the east side of the Cascade Range where one can observe the axis of an east-dipping anticline formed in the CRB near Wenatchee, appearing to project over Mt. Stuart, the highest non-volcanic peak in the central Cascades (>2800 m elevation), to the west. In between this anticline and the Cascade Range is the Columbia River valley. This "projection" argument for a low-relief Cascades region prior to the emplacement of the CRB has remained inconclusive because, while the western margin of basalt in that area is clearly erosional, the extent to which that basalt flowed further west is unknown. Without independent estimates of the amount of erosion since the deposition of the basalt, determining the geometry of the pre-CRB surface is not possible. However, such data now exist for the Cascades in the form of low-temperature thermochronmetric studies (Reiners et al., 2002, 2003).

Apatite (U-Th)/He (AHe) thermochronometric dating can measure the time and rate at which rocks pass upward through a particular geotherm due to exhumation (e.g., Farley, 2002). If one makes the assumption that exhumation-rate is constant, it is possible to calculate long-term average exhumation rates and estimate the vertical distance of exhumation for a particular period of time. Using the methods of Brandon and others (1998), these rates and distances were calculated using geothermal gradients ($^{\circ}$ km^{-1}) from Blackwell (1990), elevation data from the DEM, and AHe ages in the Cascades (Reiners et al, 2002; 2003; unpublished data). I considered north-south trends in the long-term average exhumation rates because it has been suggested that the North Cascades are higher, more deeply exhumed, and lack CRB cover today because they experienced greater late- and post-Miocene uplift and thus greater erosion than the southern Cascades (E. Cheney, personal communication, 2001). Alternatively, the North Cascade Range may now be high, deeply exhumed, and lack CRB cover because this region was already a topographic high during the Miocene and has been experiencing erosional exhumation for a longer time, not at a faster rate, than the south.

I also estimated the position of the deformed 15-My "datum" calculated by adding back the vertical distance of erosion to the altitude of apatite (U-Th)/He (AHe) samples (P.W. Reiners, unpublished data). Fifteen My was chosen because it represents

the end of Grande Ronde Basalt deposition; none of the younger CRB flows covered as large an area or reached as close to the modern crest of the Cascade Range in Washington (e.g., Reidel and others, 1989). I then make a simple linear reconstruction connecting the easternmost projected datum to the western limit of the GRB exposures. This reconstruction shows the simplest estimation of the position of the deformed land surface had no erosion taken place. If the original landscape had low relief and enough erosion has taken place to remove any basalt—if it originally covered the surface—the reconstruction should project over the existing topography without intersecting it. Alternatively, if there was pre-existing high topography between the modern edge of the basalt and the location of AHe samples at 15 My ago, and this high topography has not eroded away, the projection should intersect the modern topography. Another condition that could cause the basalt surface projection to intersect topography is post-Miocene deformation more complex than a simple anticline, for example, faulting with significant vertical offset between the western edge of the basalt and the easternmost AHe samples.

Results

The North Cascades and southern Cascade Range in Washington have previously been differentiated primarily on the basis of geology (e.g., by Haugerud, 2004). A glance at generalized geologic maps of Washington State (e.g., Schuster, 1992; Weissenborn, 1969) shows that primarily pre-Cenozoic metamorphic and intrusive igneous and lower Tertiary sedimentary rocks are exposed north of Snoqualmie Pass, whereas south of Snoqualmie Pass, primarily Tertiary volcanic and sedimentary rocks are exposed. However, the differences in the altitude-derived topographic indices between these two regions are gradational and subtle. In contrast, average slope and relief are more distinct between the northern and southern Cascades. As discussed later, many of the topographic distinctions between the north and south are less apparent on the western flank of the range than on the eastern flank.

When eastern and western regions of the range are analyzed together, the "average maximum altitudes" (the maximum altitudes determined within 10 km^2 blocks averaged within the 10 km-wide, W-E trending swaths) are highest in the northern Cascades (~2000 m) and decrease linearly to the south (~1100 m) at a rate about 2.8 m km^{-1} (Figure 2.4). In addition, there is so little difference in the N-S altitude gradient between the northern and southern parts of the range that least squares linear regressions of the northern and southern regions do not differ from those taking into account the entire region; that is to say, there is no "break" in this topographic trend as one might expect at the geologic transition near Snoqualmie Pass. However, this maximum altitude gradient is low enough that the standard deviations (1σ) for the maximum altitudes overlap across the entire N-S distribution. When divided into eastern and western regions, the average maximum altitudes decrease to the south at a slightly steeper gradient on the eastern flank than on the western flank.

Average mean altitudes (see explanation for "average maximum altitudes" above) are also highest in the north (~1200 m) and decrease approximately linearly to the south (~700 m), although the gradient is lower (~1.3 m km^{-1}) than it is for the maximum altitudes (Figure 2.5). As with the maximum altitudes, the separate least squares linear regressions of the northern and southern regions do not differ substantially from the regression of the entire range. This lack of a break in the mean altitude trend holds for the entire range, as well as for the western and eastern flanks when analyzed separately, though the goodness of fit of the regression for the west side ($R^2 = 0.22$, $p < 0.05$) is much less than for either the region as a whole ($R^2 = 0.71$, $p < 0.05$) or the eastern flank ($R^2 = 0.79$, $p < 0.05$) (Figure 2.5).

In contrast, there is a difference in mean relief, the difference between the highest and lowest altitudes measured within 10 km^2 windows and then averaged across latitudinal bins, between the northern and southern Cascades. The average relief ranges from 750 to 1000 m in the southern Cascades, with a weak to no north-south trend (Figure 2.6). This lack of a statistically significant N-S trend in relief in the south is particularly striking on the west side of the range. North of Snoqualmie Pass, however,

overall relief increases towards the north, with relief reaching > 1500 m in the northernmost part of the range. On the west side of the northern Cascades, this increase in relief with increasing latitude is strongly linear, with relief increasing from about 800 m at Snoqualmie Pass to nearly 2000 m at the Canadian border, at a gradient of 4.9 m km^{-1}. On the east side of the range, there is no trend ($R^2 < 0.001$, $p = 0.96$), with a peak in relief about midway between Snoqualmie Pass and the northern border.

The average slopes of E-W trending latitudinal swaths are also generally higher in the North Cascades than in the southern Cascades. The increase in slope from south to north is linear on the west flank of the range, but there is a sharp break in the trend in slopes on the east flank of the range (Figure 2.7). When both the east and west flanks are considered, the average slope is approximately constant at ~ 23° from Snoqualmie Pass to the northern border; when only the eastern flank is considered, there is a decrease in average slope north of Snoqualmie Pass. South of the pass, the average slope is generally less than in the north, ranging from 10° to 20°, with higher slopes on the western side of the range than on the eastern side. There is also a slight northerly increase in slope in the southern Cascades; this gradient of the slope trend is both steeper and stronger on the eastern side of the range than on the western side.

I have also determined the averages of all the altitude, relief, and slope measurements for the four "quadrants" of the range: northeast, northwest, southeast, and southwest (Figure 2.8). Maximum and mean altitudes are very slightly higher (and overlap with their 1σ standard deviations) in the east than the west in the northern Cascades, and vice versa in the southern Cascades. There is no statistical difference in relief or slope in the northern Cascades between east and west, but both relief and slope are lower on the east flank than the west flank in the southern Cascades.

Spatial and Topographic Patterns of the Grande Ronde Basalt

Topographic profiles show the deformation of the Grande Ronde Basalt (GRB) on the east flank of the Cascades (Figure 2.9). In the southernmost swaths (1-10), the upper surfaces of the N2 and R2 GRB flows extend up and westward to the altitude of

the range crest, and in places, have crossed the modern drainage divide. The extent of the basalt in the south relative to the edge and crest of the range stands in stark contrast to the North Cascades (swaths 11-15) where the basalt is limited to the eastern edge of the range. No N2 or R2 GRB is exposed in swaths 16-19. Again, the key question is whether basalt is missing from the landscape because it has been eroded or because it was never deposited there.

CRB is found at higher altitudes in the southern Cascades in both absolute and relative terms. The highest basalt in the southernmost swaths is found at ~1500 m, increasing to ~2000 m in swaths 5-10. In each of these southern Cascade swaths, the basalt reaches 80% to 100% of the highest altitude found in the entire swath, excluding the Quaternary volcanoes (Figure 2.10). For example, in swath 6, the highest point in the swath (2100 m) is an exposure of N2 GRB. Conversely, the highest basalt in the North Cascades (swaths 11 through 15) is at 1500 m, decreasing to < 1000 m in the northernmost swaths. In addition, these basalt exposures reach a smaller percentage of the total range altitude, only 30 to 60% of each swath's highest non-volcanic point. There are no GRB exposures in swaths 16 through 19.

Grande Ronde Basalt exposures are present significantly closer to the crest of the southern Cascades than to the crest of the North Cascades (Figure 2.9 and 2.11). In far southern Washington (swaths 1 and 3), the basalt is found on the west side of the modern drainage divide, and in swaths 4 through 8, the basalt has flowed > 50% of the distance from the eastern margin of the range toward the present divide. However, in swaths 11 through 15, the basalt reaches < 10% of the distance between the edge of the range and the divide.

Exhumation Rate Trends from AHe Thermochronometry

AHe data are only available for swaths 10 through 14, in the central part of the range. Assuming a constant exhumation rate through time, the linear reconstructed 15 My surfaces connecting the basalt to the AHe projections project over the existing topography in swaths 10 and 11, but intersect existing topography in swaths 13 and 14

(Figure 2.12). Interpretation of the projection is ambiguous in swath 12, and thus not shown in Figure 2.12.

The AHe data from Reiners et al. (2002, 2003) span a 100-km N-to-S distance in the Cascade Range, primarily in what I have defined as the North Cascades. In the area covered by these data, long-term average exhumation rates range from 0.02 to 0.1 km Ma^{-1} east of the drainage divide, and do not have any N-S trend (Figure 2.13). West of the drainage divide, however, exhumation rates range from 0.05 to 0.11 km Ma^{-1} in the north and generally increase to a maximum of 0.33 km Ma^{-1} to the south (Figure 2.13).

Discussion

The topographic, geologic, and thermochronometric evidence collectively supports the polygenetic model for topographic development of the Cascade Range in Washington. Indeed, the polygenetic model also resolves evidence previously considered to provide contradictory support for either low- or high-relief paleotopography.

Grande Ronde Basalt and Topography

The topographic and spatial relationships of the GRB to Cascade topography confirm there was low relief in the area now forming the southeastern flank of the Cascades during the middle Miocene. Given that basalt does not flow uphill and assuming that the upper surfaces of the GRB flows initially were roughly horizontal, the areas where surfaces of basalt flows are preserved had low relief during the middle Miocene. Because this low-relief footprint covers the entire eastern flank of the southern Cascades, any basalt-blocking relief in the Miocene must have been 20 to 50 km west of the current eastern edge of the Cascades 17 My ago. As suggested by Mackin and Cary (1965), low relief topography could have extended beyond the footprint indicated by the basalt in southern Washington, and connected with the other CRB flows found closer to the Washington coast. In the North Cascades, the footprint of definitively low Miocene relief is limited to within 4 to 12 km of the eastern edge of

the modern range and is consistent with the North Cascades standing above the encroaching basalt flows. If the basalt in the north was once more extensive but has since been eroded away, there must be an explanation for why it was preferentially removed in the north.

Not only do modern GRB exposures exist closer to the drainage divide in the southern Cascades than in the North Cascades, the basalt outcrops also reach altitudes ~1000 m higher and are even exposed at the crest of the range in the south. This N-S difference in basalt altitude could be explained by several hypotheses. If the Cascades existed prior to the emplacement of the CRB and the modern basalt margin is depositional across both the North and southern Cascades, the basalt could be higher in the south because it either flowed closer to the axis of post-Miocene uplift in the south than it did in the north, or the amount of rock uplift was greater in the south than in the north. Alternatively, if the basalt margin on the east flank of the Cascades is erosional, the difference in basalt altitude between the north and south could be due to greater erosional stripping of the basalt in the north. Porter (1976a) suggested that CRB may have once covered more of the eastern North Cascades, preserving a series of low-relief, tilted erosion surfaces that appear to follow the trend of basalt flow surfaces. This hypothesis raises the same question as above; if pre-CRB topography had low relief and CRB once covered the entire range, why would the basalt be missing from the North Cascades but be preserved in the southern Cascades? This question is especially pertinent on the east side of the range, where precipitation and long-term exhumation rates are quite low (< 0.1 km Ma^{-1}, Reiners et al., 2002, 2003).

One possible explanation is that glacial erosion preferentially removed basalt from the north and not the south. For example, only the Cascades in far northern Washington were covered by ice of the Cordilleran Ice Sheet (Booth et al., 2004) (Figure 2.14A). However, the Cascade Range in central and southern Washington was also extensively covered with alpine valley glaciers during the last several Quaternary glaciations (S.C. Porter, personal communication, 2003) (Figure 2.14A). A comparison between the Quaternary maximum glacial extent and the modern extent of the CRB

shows that the ice extended eastward to (and locally overlaps) what is now the edge of the basalt in the southern Cascades (Figure 2.14B). The overlap between the glacial and CRB margins in the southern Cascades is consistent with glaciers having removed CRB from the landscape, at least along the main valleys. However, north of Snoqualmie Pass, the ice extent at the glacial maximum does not abut or overlap the modern CRB limit (Figure 2.14B). One thus cannot invoke preferential glacial erosion to explain the lack of CRB on the east flank of the North Cascades.

Recognizing the limitations imposed by the assumptions required of the exhumation-rate analysis, the projections of the 15 My surface are also consistent with a polygenetic topographic history of the range. The linearly projected 15 My surfaces do not intersect existing topography in swaths 10 and 11 (the swaths containing AHe data south of Snoqualmie Pass), and so it is possible that no elevated topography stood between the western edge of the basalt and the easternmost AHe sample localities at 15 My ago. However, the linear 15 My datum projections in the northern swaths 13 and 14 intersect existing topography, thus either complex deformation of the 15 My "surface" occurred between the western edge of the basalt and the easternmost available exhumation rate data, or elevated topography already existed between these two areas (Figure 2.12). I prefer the latter explanation due to the lack of identifiable structures that could accommodate hundreds of meters of post-Miocene offset (Campbell, 1988).

The N-S trends in long-term average exhumation rate also support the interpretation that the North Cascades had significant relief prior to the emplacement of the CRB, and that the two regions of the Cascades have not experienced greatly different exhumation histories since the middle Miocene. Although exhumation rate data is unavailable from the far northern and southern portions of the study area, data from the central and northern part of the study area suggest that exhumation rates either do not change or increase to the south. If the entire range had low relief at the time of CRB emplacement, and the North Cascades have subsequently been uplifted and exhumed to a much greater extent than the southern Cascades, one should expect exhumation rates to be higher in the north than the south. In this polygenetic hypothesis

with post-Miocene uplift acting upon an already-high North Cascades and a low-relief southern Cascades, one would expect to see reasonably constant exhumation rates across the area if the uplift rate were also constant, or higher exhumation rates in the south if uplift was more rapid there. Although of limited spatial extent, these data support the polygenetic model (Figure 2.12).

Geologic Context

A polygenetic origin of Cascades topography is not only consistent with the geographic and thermochronologic data and analyses, but such an interpretation of the Cascade Range topographic evolution is also consistent with the geologic history and geophysical setting of the range. In the following section, I discuss the geologic and tectonic history of the Cascades, and how these relate to the polygenetic physiographic hypothesis.

The history of mountain building in Washington State long precedes the Miocene. The main backbone of the northern Washington Cascades accreted during the middle Cretaceous (e.g., Saleeby et al., 1992). Deformation resulting from the docking and suturing of terranes on the west coast of North America at this time caused up to 500 km of shortening, resulting in extensive crustal thickening and metamorphism. The current exposure of highly metamorphosed formations in the northern Washington Cascades today attests to tens of kilometers of structural and erosional exhumation since that time (Haugerud et al., 1991; McGroder, 1991, Valley et al., 2003). This evidence of crustal thickening and exhumation suggests that the middle Cretaceous was a time of mountain building in northern Washington State, with a significant amount of relief (e.g., Mackin and Cary, 1965). Although the pre-Tertiary basement of the southern Washington Cascades is almost completely covered by Cenozoic sedimentary and volcanic rocks, gravity data and a southern Cascade exposure of pre-Tertiary melange and metamorphic rocks correlates with those exposed in the northern Cascades and suggests that a relatively continuous accreted crystalline core probably underlies the

entire Cascades and plunges under the Cenozoic cover in southern Washington (Miller, 1989; Saltus, 1993).

During the early Cenozoic, collision and subduction appear to have slowed while sedimentation and extension of fault-bounded basins began (Johnson, 1984; Christensen et al., 1992). During this time, extensive and km-thick fluvial and shallow marine sediments were deposited along the western edge and across the middle of the Cascade Range in Washington (Figure 2.15A). These sediments are thought to have been "deposited by meandering rivers that flowed westward across a broad coastal plain that existed prior to the uplift of the Cascade Range," indicating low relief at that time (Johnson, 1984). The great thickness (some sections are 6 km thick), volume, and grain size of these Eocene sediments attest both to the rapid subsidence of the basins, and to the presence of a nearby, rapidly uplifting source region (Johnson, 1984; Christiansen and Yeats, 1992). The source regions of these sediments include distant terrains to the north and east of the Cascades (R.C. Evarts, personal communication, 2005; Mathews, 1981), as well as the rocks now exposed in the core of the North Cascades, including the Chiwaukum Schist and Mt. Stuart batholith (Johnson, 1984; Vance, 2002). The presence of these lithologies in Eocene sediments indicates that the crystalline core of the North Cascades was exposed and shedding sand- to gravel-sized sediment at that time. All of these early Eocene sedimentary deposits were subsequently folded and faulted (Foster, 1960; Gresens, 1980).

The next geomorphically significant phase in Cascade geology was the renewal of arc volcanism, fed by the renewed subduction of the Farallon/Juan de Fuca plate to the west beginning ~40 My ago (Smith, 1993). In the North Cascades, this period of magmatic activity is evidenced by the development of numerous intrusive igneous bodies (Dragovich et al., 2002) (Figure 2.15B). It is thought that these batholiths and plutons are the crystallized magma chambers that may have once fed a chain of volcanoes of unknown extent and altitude. In the north, any extrusive rocks of these volcanoes have long since eroded away, potentially indicating that relief in the north was high enough to drive relatively rapid erosion of the volcanoes. Conversely, both

extrusive and intrusive rocks are widely preserved in the southern Cascades of Washington (e.g., Walsh et al., 1987). During or after this interval of volcanic activity, the southern Cascades subsided, deforming these volcanic rocks into a broad syncline with the axis near the modern drainage divide of the range (Evarts and Swanson, 1994; Hammond, 1998). These volcanic deposits subsided so much that great thicknesses were preserved and were later intruded by slightly younger Miocene plutons (Evarts and Swanson, 1994; Power et al., 1981). The evidence of subsidence and lack of erosion of the volcanic rocks suggests low relief in southern Washington at this time.

By the middle Miocene, volcanic activity was still a dominant process throughout the range. Clasts of extrusive rocks associated with middle Miocene plutonism in the southern Cascades occur in sedimentary and volcaniclastic deposits that flank the Cascades (Smith and others, 1988). The Ellensburg Formation (16-7 My, Smith and others, 1988) consists of fluvial and pyroclastic deposits of primarily volcanic and volcaniclastic origin preserved on the east side of the Cascades (Figure 2.15C). The Ellensburg Formation crops out primarily south and east of Snoqualmie Pass, though small exposures exist as far north as Wenatchee. The contemporaneous Mashel Formation, which also consists of fluvially transported volcanic sediment, is found on the west side of the range (Mullineaux et al., 1959; Walters and Kimmel, 1968). These coarse-grained deposits, much like the earlier Eocene sediments, must have formed on or adjacent to topography steep enough to generate and transport large clasts, e.g., on the flanks of volcanoes. However, as Mackin and Cary (1965) suggested, middle to late Miocene volcanoes did not necessarily form a continuous upland in southern Washington. Any parts of the landscape high enough to block the flow of nearly planar sheets of fluid lava must have been located to the west of the modern basalt outcrops. However, this does not exclude the possibility that the basalt once covered more of the Cascade Range in southern Washington; subsequent uplift and differential erosion on the wetter west side of the range could have removed any CRB that may have once covered the area.

The paleobotanical and isotopic evidence of rainshadow formation is also

consistent with a polygenetic topographic history of the Cascades in Washington. The majority of fossil evidence for the transition from mesic to xeric ecosystems in eastern Washington comes from central and southern regions of the state (e.g., Chaney, 1938; Beck, 1945; Smiley, 1963; Leopold and Denton, 1987; Takeuchi and Larson, 2005) (Figure 2.15D). Chaney (1938, 1959) focused on eastern Oregon, studying only a few sites in southern Washington and no sites north of Snoqualmie Pass. Smiley (1963) worked in the Ellensburg Formation of south-central Washington. Although this formation is found further to the north, Smiley (1963) did not study any sections north of Wenatchee. Leopold and Denton (1987) and Takeuchi and Larson (2005) also had sites located only in southern Washington (Figure 2.15D). Thus, while the evidence appears conclusive that a significant climate changed occurred in south- and central-eastern Washington from ~16-8 My ago, there appear to be no data documenting a similar phenomenon in northern Washington. Therefore, possibly there was already significant relief in northern Washington 16 My ago as the southern Washington Cascades rose and created an orographic rainshadow.

Tectonic Context

Although the tectonic explanation for the post-Miocene uplift of the Cascades in Washington remains a matter of debate, there appears to have been a pulse of rapid exhumation, and therefore rapid rock uplift, along much of the northwestern coast of North America between 10 and 12 My ago (Reiners et al., 2002). Evidence for this pulse of exhumation has been found from Mt. Rainier north to Juneau, Alaska, suggesting regional-scale uplift, possibly related to a change in relative plate motions or delamination of the lower crust (Reiners et al., 2002). In addition to this regional uplift, there is tectonic evidence that the southern Cascade Range is also experiencing north-south compression and shortening. This tectonic evidence includes paleomagnetic evidence of post-Miocene rotation, GPS measurements of modern crustal movements, and historic seismicity.

Determinations of crustal motions from paleomagnetic and GPS data suggest

that southern Washington is being rotated and compressed against the crystalline foundation of the North Cascades and Coast Range of British Columbia. Paleomagnetic data show that there has been significant (10°-35°) clockwise rotation in < 30 My old rocks in the southern Cascades relative to a fixed North American datum (Bates et al., 1981; Wells, 1990; England and Wells, 1991; Hagstrum et al., 1999). Rotation and northeastern movement of the Cascade Range in southern Washington is also evident in GPS velocities (for example, Wells et al., 1998; Svarc et al., 2002; Mazzotti et al., 2003) and north-south compression is evident in recent seismicity (Stanley et al., 1996). This rotation in southern Washington is probably due to a combination of dextral shear resulting from the subduction angle at the plate margin and effects of Basin and Range extension (Figure 2.1B) (Wells, 1990; Hagstrum et al., 1999). In contrast, rocks in the North Cascades have not experienced rotation since the Miocene, are not currently moving to the northeast relative to a fixed North America, and are relatively seismically inactive (e.g., Wells, 1990; Stanley et al., 1996; Wells et al., 1998; Svarc et al., 2002). Although I have not modeled the specific effects of tectonic differences on the uplift of the Cascades, the observed differences in past and present rotation and seismicity are consistent with the hypothesis that the southern Washington Cascades experienced additional regional uplift superimposed upon the larger-scale (and still enigmatic) uplift that affected the entire northwestern Pacific coast during the Miocene. This north-south compression of the southern Cascades against the North Cascades likely explains why the highest CRBs are found right at the transition between the two regions, as that is where the gradient in crustal velocity is the highest.

Modern Topography

Despite substantial differences in both geologic and tectonic history between the northern and southern Cascades, why are the differences in the maximum and mean altitudes between the regions subtle and gradational, particularly on the western flank? First, greater uplift in the originally lower southern Cascades due to additional north-south compression may have obscured original differences in altitude between the two

regions. In addition, I suggest that erosional processes masked the topographic differences between the northern and southern Washington Cascades since the uplift of the Cascade Range antiform. There are two distinct climatic gradients in the Cascades that affect erosion patterns: the strong W-E variation in precipitation resulting from the rainshadow effect, and the strong altitudinal control on glacial erosion processes (Mitchell and Montgomery, 2006). Once the range, northern and southern, became high enough to interfere with weather systems bringing in moisture from the west, increased precipitation rates on the west side caused fluvial and glacial erosion rates to increase, while precipitation and erosion rates decreased on the east side (Reiners et al., 2003)—although it is worth noting that the largest alpine glacier systems in the Cascades were on the east side (Porter, 1976b). Also, once the climate was cold enough and the range high enough to intersect the glacial equilibrium line altitude, glacial erosion increased erosion rates and limited how high the peaks could rise on the west flank of the range, regardless of uplift rate. The spatial correspondence of the edge of alpine glaciation and the extent of the CRB suggests that glacial erosion also contributed to the removal of CRB from the southern part of the range. Both of these climatic influences on post-uplift erosion are largely independent of rock type and of latitude, and thus this erosion may have erased any prior differences in peak altitude between the northern and southern Cascade Range in Washington, most noticeably on the western flank.

The increase in average slope and relief towards the north could be due to differences in the average rock hardness and resistance to erosion in the two regions. Resistant, crystalline rocks that form most of the northern part of the range may be capable of maintaining steeper slopes and thus higher relief than the less-resistant, more jointed volcanic and sedimentary rocks in the south (e.g., Schmidt and Montgomery, 1995). Even with steeper slopes and more relief, the harder rocks exposed in the northern Cascades appear to be eroding, based on AHe data from Reiners et al. (2002, 2003), at a similar or slower average rate as those in the south, particularly on the east flank of the range (Figure 2.13).

Conclusions

Because previous investigations of Cascades physiography focused on particular regions, outcrops, or features, prior interpretations regarding topographic development are biased according to the location and type of evidence available. By integrating topographic and exhumation-rate analyses with the geologic evidence previously used to infer local paleotopography into a regional context, I am able to resolve apparent contradictions in prior ideas and observations regarding the topographic evolution of the range. Specifically, this reanalysis of prior studies in light of new topographic and AHe analyses support a polygenetic model for development of the topography of the modern Cascade Range in Washington State. I conclude that the North Cascades had significant relief before the Miocene, blocking the CRB flows. During this same time, the southern Cascades probably had low to modest relief, punctuated by isolated volcanic centers. The Cascade Range was later uplifted at least ~1000 m more, as evidenced by the deformation of the CRB on the eastern flank of the range. The polygenetic model provides a reasonable singular underlying explanation for many of the observed phenomena, including: 1) the spatial distribution and vertical deformation of the CRB relative to the topography of the Cascade Range, 2) observed climate change in eastern Washington resulting from the raising of an orographic barrier, and 3) the spatial relationship between CRB outcrops and the extent of glaciation. This polygenetic model is also consistent with the differences in geology and tectonics between the two regions. Subsequent topographic modification of the range due to orographic effects and glacial erosion masked the differences in geology and topographic history, resulting in a single physiographic entity with a complex, polygenetic origin.

Figure 2.1: A. Physiographic and generalized geologic map of Washington State. "North Cascade" and "southern Cascade Range" areas (from Haugerud, 2004) are shaded in gray and Snoqualmie Pass (SP) noted. The drainage divide is the fine dashed black line, and the generalized outcrop limit of the Grande Ronde Basalt is shown as the dark gray dashed line. The hatchured region shows the pre-Tertiary crystalline core of the North Cascades and northern Washington. Quaternary volcanoes Mt. St. Helens (MSH), Mt. Adams (MA), Mt. Rainier (MR), Glacier Peak (GP), and Mt. Baker (MB) are indicated by the triangles. B. Generalized tectonic map of the Pacific Northwest. Physiographic provinces from Haugerud (2004) outlined in gray include: North Cascades (NC), Western Cascades (WC), High Cascades (HC), Columbia Plateau (CP), Olympic Mountains (OM), Coast Ranges (CR), and Basin and Range (B and R). Note that the area shaded in gray is the same as in Figure 2.1A. Tectonic boundaries (Haugerud, 2004) include spreading centers (double line), transform faults (solid lines), and the Cascadia subduction zone (heavy black line with teeth).

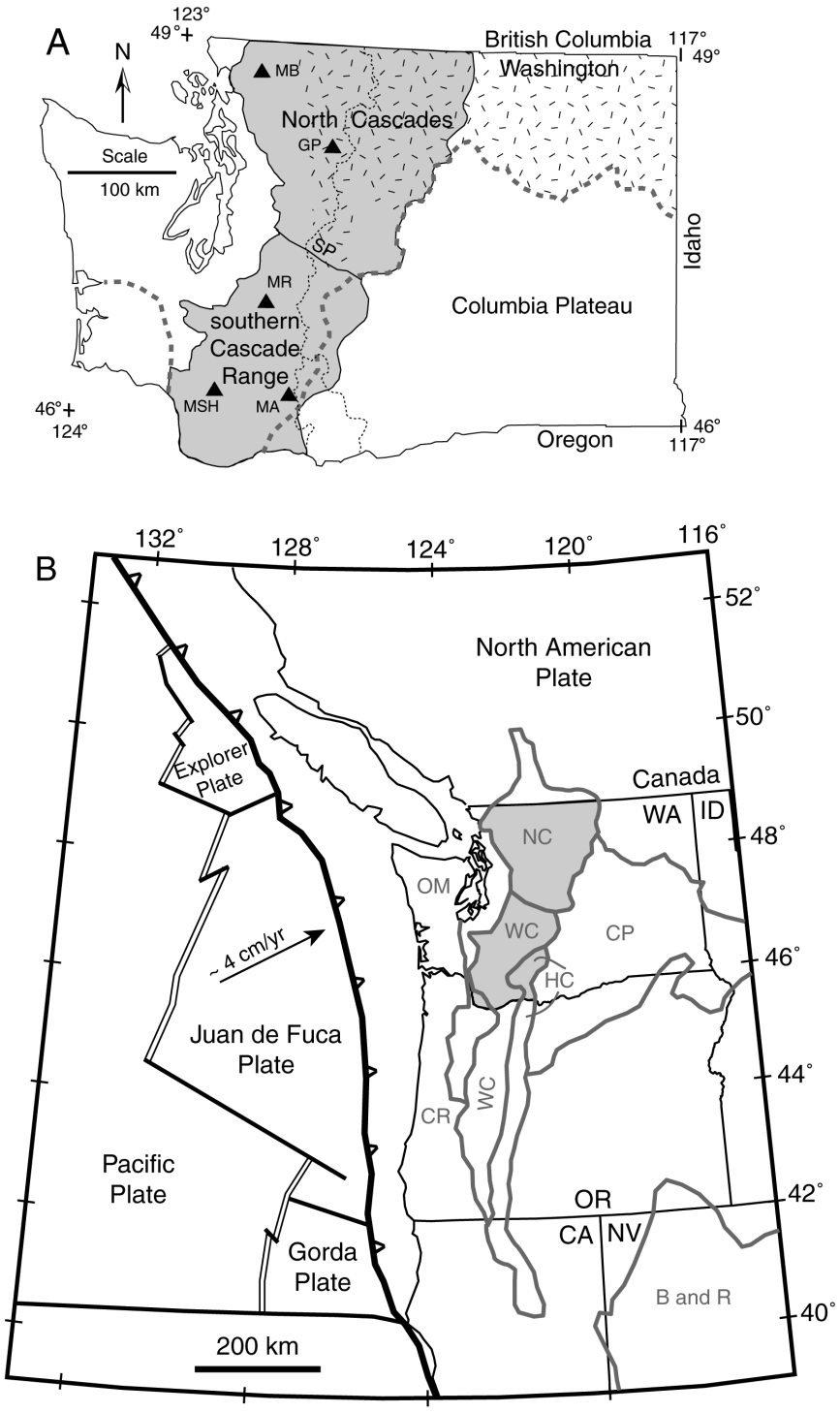
A
123°
49°
N
British Columbia
Washington
117°
49°
MB
North Cascades
GP
Scale
100 km
SP
Idaho
MR
Columbia Plateau
southern
Cascade
Range
MSH
MA
46°
124°
Oregon
46°
117°
B
132°
128°
124°
120°
116°
52°
North American
Plate
50°
Explorer
Plate
Canada
WA
ID
NC
48°
OM
WC
CP
46°
HC
~ 4 cm/yr
Juan de Fuca
Plate
44°
CR
WC
Pacific
Plate
OR
42°
CA
NV
Gorda
Plate
B and R
40°
200 km

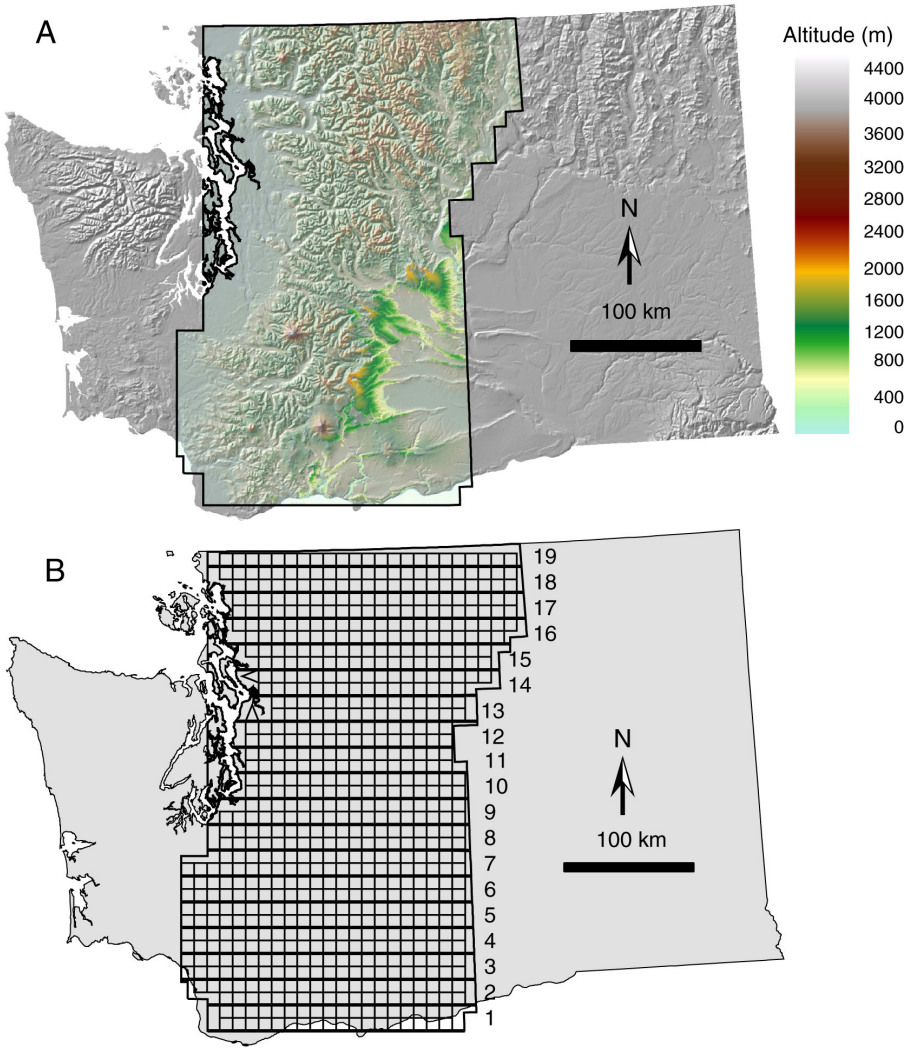

Figure 2.2: A. Shaded relief and altitude map of Washington State derived from the DEM of study area. Study area for topographic analyses is outlined in black, altitudes are indicated in pale color. Intensely colored regions inside study area indicate modern exposures of Grande Ronde Basalt (GRB); GRB outside study area is not shown. B. Grid showing analysis windows for topographic calculations. Bold lines show the position of "swaths" used to make topographic profiles, numbers on the right indicate the swath number. Fine lines show the position of 10 km^2 windows used for morphometric analyses.

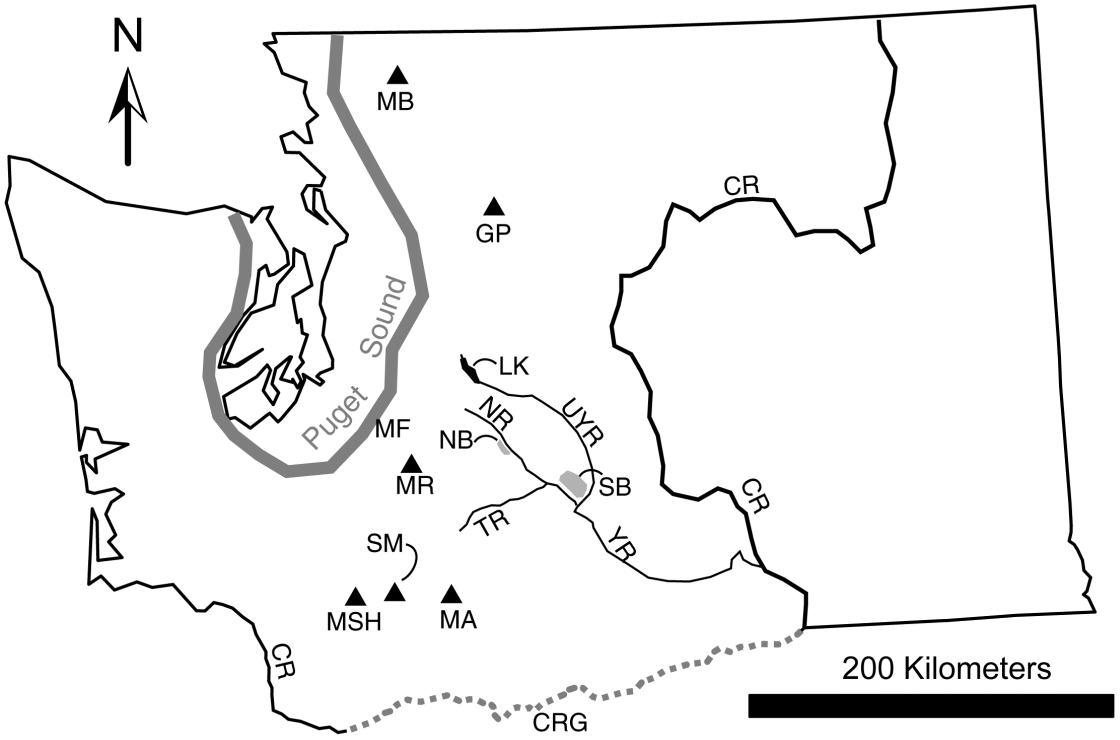

Figure 2.3: Geographic place names used in Chapter 2. Quaternary volcanoes (triangles) are labeled as in Figure 2.1. CR = Columbia River; CRG = Columbia River Gorge (dashed gray line), LK = Lake Keechelus; MF = Mashel Formation; NB = Nile Basin; NR = Naches River; SB = Selah Basin; SM = Steamboat Mountain; UYR = Upper Yakima River; YR = Yakima River.

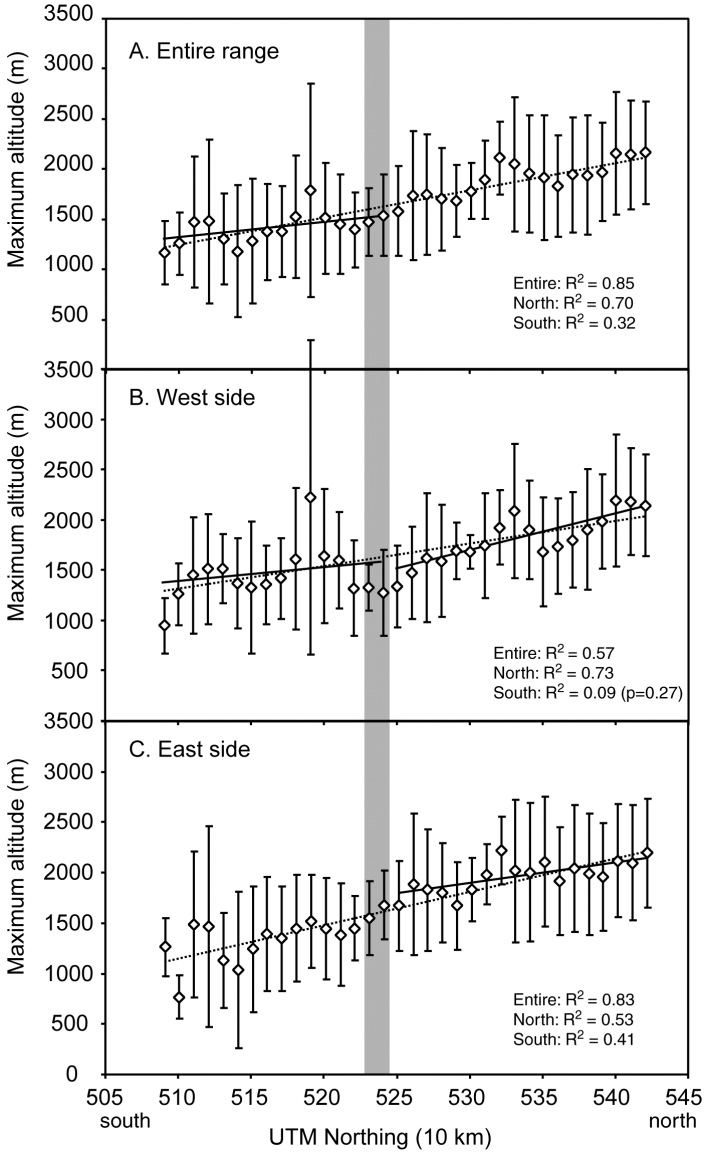

Figure 2.4: Maximum altitudes (diamonds) averaged across 10-km-wide latitudinal bins for: A, the entire range; B, west of the range crest; and C, east of the range crest. Error bars indicate the 1σ standard deviation. The vertical gray bar denotes the approximate latitude of Snoqualmie Pass, dividing the range into northern (right) and southern (left) regions. Least squares linear regressions for the average maximum altitude for the entire (dashed line), northern (solid line), and southern (solid line) areas of the range are also shown (note: if the regression for a subregion overlaps the regression for the entire region, only the latter is shown). All p-values are < 0.01 unless noted.

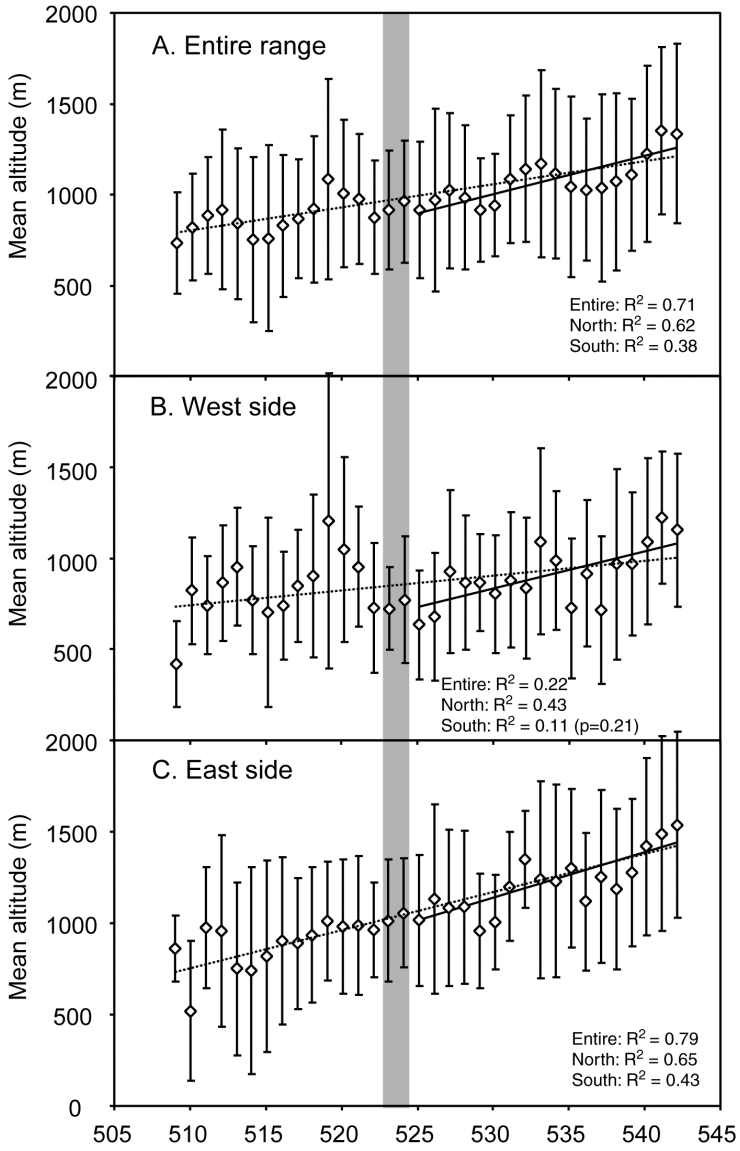

Figure 2.5: Mean altitudes (diamonds) of 10-km-wide latitudinal bins for: A, the entire range; B, west of the range crest; and C, east of the range crest. The vertical gray bar denotes the approximate latitude of Snoqualmie Pass. Least squares linear regressions for the average altitudes for the entire (dashed line), northern (solid line), and southern (solid line) areas of the range are also shown (note: if the regression for a subregion overlaps the regression for the entire region, only the latter is shown). All p-values are < 0.01 unless noted.

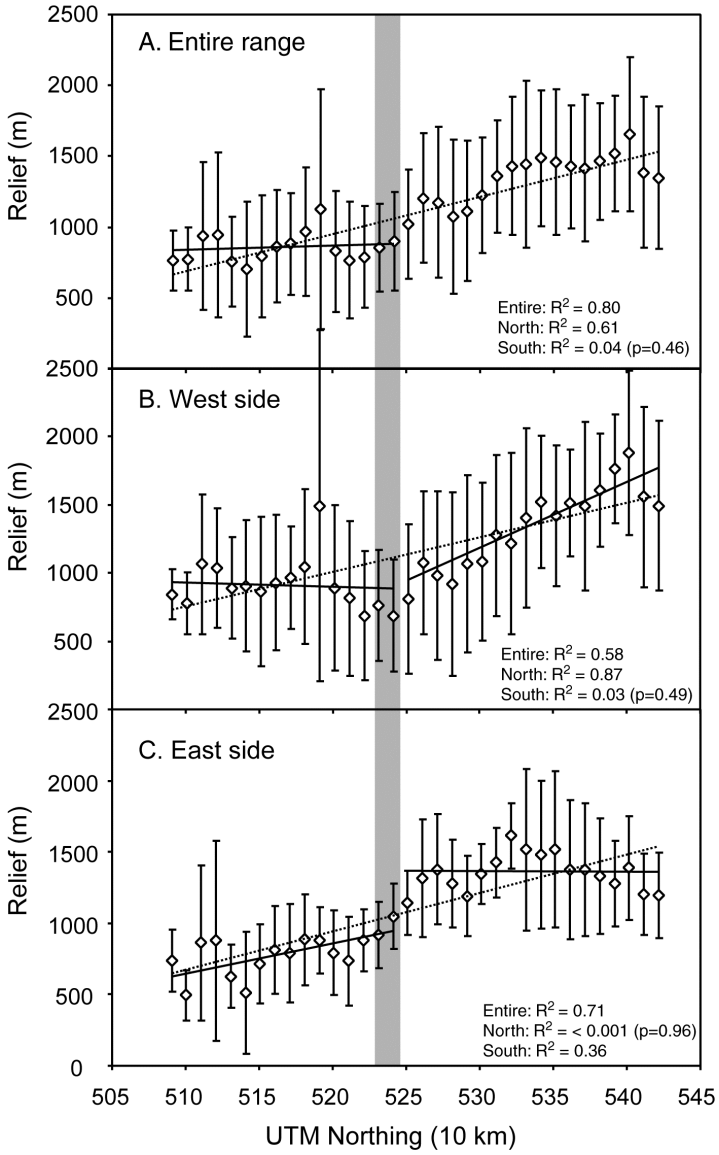

Figure 2.6: Mean relief (diamonds) of 10-km-wide latitudinal bins for: A, the entire range; B, west of the range crest; and C, east of the range crest. The vertical gray bar denotes the approximate latitude of Snoqualmie Pass. Least squares linear regressions for the average relief for the entire (dashed line), northern (solid line), and southern (solid line) areas of the range are also shown (note: if the regression for a subregion overlaps the regression for the entire region, only the latter is shown). R^2 values are indicated for each regression, all p-values are < 0.01 unless noted. Generally, relief is higher in the north than in the south.

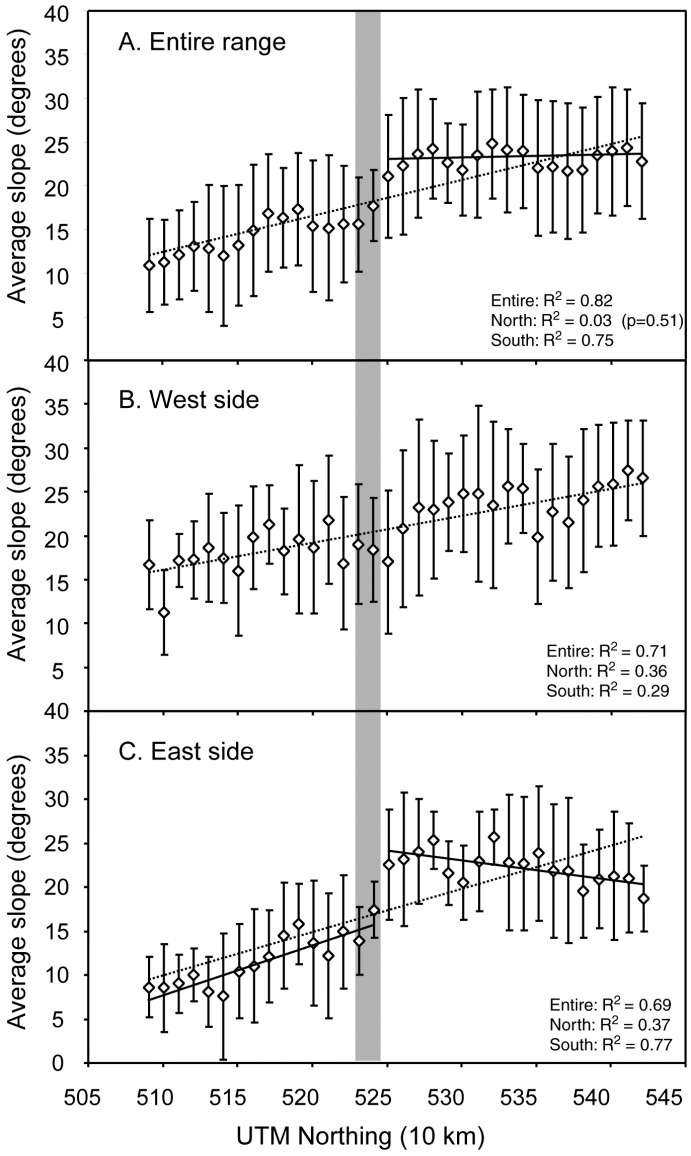

Figure 2.7: Average slope (diamonds) of 10-km-wide latitudinal bins for: A, the entire range; B, west of the range crest; and C, east of the range crest. The vertical gray bar denotes the approximate latitude of Snoqualmie Pass. Least squares linear regressions for the average relief for the entire (dashed line), northern (solid line), and southern (solid line) areas of the range are also shown (note: if the regression for a subregion overlaps the regression for the entire region, only the latter is shown). All p-values are < 0.01 unless noted.

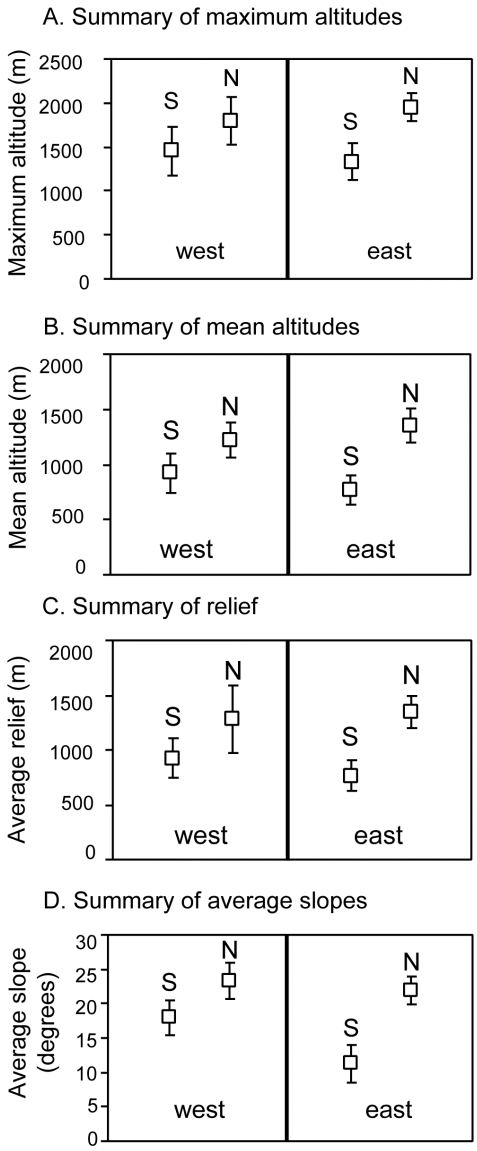

Figure 2.8: Summary diagrams showing average values of: A) maximum altitudes, B) mean altitudes, C) relief, and D) slope for four quandrants of the Cascades, divided W-E by the drainage divide and N-S by Snoqualmie Pass. There is little overall distinction in any of the topographic parameters between west and east in the northern Cascades. In the southern Cascades, there is little distinction between east and west in altitude or relief, but slopes are significantly lower on the east side than the west side.

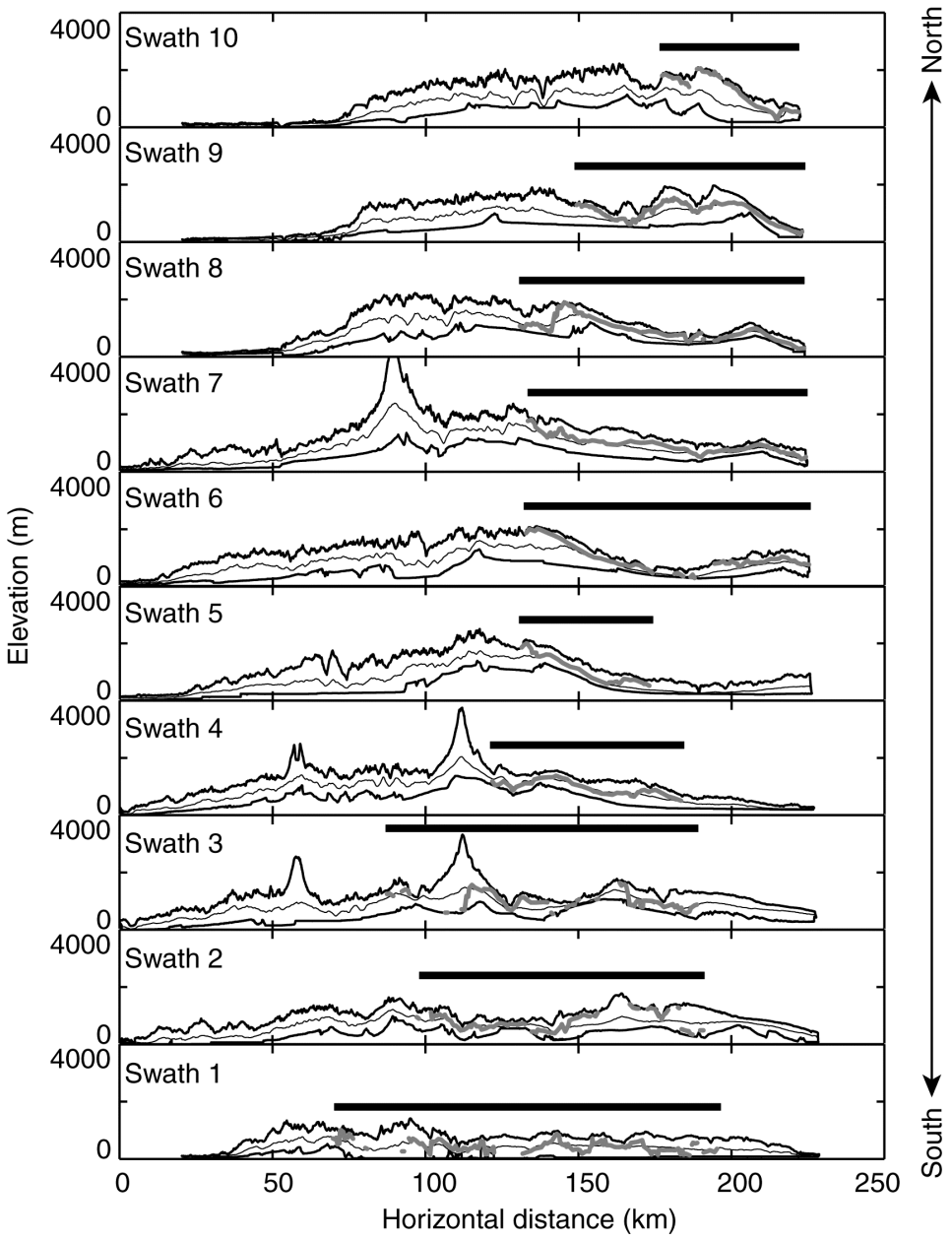

Figure 2.9A: Topographic profiles across swaths 1-10. Maximum, mean, and minimum topography shown as thin upper black, middle gray, and lower black lines, respectively. Upper surfaces of GRB shown in gray. Black bars highlight the horizontal extent of GRB within each swath.

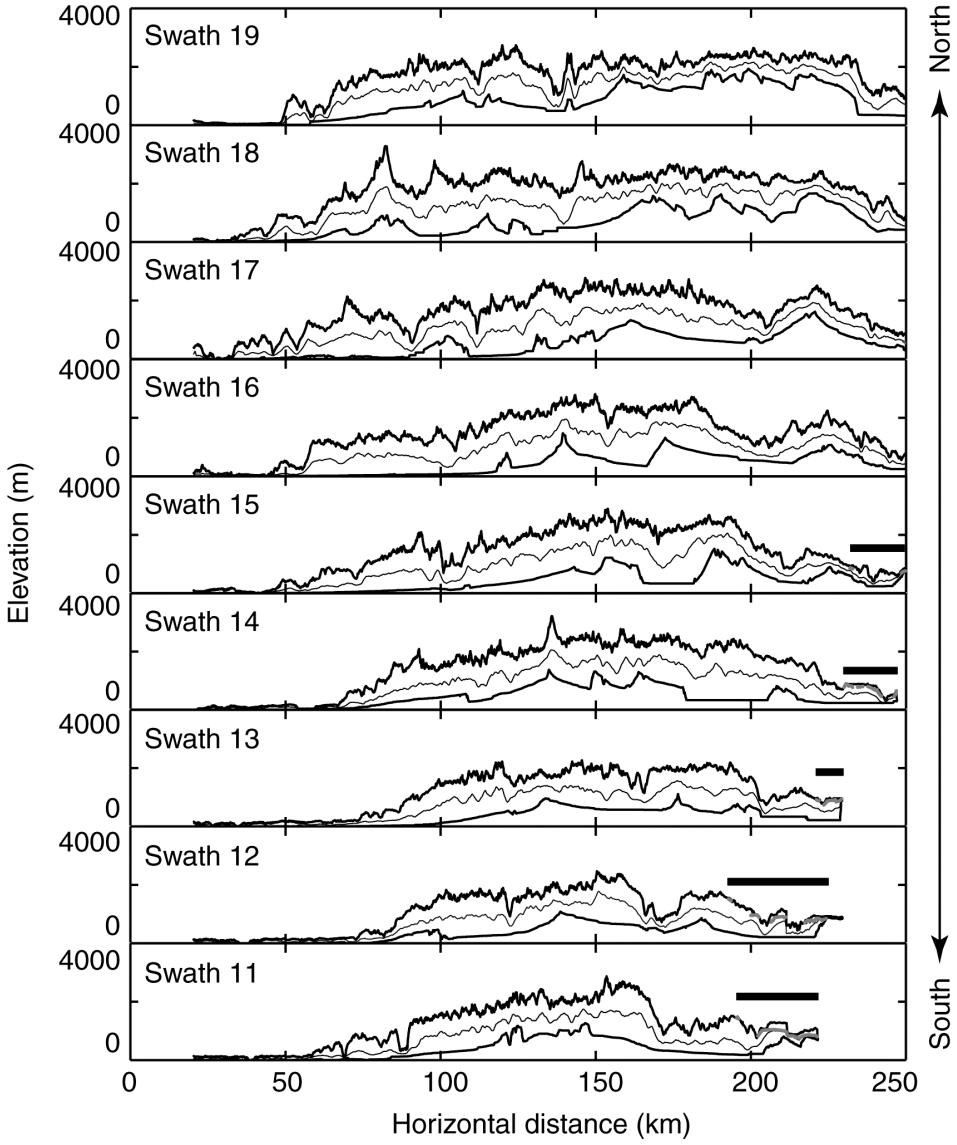

Figure 2.9B: Topographic profiles across swaths 11-19. Maximum, mean, and minimum topography shown as thin upper black, middle gray, and lower black lines, respectively. Upper surfaces of GRB shown in gray. Black bars highlight the horizontal extent of GRB within each swath.

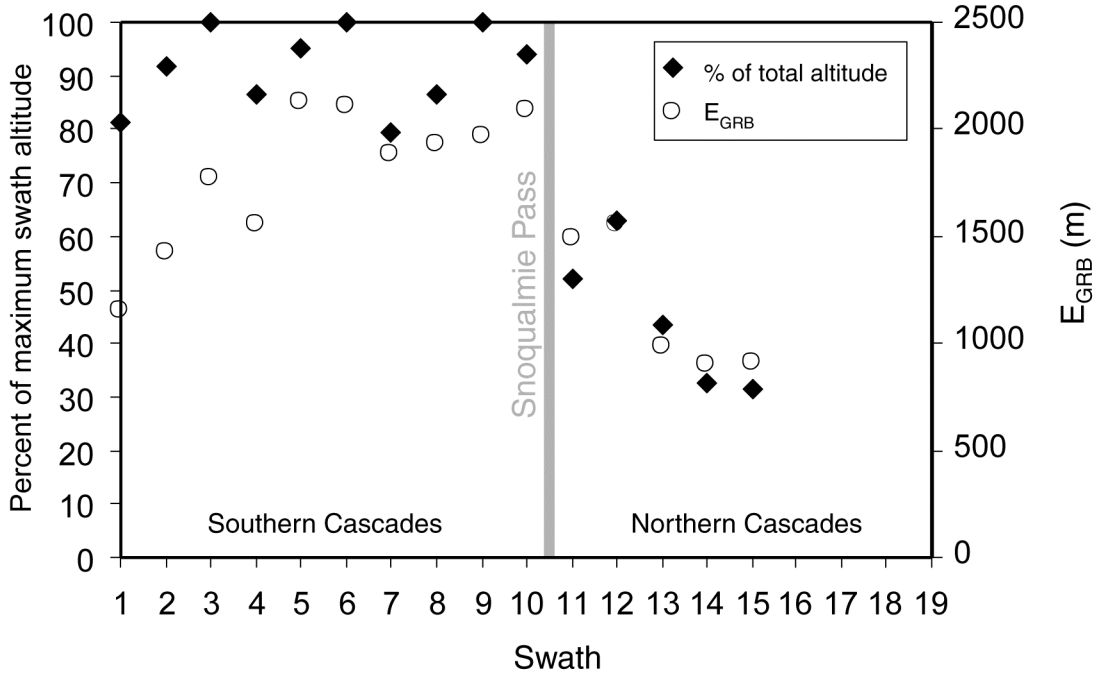

Figure 2.10: Open circles show the elevation of the highest exposure of GRB (E_{GRB}) in each swath, black diamonds show E_{GRB} as a percentage of the maximum elevation within each swath, excluding Quaternary volcanoes. Note there are no GRB exposures in swaths 16 to 19.

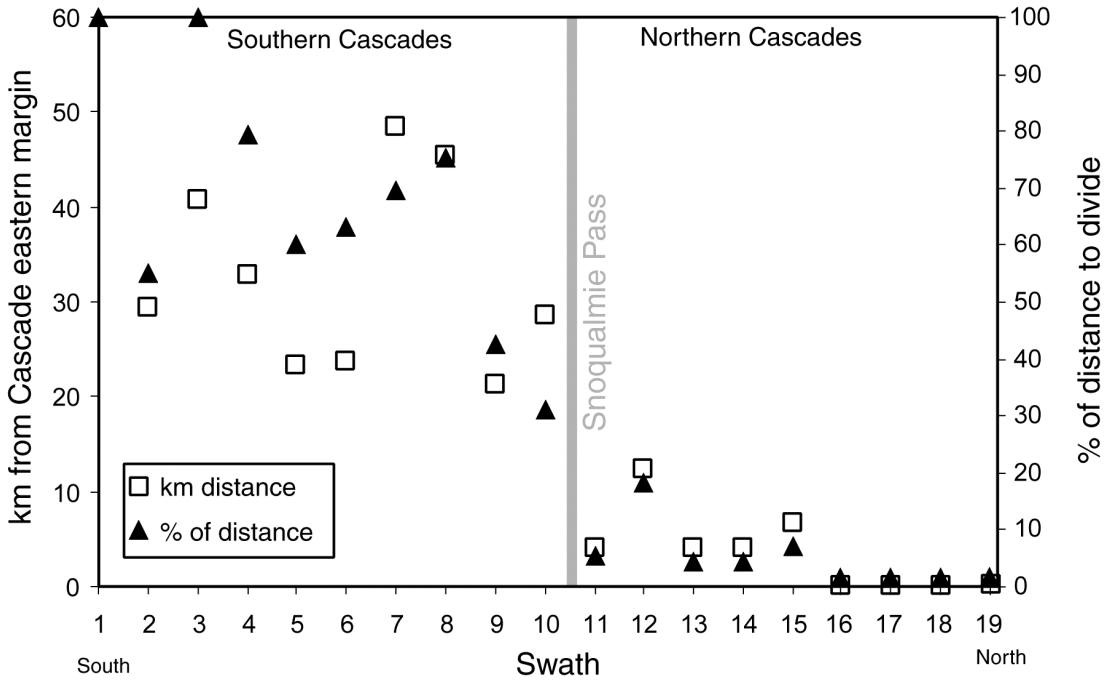

Figure 2.11: Absolute and relative position of western margin of GRB. Open squares show the distance between the western GRB limit and the eastern edge of the range. Black triangles indicate the location of the western GRB limit relative to the width of the range between the drainage divide and the eastern limit (100% means the GRB reaches the divide, 0% means no GRB is located within the Cascade physiographic province).

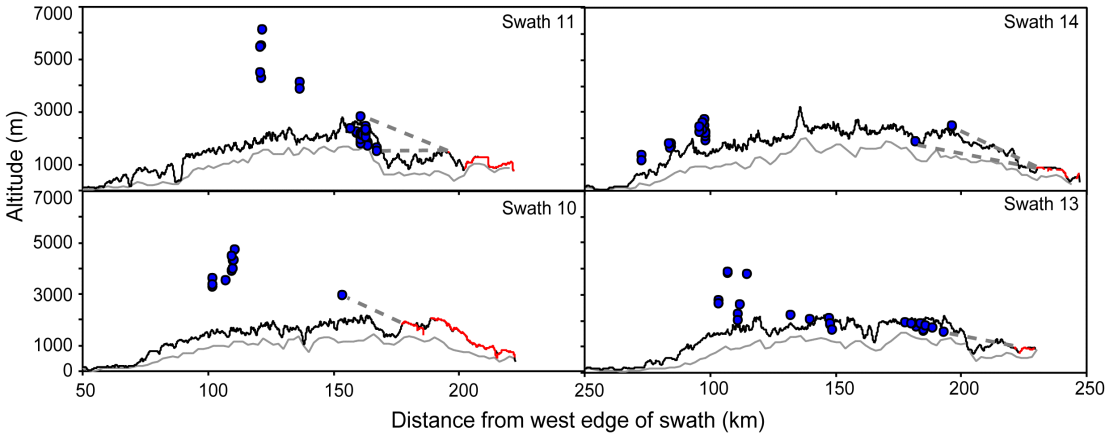

Figure 2.12: Generalized topographic profiles of swaths 10-14, showing maximum and mean altitudes. Red shows the top surfaces of exposed GRB. Blue circles show the estimated altitude of a hypothetical 15 Ma surface, calculated from AHe sample altitudes and exhumation rates (Reiners and others, 2002; 2003, P.W. Reiners, unpublished data). Gray dashed lines connecting the westernmost basalt limit to the easternmost AHe sample locations represent the simplest possible 15 Ma "paleosurface" reconstruction. Note that this reconstruction projects over existing topography in the southern swaths 10 and 11 (on left) but cross through topography in northern swaths 13 and 14 (on right). The projection is somewhat ambiguous in swath 12, and thus is not shown here.

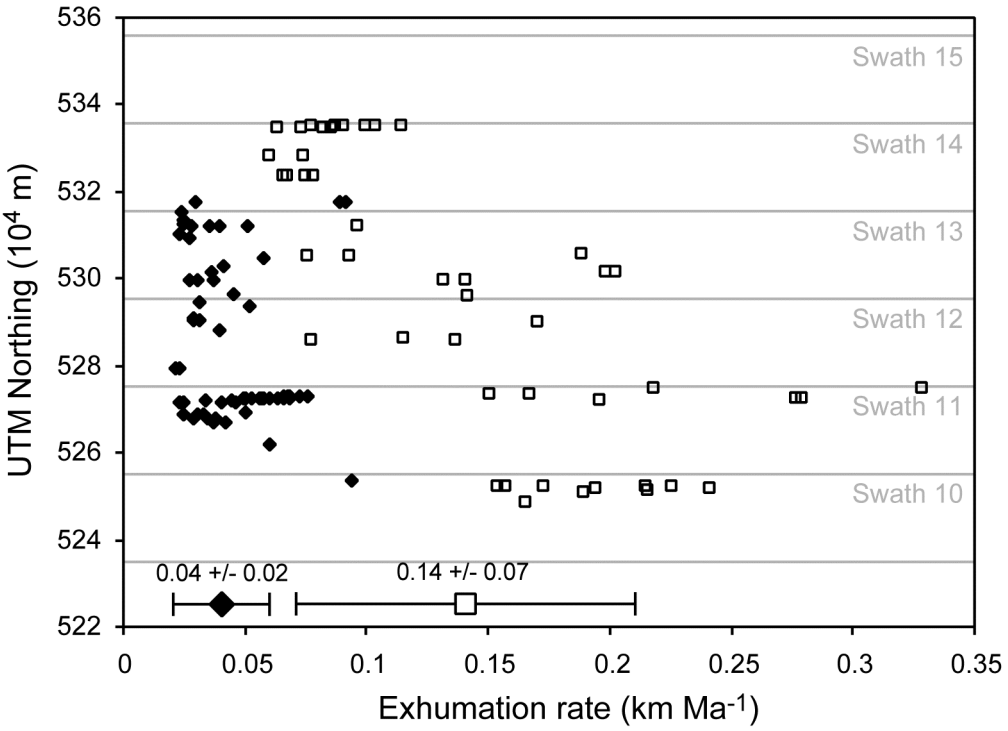

Figure 2.13: North-south trends in long-term average exhumation rate, determined from apatite U-Th/He thermochonometric ages from exposed plutons (Reiners and others, 2002; 2003; unpublished data). Diamonds are from samples located east of the drainage divide, squares are from samples located west of the divide. Swaths are shown in gray; note that the southernmost sample is located in Swath 10. There is no north-south linear trend in exhumation rate on the east side of the range, while exhumation rates decrease towards the north on the west side of the range. Large symbols with error bars at bottom indicate mean and standard deviation for each population of exhumation rate data.

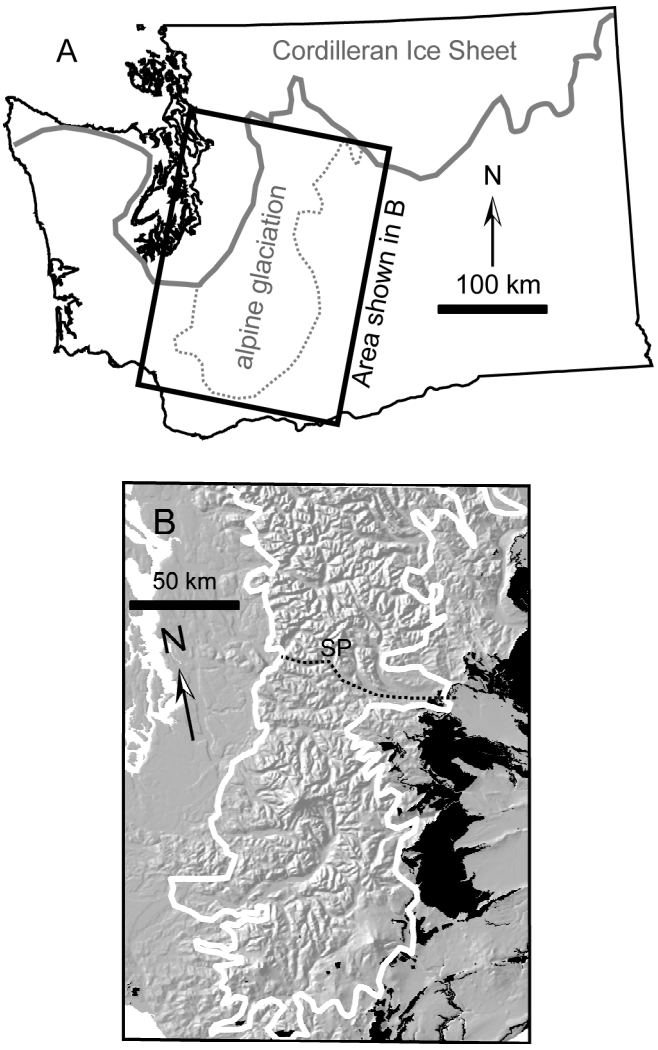

Figure 2.14: A. Approximate Quaternary maximum glacial limits in Washington. Solid gray line indicates the southern limit of the Cordilleran Ice Sheet (Booth and others, 2004); dotted gray line indicates the approximate limit of Cascade alpine glaciers (S.C. Porter, personal communication, 2005). B. Detailed view of Quaternary maximum glacial extent in the Cascade Range. The heavy white line shows the downstream limit of alpine glaciers, excluding nunataks that were exposed in the core of the range (S.C. Porter, personal communication, 2005). Solid black areas show exposures of Grande Ronde Basalt. Snoqualmie Pass (SP) is labeled, and the boundary between the northern and southern regions is marked with a dashed line. The basalt and glacial margins locally overlap in the south but do not in the north.

Figure 2.15: A. Major Eocene sedimentary units. Continental (fluvial) deposits including sandstones and conglomerates of the Chuckanut (CT), Swauk (S) and Chumstick (CK) Formations are shown in black, fine-grained marine deposits are shown in gray. B. Plutons resulting from Cascade arc magmatism, Eocene to Miocene age. C. Mid-Miocene continental sediments, including the Ellensburg Formation (E) and the Mashel Formation (M). D. Location of paleobotany and oxygen isotope samples from Washington used to infer the development of an orographic rainshadow during the Miocene. Samples for oxygen isotope analysis (Takeuchi and Larson, 2005) shown as gray squares. These samples range in age from <1 My to 15.6 My, and show a progressive lightening of $\delta^{18}O$ values through that time. Field locations of flora from the Ellensburg Formation from Smiley (1963) are shown as crosses. Locations of other well-known Miocene floras indicating a more humid ecosystem than today are shown as closed circles (Mustoe, 2001) and open circles (Leopold and Denton, 1987). Locations of Miocene forests from Beck (1945) are marked with stars; however, these sites only show a single snapshot of climate, not a temporal evolution like the other data sets. Finally, the Washington field site of Chaney (1938) is shown as an open triangle. Generalized contacts are derived from the digitized version of a 1:500,000-scale geologic map of Washington State (Hunting and others, 1961); geologic formation identifications are from the 60-minute, 1:100,000-scale geologic maps of Washington State (Tabor and Cady, 1978; Tabor and others, 1982; Frizzell and others, 1984; Walsh, 1986b; Korosec, 1987a; Korosec, 1987b; Logan, 1987; Phillips, 1987a; Phillips, 1987b; Phillips and Walsh, 1987; Schasse, 1987a; Schasse, 1987b; Tabor and others, 1987; Walsh, 1987a; Walsh, 1987b; Tabor and others, 1988; Whetten and others, 1988; Bunning, 1990; Gulick and Korosec, 1990a; Soffel and McGroder, 1990; Yount and Gower, 1991; Tabor and others, 1993; Schuster, 1994a; Schuster, 1994b; Schuster, 1994c; Tabor and others, 1994; Dragovich and Norman, 1995; Tabor and others, 2003).

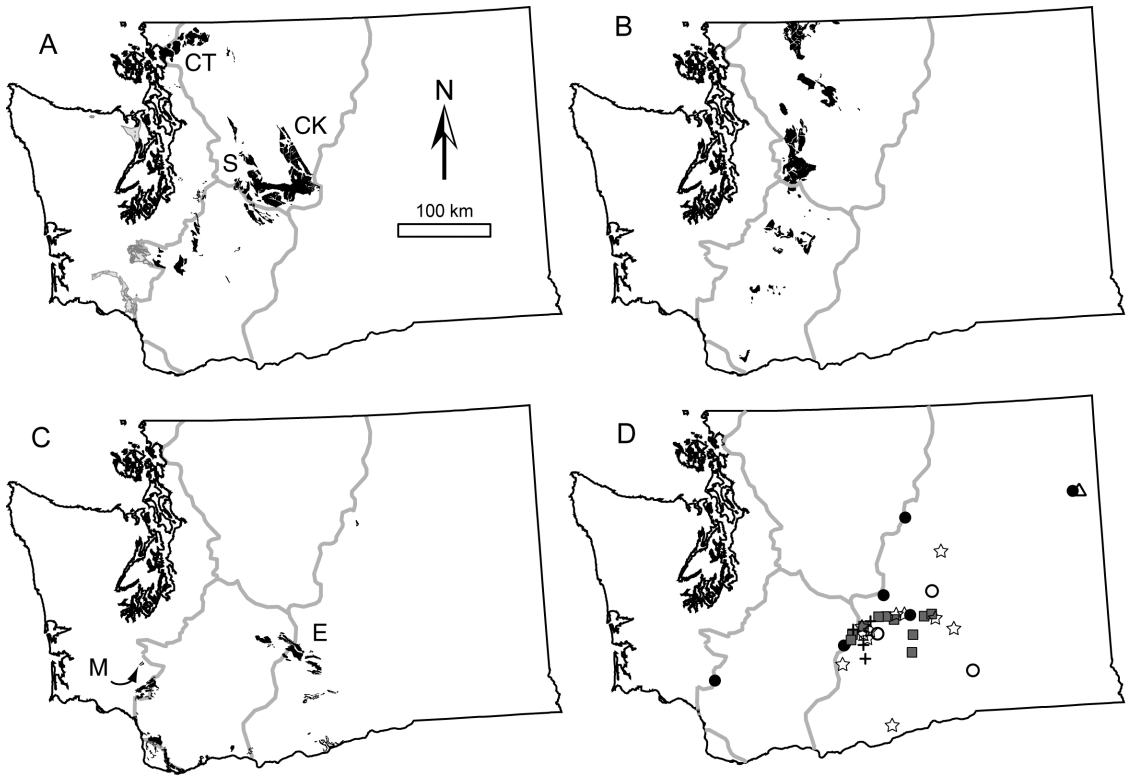
A
CT
CK
S
N
100 km
B
C
M
E
D

Notes to Chapter 2

Anderson, J.L., and Vogt, B.F, 1987, Intracanyon flows of the Columbia River Basalt group in the southwest part of the Columbia Plateau and adjacent Cascade Range, Oregon and Washington, in, Schuster, J.E., editor, Selected papers on the geology of Washington: Bulletin of the Washington Department of Natural Resources, Division of Geology and Earth Resources, v. 77, p. 249-267.

Bates, R.G., Beck, M.E., Jr., and Burmester, R.F., 1981, Tectonic rotations in the Cascade Range of southern Washington: Geology, v. 9, no. 4, p. 184-189.

Beck, G.F., 1945, Ancient forest tress of the sagebrush area in central Washington: Journal of Forestry, v. 43, no. 5, p. 334-338.

Beeson, M.H., and Tolan, T.L., 1989, The Columbia River Basalt Group in the Cascade Range—a middle Miocene reference datum for structural analysis, *in* Muffler, L.J.P., Weaver, C.S., Blackwell, D.D. editors, Proceedings of workshop XLIV—Geological, geophysical and tectonic setting of the Cascade Range: US Geological Survey Open File Report 89-178, p. 257-290.

Booth, D.B., Troost, K.G., Clague, J.J., and Waitt, R.B., 2004, The Cordilleran Ice Sheet, in Gillespie, A.R., Porter, S.C. and Atwater, B.F., editors, The Quaternary Period in the United States: Developments in Quaternary Science, v. 1, p. 17-43.

Brandon, M.T., Roden-Tice, M.K., and Garver, J.I., 1998, Late Cenozoic exhumation of the Cascadia accretionary wedge in the Olympic Mountains, Northwest Washington State: Geological Society of America Bulletin, v. 110, no. 8, p. 985-1009.

Bunning, B.B., 1990, Geologic map of the east half of the Twisp 1:100,000 quadrangle, Washington: Washington Division of Geology and Earth Resources Open File Report 90-9, 51 p., 1 plate.

Campbell, N.P., 1988, Structural geology along the northwestern Columbia River basalt margin, Washington: Washington Division of Geology and Earth Resources Open File Report 88-5, 108 p., 8 plates.

Chamberlain, C.P., and Poage, M.A., 2000, Reconstructing the paleotopography of mountain belts from the isotopic composition of authigenic minerals: Geology v. 28, no 2, p. 115-118.

Chaney, R.W., 1938. Paleoecological interpretations of Cenozoic plants in western North America: Botanical Review, v. 4, p. 371-396.

Chaney, R.W., 1959, Miocene floras of the Columbia Plateau—Part 1, Composition and interpretation: Carnegie Institution of Washington Publication 617, p. 1-34.

Cheney, E.S., 1997, What is the age and extent of the Cascade magmatic arc?: Washington Geology, v. 25, no. 2, p. 28-32.

Christiansen, R.L., Yeats, R.S., Graham, S.A., Niem, W.A., Niem, A.R., and Snavely, P.D. Jr., 1992, Post-Laramide geology of the U.S. Cordilleran region, *in* Burchfiel, B.C., Lipman, P.W., and Zoback, M.L., editors, The Cordilleran Orogen; conterminous U.S.: The Geology of North America v. G-3, Geological Society of America, p. 261-406.

Dragovich, J.D., Logan, R.L., Schasse, H.W., Walsh, T.J., Lingley, W.S., Norman, D.K., Gerstel, W.J., Lapen, T.J., Schuster, J.E., and Meyers, K.D., 2002, Geologic map of Washington; northwest quadrant: Washington Division of Geology and Earth Resources Geologic Map GM-50, 3 sheets, scale 1:250,000, with 72 p. text.

Dragovich, J.D., and Norman, D.K., 1995, Geologic map of the west half of the Twisp 1:100,000 quadrangle, Washington: Washington Division of Geology and Earth Resources Open File Report 95-3, 63 p., 1 pl.

England, P.C., and Molnar, P., 1990, Surface uplift, uplift of rocks, and exhumation of rocks: Geology, v. 18, no 12, p. 1173-1177.

England, P.C., and Wells, R.E., 1991, Neogene rotations and quasicontinuous deformation of the Pacific Northwest continental margin: Geology, v. 19, p. 978-981.

Evarts, R.C., and Swanson, D.A., 1994, Geologic transect across the Tertiary Cascade Range, southern Washington, *in* Swanson, D. A.; Haugerud, R. A., editors, Geologic field trips in the Pacific Northwest: University of Washington Department of Geological Sciences, v. 2, p. 2H 1 - 2H 31.

Farley, K.A., 2002, (U-Th)/He dating: Techniques, calibrations, and applications *in*: Noble Gases in Geochemistry and Cosmochemistry, Reviews in Mineralogy and Geochemistry, v. 47, p. 819-844.

Foster, R.J., 1960, Tertiary geology of a portion of the central Cascade Mountains, Washington: Bulletin of the Geological Society of America, v. 71, p. 99-126.

Frizzell, V.A., Jr., Tabor, R.W., Booth, D.B., Ort, K.M., and Waitt, R.B., 1984, Preliminary geologic map of the Snoqualmie Pass 1:100,000 quadrangle, Washington: U.S. Geological Survey Open-File Report 84-693, 43 p., 1 plate, scale1:100,000.

Gulick, C. W., and Korosec, M.A., 1990a, Geologic map of the Banks Lake 1:100,000 quadrangle, Washington: Washington Division of Geology and Earth Resources Open File Report 90-6, 20 p., 1 plate.

Gulick, C.W., and Korosec, M.A., 1990b, Geologic map of the Omak 1:100,000 quadrangle, Washington: Washington Division of Geology and Earth Resources Open File Report 90-12, 52 p., 1 plate.

Gresens, R.L., 1980, Deformation of the Wenatchee Formation and its bearing on the tectonic history of the Chiwaukum Graben, Washington, during Cenozoic time: Geological Society of America Bulletin, v. 91, no. 1, p. ?

Hagstrum, J.T., Swanson, D.A., and Evarts, R.C., 1999, Paleomagnetism of an east-west transect across the Cascade arc in southern Washington--Implications for regional tectonism: Journal of Geophysical Research, v. 104, no. B6, p. 12,853-12,863.

Hammond, P.E., 1998, Tertiary andesitic lava-flow complexes (stratovolcanoes) in the southern Cascade Range of Washington—observations on tectonic processes within the Cascade arc: Washington Geology, v. 26, no. 1, p. 20-30.

Hammond, P.E., Brunstad, K.A., Hooper, P.R., and Cole, S.F., 1992, Isolated occurrences of Columbia River basalt flows at Steamboat Mountain, southern Washington Cascade Range--Indication of yet greater westward extent of these flood-basalt flows: Oregon Academy of Sciences, Proceedings--Volume XXVIII: Oregon Academy of Science, p. 38.

Hammond, P.E., 1988, The Cascade paleosurface: Geological Society of America Abstracts with Programs, v. 20, no. 7, p. A284.

Haugerud, R.A., 2004, Cascadia—Physiography: USGS Miscellaneous Investigations Map I-2689.

Haugerud, R.A., van der Heyden, P., Tabor, R.W., Stacey, J.S., and Zartman, R.E., 1991, Late Cretaceous and early Tertiary plutonism and deformation in the Skagit Gneiss Complex, North Cascade Range, Washington and British Columbia: Geological Society of America Bulletin, v. 103, p. 1297-1307.

Hunting, M.T., Bennett, W.A., Livingston, V.E., Jr., and Moen, W.S., 1961, Geologic Map of Washington: Washington Department of Conservation, Division of Mines and Geology, 1 plate, scale 1:500,000.

Johnson, S.Y., 1984, Stratigraphy, age, and paleogeography of the Eocene Chuckanut Formation, Northwest Washington: Canadian Journal of Earth Sciences, v. 21, no. 1, p. 92-106.

Korosec, M.A., 1987a, Geologic map of the Hood River quadrangle, Washington and Oregon: Washington Division of Geology and Earth Resources Open File Report 87-6, 40 p., 1 plate, scale 1:100,000.

Korosec, M.A., 1987b, Geologic map of the Mount Adams quadrangle, Washington: Washington Division of Geology and Earth Resources Open File Report 87-5, 39 p., 1 plate, scale 1:100,000.

Leopold, E.B., and Denton, M.F., 1987, Comparative age of grassland and steppe east and west of the northern Rocky Mountains: Annals of the Missouri Botanical Garden, v. 74, p. 841-867.

Logan, R.L., 1987, Geologic map of the Chehalis River and Westport quadrangles, Washington: Washington Division of Geology and Earth Resources Open File Report 87-8, 16 p., 1 plate, scale 1:100,000.

Mackin, J.H., and Cary, A.S., 1965, Origin of Cascade landscapes: Washington Division of Mines and Geology Information Circular 41, 35 p.

Mathews, W.H., 1981, Early Cenozoic resetting of potassium-argon dates and geothermal history of North Okanagan area: British Columbia. Canadian Journal of Earth Sciences, v. 18, no. 8, p. 1310-1319.

Mazzotti, S., Dragert, H., Henton, J., Schmidt, M., Hyndman, R., James, T., Lu, Yuan and Craymer, M., 2003, Current tectonics of northern Cascadia from a decade of GPS measurements: Journal of Geophysical Research, v. 108, no. B12, doi: 10.1029/2003JB002653.

McDaniel, P.A., Othberg, K.L., and Breckenridge, R.M., 1998, Paleogeomorphic evolution of the Columbia River basalt embayments, western margin of the northern Rocky Mountains—Part II, Miocene paleosols: Geological Society of America Abstracts with Programs, v. 30, no. 6, p. 15.

McGroder, M.F., 1991, Reconciliation of two-sided thrusting, burial metamorphism, and diachronous uplift in the Cascades of Washington and British Columbia: Geological Society of America Bulletin, v. 103, no. 2, p. 189-209.

Miller, R.B., 1989, The Mesozoic Rimrock Lake inlier, southern Washington Cascades: Implications for the basement to the Columbia Embayment: Geological Society of America Bulletin, v. 101, p. 1289-1305.

Mitchell, S.G., and Montgomery, D.R., in press, Influence of a glacial buzzsaw on the height and morphology of the Washington Cascade Range, USA: Quaternary Research.

Mullineaux, D.R., Gard, L.M., and Jr., Crandell, D.R., 1959, Continental sediments of Miocene age in Puget Sound lowland, Washington: American Association of Petroleum Geologists Bulletin, v. 43, no. 3, pt. 1, p. 688-696.

Mustoe, G.E., 2001, Washington's fossil forests: Washington Geology, v. 29, p. 10-20.

Phillips, W.M., and Walsh, T. J., 1987, Geologic map of the northwest part of the Goldendale quadrangle, Washington: Washington Division of Geology and Earth Resources Open File Report 87-13, 7 p., 1 pl., scale 1:100,000.

Phillips, W.M., 1987a, Geologic map of the Mount St. Helens quadrangle, Washington and Oregon: Washington Division of Geology and Earth Resources Open File Report 87-4, 59 p., 1 plate, scale 1:100,000.

Phillips, W.M., 1987b, Geologic map of the Vancouver quadrangle, Washington [and Oregon]: Washington Division of Geology and Earth Resources Open File Report 87-10, 27 p., 1 plate, scale 1:100,000.

Porter, S.C., 1976a, Geomorphic evidence of post-Miocene deformation of the eastern north Cascade Range: Geological Society of America Abstracts with Programs, v. 8, no. 3, p. 402-403.

Porter, S. C., 1976b. Pleistocene glaciation on the southern part of the North Cascade Range, Washington. Geological Society of America Bulletin 87, 61-75.

Power, S.G., Field, C.W., Armstrong, R.L., and Harakal, J.E., 1981, K-Ar ages of plutonism and mineralization, western Cascades, Oregon and southern Washington: Isochron/West, no. 31, p. 27-29.

Reidel, S.P., Tolan, T.L., Hooper, P.R., Beeson, M.H., Fecht, K.R., Bentley, R.D., and Anderson, J.L., 1989, The Grande Ronde Basalt, Columbia River Basalt Group; Stratigraphic descriptions and correlations in Washington, Oregon, and Idaho, *in* Reidel, S. P.; Hooper, P. R., editors, Volcanism and tectonism in the Columbia River flood-basalt province: Geological Society of America Special Paper 239, p. 21-53.

Reiners, P.W., Ehlers, T.A., Garver, J.I., Mitchell, S.G., Montgomery, D.R., Vance, J.A., and Nicolescu, S., 2002, Late Miocene exhumation and uplift of the Washington Cascade Range: Geology, v. 30, no. 9, p. 767–770.

Reiners, P.W., Ehlers, T.A., Mitchell, S.G., and Montgomery, D.R., 2003, Coupled spatial variations in precipitation and long-term erosion rates across the Washington Cascades: Nature, v. 426, 645-647.

Russell, I.C., 1900, A preliminary paper on the geology of the Cascade mountains in northern Washington: United States Geological Survey Annual Report, 20th, Part 2, p. 83-210.

Saleeby, J.B., Busby, S.C., Oldow, J.S., Dunne, G.C., Wright, J.E., Cowan, D.S., Walker, N.W., and Allmendinger, R.W., 1992, Early Mesozoic tectonic evolution of the Western U.S. Cordillera, *in* Burchfiel, B.C., Lipman, P.W., and Zoback, M.L., editors, The Cordilleran Orogen; conterminous U.S.: The Geology of North America v. G-3, Geological Society of America, p. 107-168.

Saltus, R.W., 1993, Upper-crustal structure beneath the Columbia River Basalt Group, Washington--Gravity interpretation controlled by borehole and seismic studies: Geological Society of America Bulletin, v. 105, no. 9, p. 1247-1259.

Schasse, H.W., 1987a, Geologic map of the Mount Rainier quadrangle, Washington: Washington Division of Geology and Earth Resources Open File Report 87-16, 43 p., 1 plate, scale 1:100,000.

Schasse, H.W., 1987b, Geologic map of the Centralia quadrangle, Washington: Washington Division of Geology and Earth Resources Open File Report 87-11, 28 p., 1 plate, scale 1:100,000.

Schmidt, K.M. and Montgomery, D.R., 1995, Limits to relief: Science, v. 270, no. 5236, p. 617-620.

Schmincke, H.U., ms, 1964, Petrology, paleocurrents, and stratigraphy of the Ellensburg Formation and interbedded Yakima Basalt flows, south-central Washington: Ph.D. thesis, Johns Hopkins University, Baltimore, 426 p.

Schuster, J.E., 1994a, Geologic maps of the east half of the Washington portion of the Goldendale 1:100,000 quadrangle and the Washington portion of the Hermiston 1:100,000 quadrangle: Washington Division of Geology and Earth Resources Open File Report 94-9, 17 p., 1 pl.

Schuster, J.E., 1994b, Geologic map of the east half of the Toppenish 1:100,000 quadrangle, Washington: Washington Division of Geology and Earth Resources Open File Report 94-10, 15 p., 1 pl.

Schuster, J.E., 1994c, Geologic map of the east half of the Yakima 1:100,000 quadrangle, Washington: Washington Division of Geology and Earth Resources Open File Report 94-12, 19 p., 1 pl.

Schuster, J.E., 1992, Geologic map of Washington: Washington State Department of Natural Resources, Division of Geology and Earth Resources, scale, 1:2,250,000. 1 p. with 1 p. text.

Searle, M.P., and Treloar, P.J., 1993, Himalayan Tectonics—an introduction, *in* Searle, M.P. and Treloar, P.J., editors, Himalayan Tectonics: Geological Society of America Special Publication, no. 74, p. 1-7.

Smiley, C.J., 1963, The Ellensburg flora of Washington: University of California Publications in Geological Sciences, v. 35, no. 3, p. 159-276.

Smith, G.A., Bjornstad, B.N., and Fecht, K.R., 1989, Neogene terrestrial sedimentation on and adjacent to the Columbia Plateau; Washington, Oregon and Idaho, *in* Reidel, S. P. and Hooper, P. R., editors., Volcanism and tectonism in the Columbia River flood-basalt province: Geological Society of America, Special Paper 239, p. 187-198.

Smith, G.A., 1988, Neogene synvolcanic and syntectonic sedimentation in central Washington: Geological Society of America Bulletin, v. 100, no. 9, p. 1479-1492.

Smith, G.O., 1903, Geology and physiography of central Washington: U.S. Geological Survey Professional Paper 19, p. 9-39.

Smith, J.G., 1993, Geologic map of upper Eocene to Holocene volcanic and related rocks in the Cascade Range, Washington: U.S. Geological Survey Miscellaneous Investigation, Map I-2005, scale 1:500,000.

Stanley, W.D., Johnson, S.Y., Qamar, A.I., Weaver, C.S., and Williams, J. M., 1996, Tectonics and seismicity of the southern Washington Cascade Range: Seismological Society of America Bulletin, v. 86, no. 1A, p. 1-18.

Stoffel, K.L. and McGroder, M.F., 1990, Geologic map of the Robinson Mtn. 1:100,000 quadrangle, Washington: Washington Division of Geology and Earth Resources Open File Report 90-5, 39 p., 1 plate.

Svarc, J.L., Savage, J.C., Prescott, W.H., and Murray, M.H., 2002, Strain accumulation and rotation in western Oregon and southwestern Washington: Journal of Geophysical Research, v. 107, no. B5, 2087, 10.1029/2001JB000625.

Swanson, D.A., 1997, Uplift of the southern Washington Cascades in the past 17 million years: Geological Society of America Abstracts with Programs, v. 29, no. 5, p. 68.

Summers, K.V., ms, 1976, Palagonite and pillow basalts of the Columbia River group: MSc. thesis, Washington State University, Pullman, 99 p.

Tabor, R.W., Haugerud, R.A., Hildreth, W., and Brown, E.H., 2003, Geologic map of the Mount Baker 30- by 60-minute quadrangle, Washington: U.S. Geological

Survey Geologic Investigations Series I-2660, 2 sheets, scale 1:100,000, with 73 p. text.

Tabor, R.W., Haugerud, R.A., Booth, D.B. and Brown, E.H., 1994, Preliminary geologic map of the Mount Baker 30- by 60-minute quadrangle, Washington: U.S. Geological Survey Open-File Report 94-403, 55p., 2 pl.

Tabor, R.W., Frizzell, V.A., Jr., Booth, D.B., Waitt, R.B., Whetten J.T., and Zartman, R.E., 1993, Geologic map of the Skykomish River 30- by 60-minute quadrangle, Washington: U.S. Geological Survey Miscellaneous Investigations Series Map I-1963, 1 sheet, scale 1:100,000, with 42 p. text.

Tabor, R.W., Booth, D.B., Vance, J.A., Ford, A.B., and Ort, M.H., 1988, Preliminary geologic map of the Sauk River 30 by 60 minute quadrangle, Washington: U.S. Geological Survey Open-File Report 88-692, 50p., 2 pl.

Tabor, R.W., Frizzell, V.A., Jr., Whetten, J.T., Waitt, R.B., Swanson, D.A., Byerly, G.R., Booth, D.B., Hetherington, M.J., and Zartman, R.E., 1987, Geologic map of the Chelan 30-minute by 60-minute quadrangle, Washington: U.S. Geological Survey Miscellaneous Investigations Series Map I-1661, 1 sheet, scale 1:100,000, with 29 p. text.

Tabor, R.W., Waitt, R.B., Frizzell, V.A., Jr., Swanson, D.A., Byerly, G.R., and Bentley, R.D., 1982, Geologic map of the Wenatchee 1:100,000 quadrangle, central Washington: U.S. Geological Survey Miscellaneous Investigations Series Map I-1311, 26 p.,1 plate, scale 1:100,000.

Tabor, R. W., and Cady, W. M., 1978, Geologic map of the Olympic Peninsula, Washington: U.S. Geological Survey Miscellaneous Investigations Series Map I-994, 2 sheets, scale 1:125,000.

Takeuchi, A., and Larson, P.B., 2005, Oxygen isotope evidence for the last Cenozoic development of an orographic rain shadow in eastern Washington, USA: Geology, v. 33, no. 4, p. 313-316.

Tolan, T.L., Reidel, S.P., Beeson, M.H., Anderson, J.L., Fecht, K.R., and Swanson, D.A., 1989, Revisions to the estimates of the areal extent and volume of the Columbia River Basalt Group, *in* Reidel, S. P.; Hooper, P. R., editors, Volcanism and tectonism in the Columbia River flood-basalt province: Geological Society of America Special Paper 239, p. 1-20.

Valley, P.M., Whitney, D.L., Paterson, S.R., Miller, R.B., and Alsleben, H., 2003, Metamorphism of the deepest exposed arc rocks in the Cretaceous to Paleogene Cascades belt, Washington: evidence for large-scale vertical motion in a continental arc: Journal of Metamorphic Geology, v. 21, p. 203-220.

Vance, J.A., 2002, Age and provenance of Eocene nonmarine sandstones in the central and Northwest Washington Cascades: fission track evidence from detrital zircons: Geological Society of America Abstracts with Programs, v. 34, no. 5.

Walsh, T.J., 1987a, Geologic map of the south half of the Tacoma quadrangle, Washington: Washington Division of Geology and Earth Resources Open File Report 87-3, 10 p., 1 plate, scale 1:100,000.

Walsh, T.J., 1987b, Geologic map of the Astoria and Ilwaco quadrangles, Washington and Oregon: Washington Division of Geology and Earth Resources Open File Report 87-2, 28 p., 1 plate, scale 1:100,000.

Walsh, T.J., Korosec, M.A., Phillips, W.M., Logan, R.L., and Schasse, H.W., 1987, Geologic map of Washington--Southwest quadrant: Washington Division of Geology and Earth Resources Geologic Map GM-34, 2 sheets, scale 1:250,000, with 28 p. text.

Walsh, T.J., 1986a, Geologic map of the west half of the Toppenish quadrangle, Washington: Washington Division of Geology and Earth Resources Open File Report 86-3, 1 sheet, scale 1:100,000, with 7 p. text.

Walsh, T J., 1986b, Geologic map of the west half of the Yakima quadrangle, Washington: Washington Division of Geology and Earth Resources Open File Report 86-4, 1 sheet, scale 1:100,000, with 9 p. text.

Walters, K.L., and Kimmel, G.E., 1968, Ground-water occurrence and stratigraphy of unconsolidated deposits, central Pierce County, Washington: Washington Department of Water Resources Water-Supply Bulletin 22, 428 p.

Weissenborn, A.E., 1969, Geologic Map of Washington: USGS Miscellaneous Geologic Investigations Map I-583.

Wells, R.E., Weaver, C.S., and Blakely, R.J., 1998, Fore-arc migration in Cascadia and its neotectonic significance: Geology, v. 26, no. 8, p. 759-762.

Wells, R.E., 1990, Paleomagnetic rotations and the Cenozoic tectonics of the Cascade arc, Washington, Oregon, and California: Journal of Geophysical Research B, v. 95, no. 12, p. 19,409-19,417.

Whetten, J. T., Carroll, P.I., Gower, H.D., Brown, E.H., and Pessl, F., Jr., 1988, Bedrock geologic map of the Port Townsend 30- by 60- minute quadrangle, Puget Sound region, Washington: U.S. Geological Survey Miscellaneous Investigations Series Map I-1198-G, 1 sheet, scale 1:100,000.

Willis, B., 1903, Physiography and deformation of the Wenatchee-Chelan district, Cascade Range, *in* Contributions to the geology of Washington: U.S. Geological Survey Professional Paper 19, p. 41-97.

Yount, J.C., and Gower, H.D., 1991, Bedrock geologic map of the Seattle 30' by 60' quadrangle, Washington: U.S. Geological Survey Open-File Report 91-147, 37 p., 4 pl.

CHAPTER 3

Influence of a Glacial Buzzsaw on the Height and Morphology of the Cascade Range in Central Washington State

Summary

Analysis of climatic and topographic evidence from the Cascade Range in Washington State indicates that glacial erosion limits the height and controls the morphology of this range. Glacial erosion linked to long-term spatial gradients in the glacial equilibrium line altitude (ELA) created a tilted, planar zone of 373 cirques across the central part of the range; peaks and ridges now rise ≤ 600 m above this zone. Hypsometric analysis of the region shows that the proportion of land area above the cirques drops sharply, and mean slopes > 30º indicate that the areas above the cirques may be at or near threshold steepness. The mean plus 1σ relief of individual cirque basins (570 m) corresponds to the ~600-m envelope above which peaks rarely rise. The summit altitudes are set by a combination of higher rates of glacial and paraglacial erosion above the ELA and enhanced hillslope processes due to the creation of steep topography. On the high-precipitation western flank of the Cascades, the dominance of glacial and hillslope erosion at altitudes at and above the ELA may explain the lack of a correspondence between stream-power erosion models and measured exhumation rates from apatite (U-Th/He) thermochronometry.

Introduction

The complex relationships among climate, tectonics, erosion, and topography in the world's mountain ranges encompass issues of substantial ongoing interest in geomorphology (Burbank et al., 1996; Montgomery et al., 2001; Whipple et al., 1999). Relatively new topographic analysis techniques using digital elevation models (Brocklehurst and Whipple, 2004; Montgomery et al., 2001), the recent application of low-temperature thermochronometry methods such as apatite (U-Th)/He dating (e.g., House et al., 1997; Reiners et al., 2002), and the development of new landscape

evolution models (MacGregor et al., 2000; Tomkin and Braun, 2002) allow the investigation of these relationships in glaciated terrain. Here I explore linkages between climate and topography as set by the physical effects of long-term glacial erosion on the height and morphology of the Cascade Range in central Washington.

The correspondence of glacier snowline altitudes to the maximum elevation of mountain ranges has been recognized for over a century (Mills, 1892), although whether such a relationship is governed by topographic controls on snowline altitude or erosional controls on topography has remained unsettled. Several recent studies have shown that glacial erosion can dominate the topographic form of mountain ranges that rise high enough to intersect the local glacier equilibrium-line altitude (ELA). Brozovic et al. (1997) showed that mean altitude, hypsometry, and slope distributions in the Himalaya correlate with the snowline, independent of large gradients in the modern uplift rate deduced from thermochronometry. Whipple et al. (1999) subsequently suggested that glaciers reduce mountain range relief by focusing glacial erosion at and above the ELA, decreasing fluvial erosion downstream from glaciers in sediment-choked valleys, and enhancing periglacial erosion on high peaks. Montgomery et al. (2001) showed a correlation between the ELA and peak altitudes in the Andes. Brocklehurst and Whipple (2002) suggested that in the eastern Sierra Nevada, glaciers concentrate overall mass removal to altitudes above the regional ELA, thus reducing overall relief. Spotila et al. (2004) used apatite (U-Th)/He thermochronometry (AHe dating) to show that denudation patterns in the Chugach-St. Elias Range of Alaska correlate with the distribution of glaciers and that erosion rates are sufficiently high to remove rock as it is uplifted due to tectonic convergence. These studies have produced an intriguing hypothesis regarding a "glacial buzzsaw" effect: that glacial erosion can rapidly denude topography raised above the ELA, regardless of rock uplift rate or lithology, and thereby limit how high mountains may rise.

Despite evidence for such an effect, key questions remain. Can one define specific topographic characteristics of a glacial buzzsaw, or identify the processes responsible for the glacial reduction of relief? Are such processes common to all

glaciated mountain ranges? Glacial erosion has been shown to sculpt landscapes into distinctive forms, and is thought to be relatively rapid (e.g., James, 2003; Hallet et. al., 1996). For example, repeated alpine glaciation increased the size and relief of valleys since the start of the Pleistocene in both the Olympic Mountains of Washington State (Montgomery, 2002) and in central Idaho (Amerson, 2005). Paraglacial processes, defined by Ballantyne (2002) as the "nonglacial earth-surface processes... directly conditioned by glaciation and deglaciation," may also enhance erosion rates through the creation of unstable or metastable landscapes upon deglaciation. I propose that in the Cascades, alpine glaciation scours out threshold hillslopes selectively at and above a zone of cirques formed at or close to the Quaternary average ELA. This enhanced erosion effectively creates a limiting envelope of peak and ridge heights tied to the ELA rather than modern fluvial processes or spatial gradients in long-term exhumation. I test this hypothesis using morphometric and thermochronologic techniques to investigate the relationship between topography, climate, geology, erosion rates, and the altitude of modern glaciers and glacial landforms.

Study Area and Previous Work

The portion of the Cascade Range in central Washington State is an ideal setting in which to investigate the relationship between glacial activity and topography (Figure 3.1). First, the topography and geology have been mapped in detail. Spatial data for this region include topography from 10-m-grid-size digital elevation models (DEMs) constructed from USGS quadrangles (Figure 3.2A), and digital geologic maps at 1:100,000 scale (Figure 3.2B). Second, the N-S-trending range crest is approximately perpendicular to a strong, west-east precipitation gradient caused by the orographic disruption of the eastern trajectory of weather systems originating in the Pacific Ocean. Precipitation data obtained from the Spatial Climate Analysis Service, Oregon State University (http://www.ocs.orst.edu/prism) show that the modern average annual precipitation ranges from > 4 m yr^{-1} in the central part of the study area to < 1 m yr^{-1} at the far eastern edge of the range (Figure 3.2C). This precipitation gradient creates

distinct spatial gradients in both fluvial erosion potential and the ELA (Porter, 1964; Roe et al., 2002). Third, previous studies in the Cascades provide us with ~90 low-temperature thermochronometry ages with which to investigate the relationship between long-term exhumation and topography (Reiners et al., 2002, 2003).

The Cascades were extensively glaciated in Washington during the Pleistocene. The glacial geology and glacial limits of major Cascade valleys have been mapped, and the trends in modern and Pleistocene ELAs are known for much of the Cascades (e.g., Porter, 1964, 1976a, 1989). I restricted the investigation to an area south of where the Cordilleran Ice Sheet covered high topography, an area of mountainous terrain sculpted predominantly by alpine and valley glaciers (Long, 1951; Mackin, 1941; Page, 1939; Waitt, 1975; Waitt and Thorson, 1983; Booth et al., 2004). A small part of the Puget Lowland, an area once covered by the Puget Lobe of the Cordilleran Ice Sheet, is included in the far western part of the study area; however, my analyses focus on the higher topography to the east.

This study builds upon previous physiographic investigations in the Cascade Range, including the early studies of Russell (1900), Willis (1903) and Smith (1903). Russell and Willis both noted that non-volcanic peaks and ridges in the Cascades rise to about the same altitude across the range, suggesting that the peaks were remnants of an uplifted and incised erosion surface. The remains of some relatively low-relief, high-altitude, tilted surfaces suggestive of an uplifted low-relief landscape are preserved on the eastern flank of the Cascades (Porter, 1976b). Smith (1903) acknowledged the uplifted peneplain theory, but argued that on the west side of the range, higher rates of precipitation had so dissected the terrain that the peaks today stand an unknown distance lower than the original surface, and that slow, spatially complex uplift probably means that a table-like plateau never existed. Alternatively, Daly (1905) suggested that concordance of the peaks was a function of treeline because erosion rates should be relatively high in the exposed areas above treeline due to the lack of protective effects of trees and their roots. The treeline hypothesis was later embraced by Thompson (1962), who suggested that increased rates of mass wasting above treeline are evident

over much of the high alpine regions of the western United States, including the Cascade Range in Washington.

More recently, the relationship between large-scale trends in altitude and the extent of past and present glaciations has been the subject of investigations in the Cascades. ELAs of modern glaciers are significantly higher on the eastern flank of the Cascades than on the western flank (Porter, 1977, 1989). Porter (1977) examined cross-range trends in glacier altitude, by investigating trends in a "glaciation threshold," defined as the average altitude of the lowest glacier-bearing peak and the highest nonglaciated peak within a USGS 7.5-minute topographic quadrangle. This method avoids the problem of small-scale variability in individual mean glacier altitudes resulting from differences in slope and basin topography. However, this approach dictates that the glaciation threshold is inherently a function of nearby peak altitudes. This glaciation threshold increases in altitude to the east at a rate of about 12 m/km due to a strong W-E gradient in accumulation season precipitation (Porter, 1977). When considered as a group, the individual ELAs of existing glaciers and those of the last glacial maximum have also been found to rise eastward at about the same rate. In addition, a zone of cirques lies parallel to and between modern and last glacial maximum ELAs (Porter, 1989). Porter (1989) hypothesized that this zone of cirques defines the altitude range where active, eroding glaciers spent the most time during the Quaternary, and thus represents a Quaternary average position of the ELA.

In addition, a considerable amount of low-temperature thermochronometric data has been collected for the Cascades (Reiners et al., 2002, 2003). Exhumation data from the study area indicate that there have been strong gradients in rock uplift across the range during the Cenozoic. These data indicate a pulse of rapid rock uplift and exhumation in the Cascades occurred during the late Miocene, and that precipitation is a dominant control on the spatial pattern of exhumation rates (Reiners et al., 2002, 2003).

Methods

I applied a combination of spatial and topographic analyses to investigate the relationships between the extent of glaciation, geology, and the morphometry of my study area. I used GIS to: 1) characterized the "surface" created by the maximum topography of peaks and ridges, 2) applied three different erosion models to the topography to compare with measured exhumation rates, 3) created digital maps of modern glaciers and cirques to determine spatial trends in the ELA, 4) analyzed the hypsometry and slope distributions of the region, and 5) investigated the altitude, relief, slope, and lithology of cirque basins. I also employed the data of Reiners et al. (2002, 2003), along with topographic analysis and erosion models to investigate the influence of glacial erosion on the central Washington Cascades.

Maximum Topography and Hypsometry

I used the DEM to characterize the "peak concordance" or surface formed by the peaks and ridges in the study area. I generalized cross-range trends in altitude with W-E oriented minimum, maximum, and mean altitude profiles constructed at 10-m intervals across the analysis window. Because of N-S variations in altitude, I subdivided the study area into three 160-km-long, 40-km-wide, west-to-east profiles (16,000 by 4,000 cells).

To test the suggestion that glaciated regions have area-altitude relationships that correlate with the extent of glaciation or snowline altitude (e.g., Brocklehurst and Whipple, 2004; Brozovic et al., 1997), I generated hypsometric curves for the study area. These hypsometric curves indicate the amount of land surface area within defined altitude intervals. Because the topography of the study region has such a strong W-E trend, for the hypsometric analysis I divided the DEM into eight N-S-oriented, 20-km-wide swaths that range from west to east across the region. Within each swath, I then measured the area within 100-m altitude bins.

Exhumation Rates and Erosion Indices

Because I am interested in the relative effects of glacial erosion on the Cascades, I also considered the potential influence of fluvial and hillslope erosion processes. If long-term fluvial erosion and rock uplift have been the primary controls on the morphology of the Cascades, one might expect to see a relationship between fluvial erosion models, such as stream power or unit stream power and long-term exhumation, with high exhumation rates near channels of high discharge and slope. Similarly, if hillslope erosion drives the topography of the range, high measured exhumation rates should be found in the regions of steep slopes and high precipitation. To test these potential relationships, I generate a fluvial erosion index based on stream power, and create a hillslope erosion index for the region based on slope and precipitation to compare with exhumation patterns.

I calculate stream power using the standard equation from Bagnold (1960), quantifying the energy expenditure per unit channel length:

$$\Omega = \rho g Q S \qquad (1)$$

Where Ω is stream power, ρ is the density of water (1000 g m^{-3}), g is acceleration due to gravity (9.81 m s^{-2}), and slope (S) is a unitless parameter defining the steepest descent between each cell and any of its neighbors. Instead of making the conventional substitution of drainage area for discharge (Q), I calculate discharge (m^3 s^{-1}) for each cell by calculating a precipitation-weighted flow accumulation using annual precipitation data from 1960-1990, obtained from the Spatial Climate Analysis Service at Oregon State University (http://www.ocs.orsu.edu/prism) and a flow network generated using GIS. This discharge calculation assumes all precipitation falling on a region becomes runoff, ignoring factors such as infiltration, evaporation, and transpiration. Hence, as discussed by Finlayson and Montgomery (2003), discharges estimated by these methods need to be calibrated to represent discharges of a particular recurrence interval or frequency. Because erosion rate is proportional to bedrock erodibility, I modeled stream power to simply indicate spatial differences in erosion potential, rather than as a measure of erosion rate (Finlayson and Montgomery, 2003).

Hillslope erosion potential is calculated simply as the product of mean annual precipitation and slope. All else being equal, regions with steep slopes and high rainfall should prove more vulnerable to most hillslope processes, including discrete events such as deep-seated landslides, debris flows, as well as less-catastrophic processes such as rainsplash and creep. The potential for erosion rate to increase non-linearly on steep hillslopes (e.g., Martin and Church, 1997; Martin, 2000; Montgomery and Brandon, 2002; Roering et al., 1999) would tend to reduce any such correlation for threshold slopes.

I examine the relationship between the fluvial and hillslope erosion models with measured long-term exhumation rates. Hypothesizing that if either fluvial or hillslope erosion drives topographic development in the Cascades, and assuming a relatively low variability in bedrock erodibility across the range, I should see high exhumation in regions of high erosion potential. To test this idea, I identify the maximum fluvial and average hillslope erosion potential within a 5-km radius from each sample site for (U-Th)/He exhumation rates (Reiners et al., 2003) and plot these indices against the measured exhumation rates. The 5-km radius was chosen to approximate the average valley width; this length radius assures capturing a channel in the same basin as the sample location for the maximum fluvial erosion index measurement, and integrates a large enough portion of the landscape to avoid local effects for the hillslope erosion index. To understand the dominant geomorphic influences on exhumation, I subdivide the sample localities based on several additional parameters, including location relative to the range crest (east or west), annual precipitation, and sample elevation. Finally, I investigate the relationship between the long-term exhumation and the location and character of the maximum topographic envelope defined by the peak altitudes.

Glacial erosion is considerably more complex than fluvial erosion, and I have not attempted to model it here. However, in general, landscape evolution models incorporating glacial erosion show that it is concentrated at altitudes at and above the ELA (e.g., Tomkin and Braun, 2002; MacGregor et al., 2000). This glacial erosion can also influence rates of fluvial erosion downstream, and can act to reduce relief on a

basin-wide scale (e.g., Whipple et al., 1999). Glacial erosion, largely a function of basal ice sliding velocity, scales non-linearly with precipitation, slope, and accumulation area (e.g., Tomkin and Braun, 2002). Thus, in areas where glacial erosion dominates, long-term patterns in exhumation may not correlate spatially with fluvial processes. Conversely, I may expect to see similarities between glacial and hillslope erosion patterns, as both scale similarly with precipitation.

Topographic Trends of Glaciers and Cirques

I use the mean altitudes of modern glaciers to determine the trend in the modern ELA across the study area (Charlesworth, 1957). Glacier locations are derived from areas > 1 km^2 mapped as permanent ice on the 60-minute, 1:100,000-scale digital geologic maps of Washington State (Tabor et al., 1982, 1987, 1993, 2000), though I recognize that not all permanent ice constitutes an active glacier. These regions mapped as permanent ice are overlain on the topography of the study area and clipped to make individual DEMs of each presumed glacier. I use these individual DEMs to determine UTM coordinates of the centroid and calculate the median altitude of each glacier (Porter, 2001). Recognizing this measurement as a rough approximation (e.g., Benn and Lehmkuhl, 2000), I use this median altitude as a proxy for ELA.

Because the modern ELA represents the area of active glaciation for only a small part of the total glaciated interval, I follow the general methods of Porter (1989) and analyze the topography and geology of individual cirque basins in the study area to estimate the Quaternary average ELA. For my analysis of cirque basins, I first identify the cirques visually with digital raster graphics (DRGs) of USGS 7.5-minute topographic maps. I select semi-circular-shaped basins with bowl-shaped depressions or a broad, flat area in the center (e.g., Rudberg, 1984). Many, but not all, of the cirques have a lake on the cirque floor (i.e., a tarn). Using the DRGs as a guide, I find the UTM coordinates and altitudes of the cirque drainage outlets. I use the altitudes of these drainage outlets to define the “minimum” cirque altitudes, regardless of whether or not the cirque is overdeepened, contains a tarn, or is filled with sediment.

I then use these basin outlets and a flow-direction algorithm run on the 10-m DEM to delimit the basin areas for individual cirques; these basin areas represent the contributing watershed area for each cirque outlet, including the adjacent peaks and ridges. I verified the accuracy of the automated basin-delimiting program by overlaying the cirque basin boundaries on the DRGs of each region. Because I am particularly interested in the relationships between the minimum altitudes for each cirque and the height of its surrounding peaks, I calculated the relief in each cirque basin by subtracting the altitude of the cirque outlet from the maximum altitude in each watershed. Because the outlet may not represent the lowest altitude of the cirque, the cirque relief so defined consequently is a minimum. Finally, I identified the bedrock underlying each cirque to determine if there are relationships between rock type and cirque basin relief. Bedrock geology was identified using the 1:100,000-scale digital geologic maps of Washington State, and divided into the following broad categories: plutonic igneous, volcanic igneous, metamorphic, and sedimentary (including volcaniclastic deposits) (Tabor et al., 1982; 1987; 1993; 2000).

Slope Distributions

I also analyze differences in the steepness of the cirque basins relative to the overall topography, as well as consider whether the topography is composed of threshold slopes that stand as steep as supportable for the local relief, drainage density, and rock type (e.g., Burbank et al., 1996; Montgomery, 2001; Schmidt and Montgomery, 1995). Slopes throughout the study area were calculated from the elevations of each DEM cell's eight nearest neighbors. I generated slope distributions by determining the number of cells within single-degree bins and analyzed the slope distributions for both the entire study area and for just the small fraction of topography contained within the cirque basins.

Results

Excluding the Quaternary-aged volcanic cone of Glacier Peak, the maximum and mean altitudes in the study area systematically increase from west to east, with the maximum altitudes located 10 to 40 km east of the drainage divide. The high peaks on the western flank of the range define an inclined "surface" (Figure 3.3). This inclined peak surface increases in altitude eastward at a gradient of 9 to 15 m km^{-1} (Table 3.1). East of the range crest, the planar nature of the peak "concordance" loses its distinction.

Most of the glaciers present within the study area are concentrated in four main areas of relatively high topography: Glacier Peak, Mount Stuart, Alpine Lakes and Monte Cristo Peak (Figure 3.4). Excluding the 16 glaciers located within 2.5 km of the volcanic Glacier Peak summit, mean glacier altitudes for the entire area average 1990 ± 240 m. Overall, glacier altitudes rise eastward at a linear gradient of ~ 11 m km^{-1} (Table 3.1, Figure 3.5). This gradient is slightly less steep in the far northern part of the range. The altitudes of the 373 cirque outlets identified in the study area follow a similar linear trend, with mean altitudes rising from west to east at ~13 m km^{-1} (Table 3.1). These gradients in median glacier and cirque outlet altitudes are roughly parallel to the gradient in peak altitudes, which ranges from 9 to 15 m km^{-1}. The trend of the least squares linear regression of cirque outlets is ~ 500 m lower than the corresponding regressions for the peaks and the modern glaciers.

Hypsometry of the area shows that in the far western portion of the study area (which includes significant amounts of the Puget Lowland) most of the land is at the low end of the altitude distribution. Not surprisingly, significantly more topography is found at higher altitude near the center of the range, where altitudes are more normally distributed (Figure 3.6). The altitude-area distribution has a different shape in each of the eight swaths, and both mean and maximum altitude increase to a maximum near the center of the study area. However, one constant among the different regions is that in every swath that contains cirques, the amount of land surface area begins to drop off steeply at the altitude of the lowest cirques and a mere 4 to 14% of the land surface area exists above the highest cirque in each swath (Figure 3.6).

The relief between the cirque outlets and the adjacent peaks or ridges ranges from 35 m to nearly 1200 m, averaging 380 ± 190 m (Figure 3.7A). Only 10% of cirque basins have > 600 m of relief. Cirque relief does not appear to be controlled by lithology. Relief in cirques underlain predominantly by plutonic (N = 219), volcanic (N = 27), metamorphic (N = 59), and sedimentary rocks (N = 54) is 390 ± 180 m, 380 ± 210 m, 340 ± 140 m and 400 ± 220 m, respectively.

Neither the study area as a whole nor the areas in cirque basins have normally distributed slopes (Figure 3.7B). The average slope over the entire study region is 19°, much lower than the 29° average slope of cirque basins. Because areas with slopes less than ~5° most likely represent valley bottoms and depositional rather than erosional terrain (e.g., Montgomery, 2001), I also calculated average slopes with this "depositional" topography excluded. Removing the areas with < 5° slopes (23% of the total area and 9% of the cirque basins have slopes < 5°) results in average slopes of 24° for the overall study area and 31° for the cirque basins.

Reiners et al. (2003) showed that the highest long-term average exhumation rates in the Cascades in central Washington occur in the middle of the western flank, and the exhumation rate decreases toward the far west and east sides of the range. Within my study area, the highest exhumation rates from Reiners et al. (2003) are located 30 to 40 km west of the highest peaks (Figure 3.8). In addition, there is a difference in the relationship between the various erosion models and exhumation rates at specific locations in the western Cascade flank versus the eastern Cascade flank. On the west side of the crest, stream power is relatively low for a wide range of exhumation rates (0.06 to 0.33 km myr^{-1}) and a linear regression indicates an insignificant relationship ($R^2 < 0.01$; $P = 0.95$) (Figure 3.9A, Table 3.2). Conversely, exhumation rates on the west flank generally increase with increasing hillslope erosion potential, defining a weak, although statistically significant relationship ($R^2 = 0.19$; $P < 0.01$) (Figure 3.9B). On the east side of the range, exhumation rates increase linearly with increasing stream power ($R^2 = 0.63$, $P < 0.01$) (Figure 3.9C). In contrast, the

relationship between exhumation rate and hillslope erosion potential on the eastern flank is statistically insignificant ($R^2 = 0.01$; $P = 0.55$) (Figure 3.9D).

Discussion

The spatial relationship between the ELAs and the peak altitudes suggests the operation of a glacial buzzsaw, but by itself this relationship does not prove that glacial erosion limited the altitude of the range. One proposed signature of a "glacial buzzsaw" is topography that trends with the snowline despite significant variation in the rock uplift rate over the same area (e.g., Brozovic et al., 1997; Montgomery et al., 2001; Spotila et al, 2004). The ten-fold variation in exhumation rate on the west flank of the Cascades reported by Reiners et al. (2002, 2003) spans the same area where the summits define a planar "surface" that forms an envelope ≤ 600 m above the ELA (Figure 3.8). That this topography correlates with the ELA across an area of varying exhumation rate suggests either that glacial erosion is holding peak altitudes to a level tied to the ELA and the variation in exhumation rate shows the variation in rock uplift rate, or glacial erosion has simply removed more rock in the central west flank of the Cascades since the start of glaciation. In either case, the topography of the central Cascades demonstrates at least one of the key components of the glacial buzzsaw.

The exhumation rate data also allow us to demonstrate conclusively that the distinctive peak concordance on the western flank is not an uneroded remnant of a 15 million-year-old peneplain, now uplifted and eroded, as early workers suggested (e.g., Russell, 1900). Thermochronometric data from the western flank of the Cascades indicate that long-term average exhumation rates range from 0.14 km $myr^{-1}$to as high as 0.33 km myr^{-1}, corresponding to removal of ~2 to 5 vertical km of rock in the past 15 myr (Reiners et al., 2002, 2003). The summits on the west flank therefore were not once part of a continuous topographic surface. I contend that erosion related to glaciation created the inclined topographic "surface" of the western slope of the range by shaving off high topography.

The abundance of glacial erosion features supports my hypothesis that glacial, rather than fluvial, erosion controls peak altitudes in the Cascade Range of central Washington. The widespread occurrence of cirques on the west side of the range indicates a morphologically significant "bite" out of topography above the ELA (a mode of relief reduction favored by Whipple et al., 1999). The effects of glacial erosion are also evident in the relationship between peak altitude, cirque altitude, and cirque relief. In this area, ridges and peaks rise an average of 380 ± 190 m and only rarely more than 600 m above cirque floors (Figure 3.7A). Indeed, the cirque floors appear to define a general level above which the adjacent peaks and ridges extend ≤ 600 m higher across the study area as a whole. This height of summit altitudes above the cirques is a function of both the slope and the spacing of valleys within the topography (e.g., Schmidt and Montgomery, 1995). In the Cascades, it appears that any spatial variation in the drainage density is less important in controlling the summit altitudes than the spatial trend in the altitude of cirque floors.

Further evidence for the influence of glacial processes on the topography is that the lower limit of cirque altitudes is the altitude above which the relative proportion of land surface area steeply declines (Figure 3.6). As in the Andes (Montgomery et al., 2001), only about 10% of the total land area lies above the zone of cirques in the central Cascades. my area-altitude results contrast with those of Brozovic et al. (1997), whose analysis of the Himalaya indicated a significant proportion of the land surface area lies at the modern ELA, and Meigs and Sauber (2000), who found that half or more of the land surface area in the Chugach/St. Elias Range of Alaska was located above the modern ELA. Many of the valleys in both the Himalaya and Chugach/St. Elias are full of glacier ice, and glaciers there cover a higher percentage of the topography than in the Cascades. Because the mechanical properties of glacier ice are different than rock, ice will have much different altitude-area and slope distributions than the rock of the surrounding and underlying landscape. Hence, the differences in the topographic metrics between regions may be due to the presence of extensive modern glacier ice in Alaska and the Himalaya and the lack of it in the Cascades. Modern glaciers cover

< 0.3% of the land surface within my study area, and the modern ELA barely intersects even the highest peaks (Figure 3.5). I suggest that in the Cascades, I can define one characteristic of a "fossil" glacial buzzsaw on a landscape with few active glaciers: a steep drop off in land area above the altitude of the most erosionally significant ELA, in this case the Quaternary average ELA defined by the lower limit of the zone of cirques.

The observed lack of correlation between stream power and exhumation rates further suggests that a process other than long-term fluvial erosion governed the exhumation of the western flank of the Cascades (Figure 3.9). Glacial erosion scales non-linearly with precipitation, such that higher snow accumulation rates will increase ice thickness, thus increasing basal ice velocities and therefore erosion rates (Tomkin and Braun, 2002). Glaciers may also reduce fluvial erosion downstream of glacier termini by increasing sediment loads (Whipple et al., 1999). Glacial processes acting over the past 2 to 3 My could explain why exhumation rates near the divide on the western flank of the Cascades can be quite high where stream power is relatively low. The stronger relationship between stream power and exhumation on the eastern flank of the range suggests that fluvial erosion there has been a dominant landscape-lowering process, and that glacial erosion has removed less material on the east flank than on the west flank.

If the peak altitudes in the Cascades are ultimately controlled by the position of the ELA, then what specific processes are responsible for limiting the maximum altitude across the range? I propose that a combination of glacial and nonglacial erosion may link the ELA to the maximum altitude trends. First, the many cirques at and above the Quaternary average ELA provide direct evidence that glacial erosion removed a topographically significant volume of rock at high altitude. Subglacial bedrock erosion rates tend to be highest where ice flux and velocity are greatest; these conditions often occur at or near the ELA (MacGregor et al., 2000; Tomkin and Braun, 2000). Second, I suggest that the morphology created by glacial erosion--wide cirque bottoms with steep sides--increases the potential for hillslope processes such as bedrock landslides on the steep headwalls leading up to the ridges and peaks adjacent to the cirques. It has long

been noted that the high topography in the Cascades consists of glacial features such as horns and arêtes, examples of steep alpine features that form adjacent to glaciated valleys and not under the glaciers themselves. These nunataks exposed above the ice were subject to periglacial processes, such as frost heave and ice wedging, throughout the Quaternary. When the ice retreats, the deglaciated landscape becomes susceptible to paraglacial slope failure due to steepening, fracturing, and debutressing, thus resulting in higher erosion rates focused at and above the ELA (Ballantyne, 2002). The maintenance of steep topography at and above the ELA is supported by my slope analysis: the slopes surrounding cirque basins are very steep, with an average slope of 31°. In the Cascades, glacial erosion appears to create threshold hillslopes above the Quaternary average ELA, on which slight increases in slope lead to large increases in long-term erosion rate (e.g., Schmidt and Montgomery, 1995; Montgomery, 2001; Montgomery and Brandon, 2002). Thus, glacially enhanced erosion of these steepened slopes would impose a limit to how high ridges can rise above cirque floors.

Conclusions

I conclude that the planar trend in peak altitudes across the west flank of the Cascae Range of central Washington is most likely a function of glacial and glacially-mediated erosion processes, rather than the interplay between long-term fluvial erosion and tectonic uplift or the result of incision of an uplifted plateau. Specifically, I posit that the planar zone of cirque glaciers, which according to Porter (1989) developed under “average” glacial conditions, rapidly eroded the high topography through subglacial erosion and created steep, fractured, unstable hillsides above the cirque zone. The development of this steep topography above the Quaternary average ELA and subsequent rapid erosion has resulted in peaks that rise ≤ 600 m above the average altitude of cirque floors. This relationship between the ELA and peak altitudes holds despite steep gradients in precipitation, exhumation rate, and fluvial erosion potential.

Although I cannot exclude the possibility that some combination of tectonics and erosional processes might result in such topography, I find compelling the weight of evidence linking the ELA, cirque altitudes, slope distributions, and relief to topographic trends in Cascade peak elevations. Moreover, the topographic evidence of a glacial buzzsaw in the west-central Washington Cascades includes several distinctive characteristics. First, the peak altitude surface is located ~ 600 m above the zone of cirque floors, corresponding to the mean plus 1σ distance that ridges and peaks rise above individual cirque floors. Second, the amount of topography declines sharply above the altitude of the lowest cirques, with, at most, 14 % of the topography rising above the highest cirques. Third, the erosional topography above the Quaternary average ELA is at or close to threshold steepness. Finally, the discordance between fluvial erosion models and measured exhumation rates on the western flank suggest that processes other than fluvial and hillslope erosion are responsible for the topography of this flank of the range. Taken together, these observations provide persuasive evidence for the influence of a glacial buzzsaw on controlling the height and morphology of the Cascade Range in central Washington.

Table 3.1: Slopes and linear regressions for maximum altitudes, glaciers, and cirques.

Feature		Swath 1	Swath 2	Swath 3	All
Maximum Topography*	**Slope†**	**0.0093 ± 0.0001**	**0.0153 ± 0.0002**	**0.0124 ± 0.0003**	**0.014 ± 0.0003**
	R^2	**0.86**	**0.83**	**0.69**	**0.77**
Glaciers	**Slope**	**NA**	**0.0135 ± 0.0018**	**0.0105 ± 0.0023**	**0.0106 ± 0.0012**
	R^2	**NA**	**0.70**	**0.22**	**0.48**
Cirques	**Slope**	**0.0138 ± 0.0018**	**0.0145 ± 0.0006**	**0.0088 ± 0.0008**	**0.0131 ± 0.0005**
	R^2	**0.56**	**0.72**	**0.64**	**0.69**

Notes: All regressions are statistically significant ($P < 0.01$)
*Regressions on maximum topography calculated on western flank of the range only.
†Slopes, or cross-range gradients, are presented as unitless (km km^{-1}).

Table 3.2: Regressions* for erosion models.

	slope	intercept	R^2	P
West side fluvial	**$0.089 \pm 1.45 \times 10^{-8}$**	**0.137 ± 0.0109**	**< 0.01**	**0.95**
West side hillslope	**$7.26 \pm 2.19 \times 10^{-10}$**	**0.0352 ± 0.0320**	**0.19**	**< 0.01**
East side fluvial	**$1.23 \pm 0.154 \times 10^{-8}$**	**0.0338 ± 0.00219**	**0.63**	**< 0.01**
East side hillslope	**$-0.66 \pm 1.09 \times 10^{-10}$**	**0.0510 ± 0.00839**	**< 0.01**	**0.55**

*Coefficients and statistical parameters for the linear least-squares regression for the measured exhumation rates and erosion models shown in Figure 3.9. West and east are defined relative to the range crest, shown in Figure 3.2.

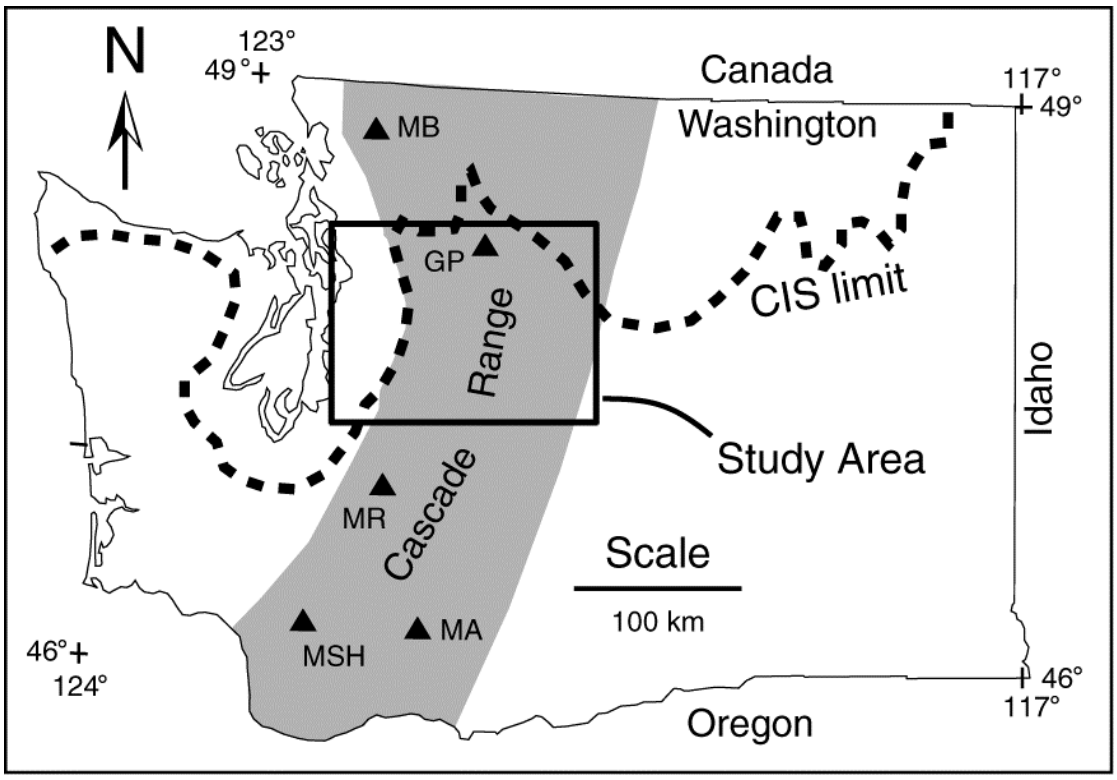

Figure 3.1: Map of study region. The area of the Washington Cascades is shaded in gray, with the study area marked by the box. Quaternary Cascade volcanoes are marked with triangles (MB = Mt. Baker, GP = Glacier Peak, MR = Mount Rainier, MSH = Mt. St. Helens, MA = Mt. Adams). Southern limit of the Cordilleran Ice Sheet (CIS) shown as heavy dashed line (Booth et al., 2004).

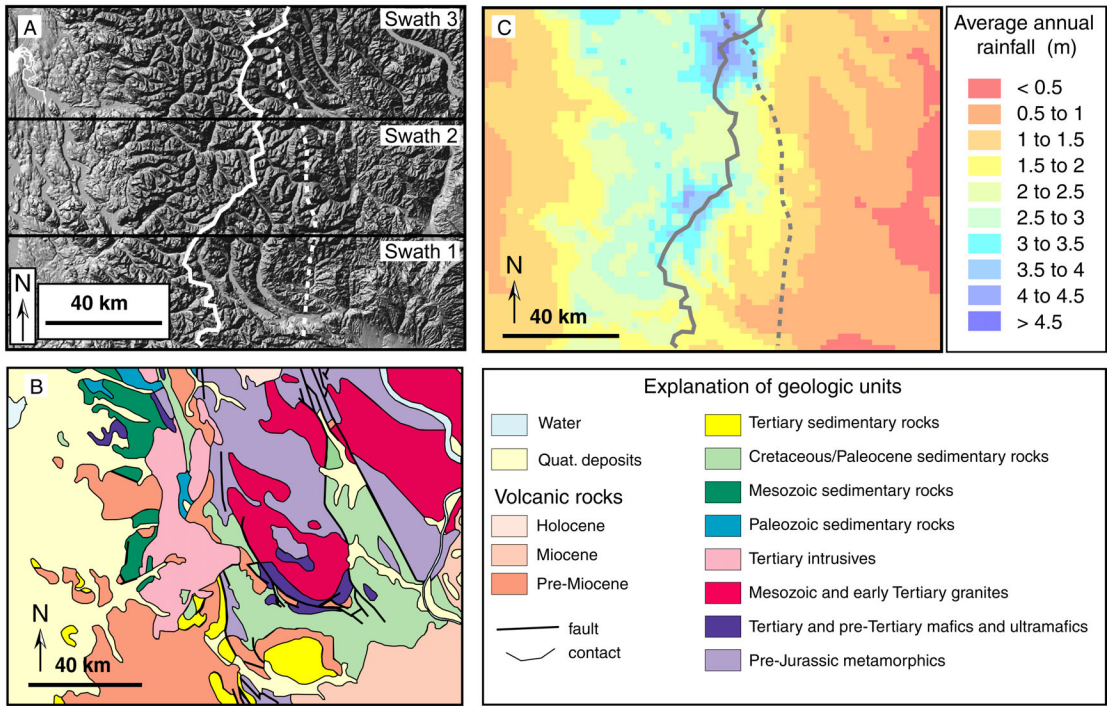

Figure 3.2: A. Shaded relief map of study area. Black horizontal lines delineate swaths 1, 2 and 3. Solid white line shows the position of the drainage divide, white dashed line shows the approximate position of the range crest. B. Generalized geology modified from Weissenborn (1969). C. Average annual precipitation (1960-1991) over the study area, in meters. The drainage divide and range crest are shown as gray solid and dotted lines, respectively. Precipitation data come from the Spatial Climate Analysis Service (Oregon State University, http://www.ocs.orst.edu/prism).

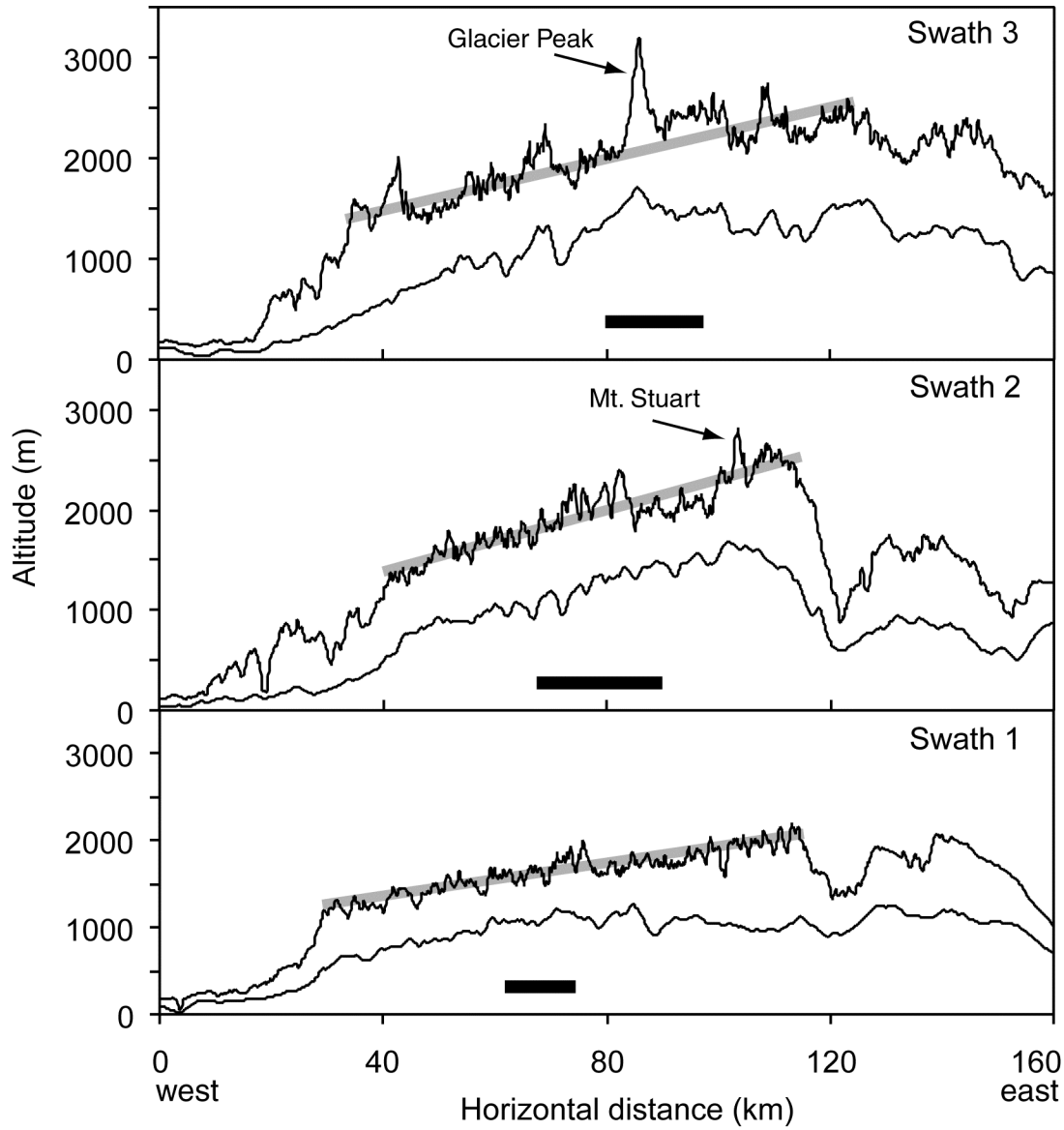

Figure 3.3: West-east topographic profiles of mean and maximum altitudes for swaths 1, 2 and 3. Linear regressions of maximum altitudes are shown as gray lines, see Table 3.1 for slope and R^2 values. Note that regressions are for the western flank of the range only. The western and eastern limits of the drainage divide in each swath are indicated by the horizontal black bars. Relative positions of swaths 1, 2 and 3 can be seen in Figure 3.1A.

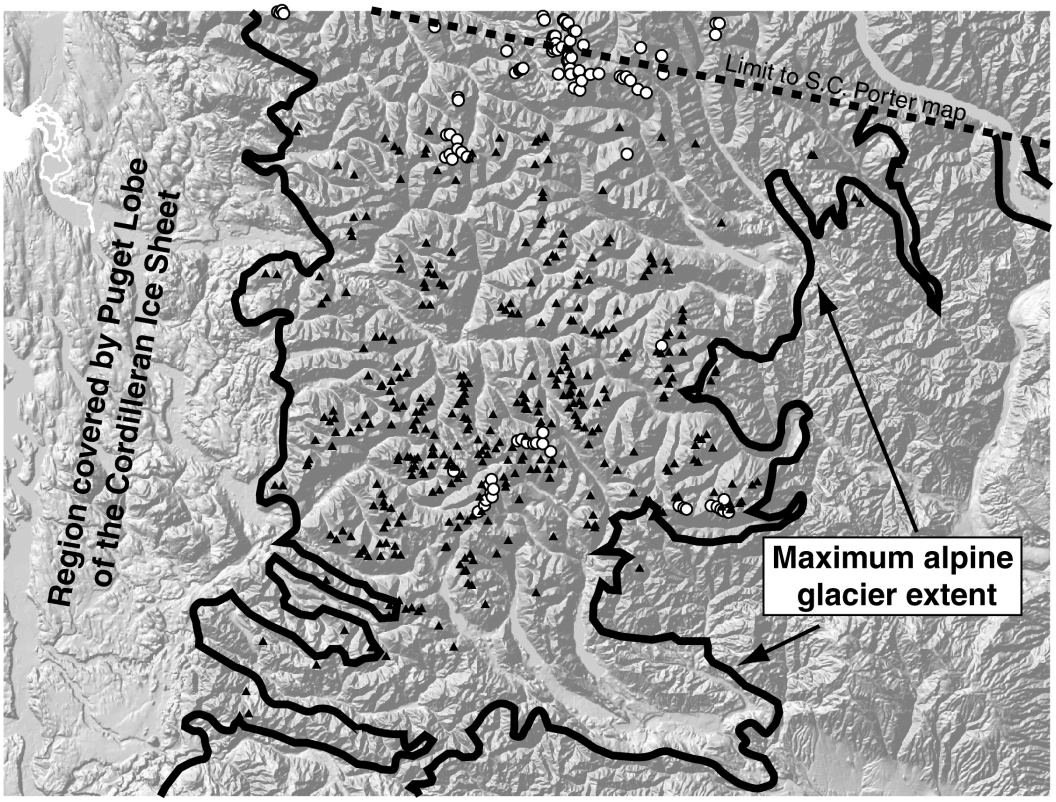

Figure 3.4: A. Spatial distribution of glaciers (open circles) and cirques (black triangles). Glaciers are concentrated in the areas of Glacier Peak (GP), Monte Cristo Peak (MCP), Mount Stuart (MS), and the Alpine Lakes (AL). Heavy black line shows the limit of valley glacier ice during the Quaternary maximum as mapped by S.C. Porter (unpublished data).

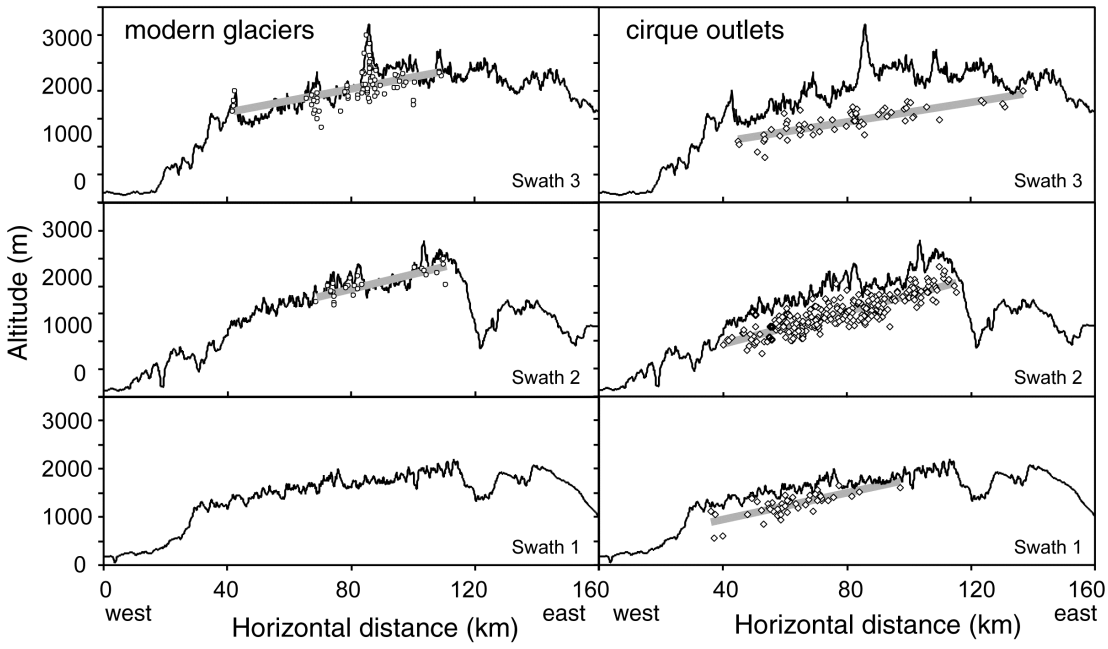

Figure 3.5: Cross-range trends in average glacier (left) and cirque outlet (right) altitudes plotted against maximum altitude profiles for comparison. Linear least-square regressions of cirque and glacier altitudes are shown as thick gray lines, slope and R^2 values are in Table 3.1.

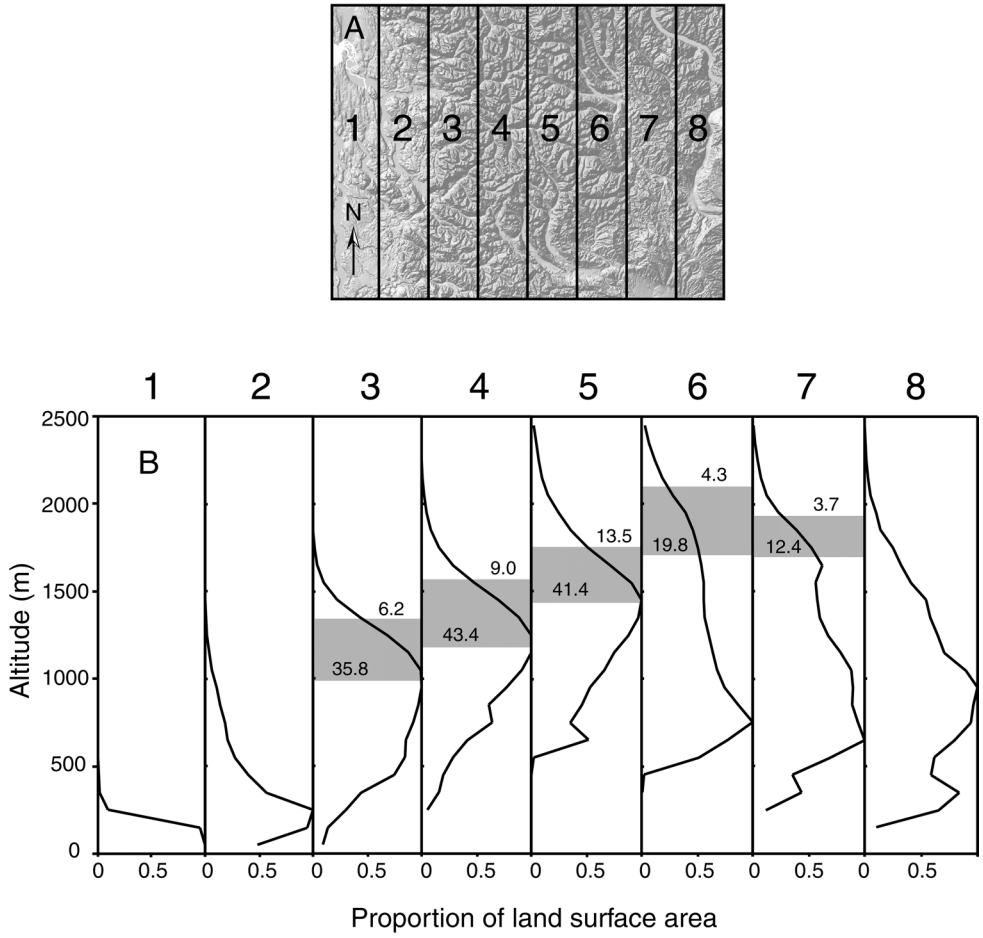

Figure 3.6: A. Index map showing subdivisions for altitude-area distributions. Each subdivision is 20 km wide. B. Normalized altitude-area distributions binned in 100 m intervals for eight subsections of study area. Distributions are shown from west to east going from left to right. The range of cirque floor altitudes within each subsection is marked with a gray box. The percentage of land area located above the lowest and highest cirques is shown for each subsection.

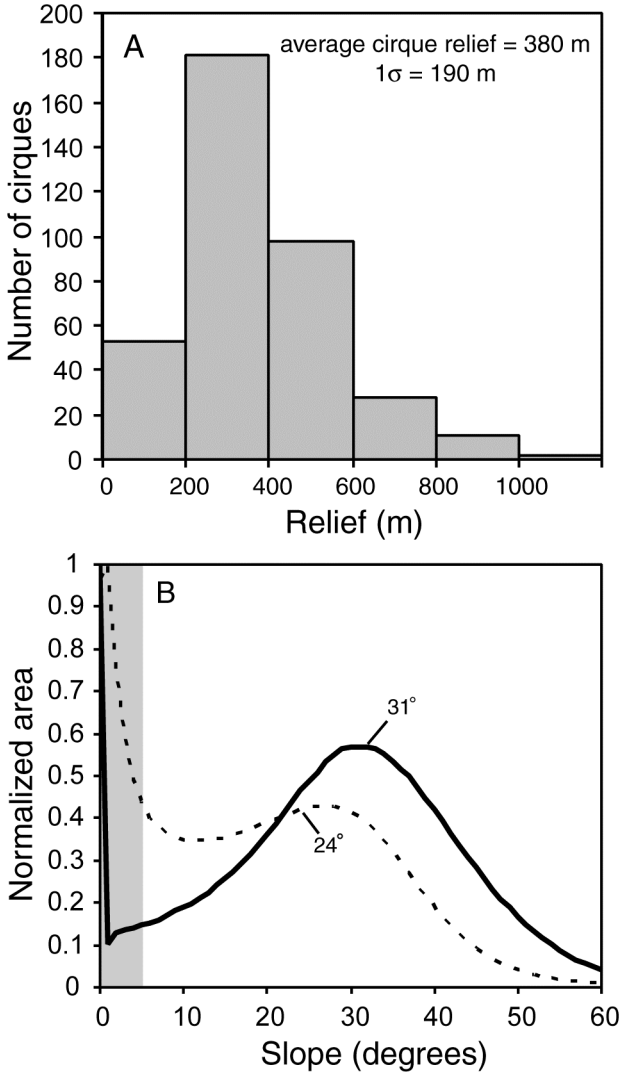

Figure 3.7: A. Distribution of cirque basin relief. Total number of cirques analyzed was N = 373. Cirque relief distributions for different rock types were similar to the overall distribution, despite probable differences in rock hardness. B. Slope distribution of entire study window (dashed line) and cirque basins only (solid line). Excluding areas with slopes < 5°, which contain the majority of depositional terrain, the average slope of the entire area is 24° and the average slope of cirque basins alone is 31°.

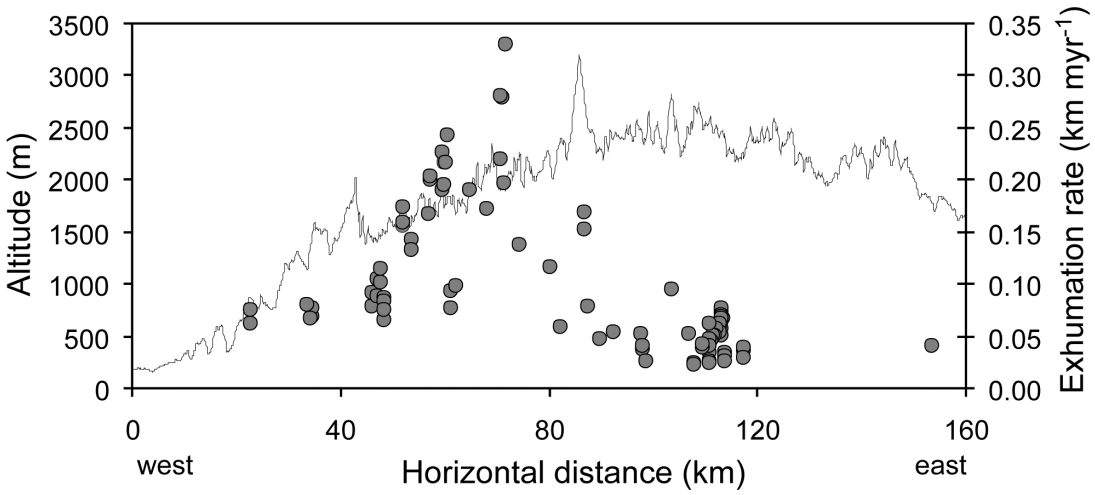

Figure 3.8: Cross-range maximum altitude profile showing spatial pattern of exhumation rates from apatite (U-Th)/He thermochronometry (open circles). All exhumation data are from Reiners et al. (2002, 2003); exhumation rates are long-term averages and assuming steady altitudes. Exhumation rates are highest ~70 km east of the western edge of the study area, whereas the highest altitudes are located 30 to 40 km farther to the east. Note that the exhumation rate varies by at least a factor of ten across the region of peak concordance.

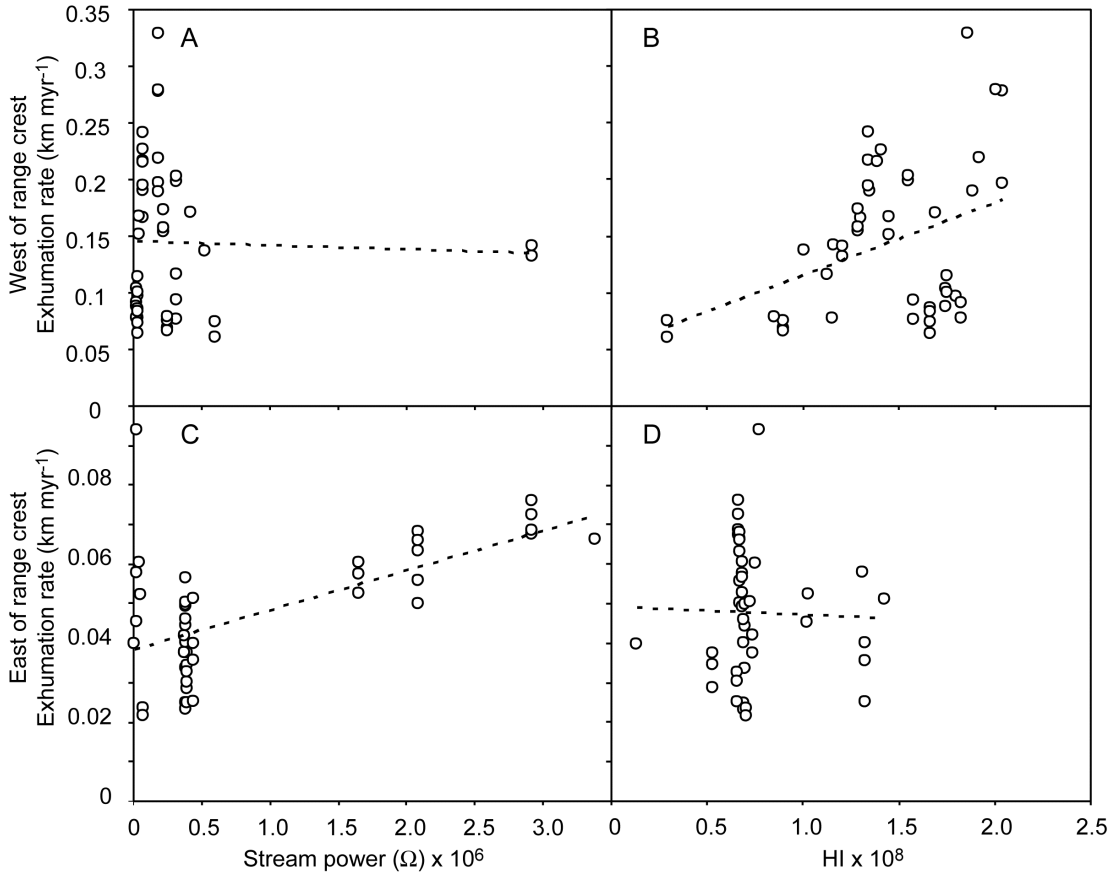

Figure 3.9: Relationships between erosion models and measured exhumation rates from AHe thermochronometry for sample locations east and west of the drainage divide (AHe data from Reiners et al. (2002, 2003). A. Maximum stream power erosion potential (Ω) within a 5 km radius has no significant relationship to exhumation rate for AHe sample locations west of the range crest. Removing the outliers with high erosion potential changes the slope, but not the intercept, R^2 value, or significance of the linear least squares trendline. B. Average hillslope erosion potential (HI) within a 5 km radius increases with increasing exhumation rate for west-side samples. C. Ω increases with increasing exhumation rate for samples located east of the range crest. D. HI has a statistically insignificant relationship with exhumation rate for samples located east of the range crest. See Table 3.2 for the slope, intercept, R^2 and P-value for all linear regressions.

Notes to Chapter 3

Amerson, B., 2005. Morphometry of fluvial and glacial valleys in central Idaho [M.S. thesis]. Seattle, University of Washington, 43 p.

Bagnold, R.A., 1960. Flow resistance in sinuous or irregular channels: part 2, A theoretical model of energy loss in curved channels. USGS Professional paper, 122-130.

Ballantyne, C.K., 2002. Paraglacial geomorphology. Quaternary Science Reviews 21, 1935-2017.

Benn, D.I. and Lehmkuhl, F., 2000. Mass balance and equilibrium-line altitudes of glaciers in high-mountain environments. Quaternary International 65/66, 15-29.

Booth, D.B., Troost, K.G., Clague, J.J., and Waitt, R.B., 2004. The Cordilleran Ice Sheet, In: Gillespie, A.R., Porter, S.C., and Atwater, B.F., eds., The Quaternary period in the United States, Developments in Quaternary Science 1, 17-43.

Brocklehurst, S.H., and Whipple, K.X., 2002. Glacial erosion and relief production in the eastern Sierra Nevada, California. Geomorphology 42, 1-24.

Brocklehurst, S.H., and Whipple, K.X., 2004. Hypsometry of glaciated landscapes. Earth Surface Processes and Landforms 29, 907-926.

Brozovic, N., Burbank, D.W., and Meigs, A.J., 1997. Climatic limits on landscape development in the northwestern Himalaya. Science 276, 571-574.

Burbank, D.W., Leland, J., Fielding, E., Anderson, R.S., Brozovic, N., Reid, M.R., and Duncan, C., 1996. Bedrock incision, rock uplift and threshold hillslopes in the northwestern Himalayas. Nature 379, 505-510.

Charlesworth, J.K., 1957. The Quaternary Era. Arnold, London.

Daly, R.A., 1905. The accordance of summit levels among alpine mountains; the fact and its significance. Journal of Geology, 105-125.

Finlayson, D.P. and Montgomery, D.R., 2003. Modeling large-scale fluvial erosion in geographic information systems. Geomorphology 53, 147-164.

Hallet, B., Hunter, L., and Bogen, L., 1996. Rates of erosion and sediment evacuation by glaciers; a review of field data and their implications. Global and Planetary Change 12, 213-235.

House, M.A., Wernicke, B.P., Farley, K.A., 1997. Dating topography of the Sierra Nevada, California, using apatite (U-Th)/He ages. Nature 396, 66-69.

James, A.L., 2003. Glacial erosion and geomorphology in the northwest Sierra Nevada, CA. Geomorphology, 55, 283-303.

Long, W. A., 1951. Glacial geology of the Wenatchee-Entiat area, Washington. Northwest Science, 25, 3-16.

MacGregor, K.R., Anderson, R.S., Anderson, S.P., and Waddington, E.D., 2000. Numerical simulations of glacial-valley longitudinal profile evolution. Geology 28, 1031-1034.

Mackin, J. H., 1941. Glacial geology of the Snoqualmie-Cedar area, Washington. Journal of Geology 49, 449-481.

Martin, Y., 2000. Modelling hillslope evolution: linear and nonlinear transport relations. Geomorphology 34, 1-21.

Martin, Y., and Church, M., 1997. Diffusion in landscape development models: on the nature of basic transport relations. Earth Surface Processes and Landforms 22, 273-279.

Meigs, A., and Sauber, J., 2000. Southern Alaska as an example of the long-term consequences of mountain building under the influence of glaciers. Quaternary Science Reviews 19, 1543-1562.

Mills, J.E., 1892. Stratigraphy and succession of the rocks of the Sierra Nevada of California. Geological Society of America Bulletin, 413-444.

Montgomery, D.R., Balco, G., and Willett, S.D., 2001. Climate, tectonics, and the morphology of the Andes. Geology 29, 579-582.

Montgomery, D.R., 2001. Slope distributions, threshold hillslopes, and steady-state topography. American Journal of Science 301, 432-454.

Montgomery, D.R., 2002. Valley formation by fluvial and glacial erosion. Geology 30, 1047-1050.

Montgomery, D.R. and Brandon, M.T., 2002. Topographic controls on erosion rates in tectonically active mountain ranges. Earth and Planetary Science Letters 201, 481-489.

Page, B.M., 1939. Multiple alpine glaciation in the Leavenworth area, Washington. Journal of Geology 47, 785-815.

Porter, S.C., 2001. Snowline depression in the tropics during the Last Glaciation. Quaternary Science Reviews 20, 1067-1091.

Porter, S.C., 1989. Some geological implications of average Quaternary glacial conditions. Quaternary Research 32, 245-261.

Porter, S.C., 1977. Present and past glaciation threshold in the Cascade Range, Washington, U.S.A.: topographic and climatic controls, and paleoclimate implications. Journal of Glaciology 18, 101-116.

Porter, S. C., 1976a. Pleistocene glaciation on the southern part of the North Cascade Range, Washington. Geological Society of America Bulletin 87, 61-75.

Porter, S. C., 1976b. Geomorphic evidence of post-Miocene deformation of the eastern North Cascade Range. Geological Society of America Abstracts with Programs, 8, 402-403.

Porter, S.C., 1964. Composite Pleistocene snow line of Olympic Mountains and Cascade Range, Washington. Geological Society of America Bulletin 75, 477-482.

Reiners, P.W., Ehlers, T.A., Mitchell, S.G., and Montgomery, D.R., 2003. Coupled spatial variations in precipitation and long-term erosion rates across the Washington Cascades. Nature 426, 645-647.

Reiners, P.W., Ehlers, T.A., Garver, J.I., Mitchell, S.G., Montgomery, D.R., Vance, J.A., and Nicolescu, S., 2002. Late Miocene exhumation and uplift of the Washington Cascade Range. Geology 30, 767-770.

Roe, G.H., Montgomery, D.R., and Hallet, B., 2002. Effects of orographic precipitation variations on the concavity of steady-state river profiles. Geology 30, 143-146.

Roering, J.J., Kirchner, J.W., and Dietrich, W.E., 1999. Evidence for nonlinear, diffusive sediment transport on hillslopes and implications for landscape morphology. Water Resources Research 35, 853-870.

Rudberg, S., 1984. Fossil glacial cirques or cirque problematica at lower levels in northern and central Sweden. Geografiska Annaler 66A, 29-39.

Russell, I.C., 1900. A preliminary paper on the geology of the Cascade Mountains in northern Washington. USGS Annual Report 20, pt. 2, 83-210.

Schmidt, K.M., and Montgomery, D.R., 1995. Limits to relief. Science 270, 617-620.

Smith, G.O., 1903. Geology and Physiography of Central Washington. USGS Professional Paper 19, 1-46.

Spotila, J.A., Buscher, J.T., Meigs, A.J., and Reiners, P.W., 2004. Long-term glacial erosion of active mountain belts: example from the Chugach-St. Elias Range, Alaska. Geology 32, 501-504.

Tabor, R.W., Waitt, R.B., Frizzell, V.A. Jr., Swanson, D.A., Byerly, G.R., and Bentley, R.D., 1982. Geologic map of the Wenatchee 1:100,000 quadrangle, central Washington. USGS Miscellaneous Investigations Series Map 1-1311, 26 p.

Tabor, R.W., Frizzell, V.A. Jr., Waitt, R.B., Swanson, D.A., Byerly, G.R., Booth, D.B., Hetherington, M.J., and Zartman, R.E., 1987. Geologic map of the Chelan 30-by 60-minute quadrangle, Washington. USGS Miscellaneous Investigations Series Map I-1661, scale 1:100,000, 29 p.

Tabor, R.W., Frizzell, V.A. Jr., Booth, D.B., Waitt, R.B., Whetten, J.T., and Zartman, R.E., 1993. Geologic map of the Skykomish River 30- by 60-minute quadrangle, Washington. USGS Miscellaneous Investigations Series Map I-1963, scale 1:100,000, 42 p.

Tabor, R.W., Frizzell, V.A. Jr., Booth, D.B., Waitt, R.B., 2000. Geologic map of the Snoqualmie Pass 30 x 60 minute quadrangle, Washington. USGS Geologic Investigations Series Map I-2538, scale 1:100,000, 57 p.

Thompson, W.F., 1962. Cascade alp slopes and Gipfelfluren as clima-geomorphic phenomena. Erdkunde 16, 81-94.

Tomkin, J.H., and Braun, J., 2002. The influence of alpine glaciation on the relief of tectonically active mountain belts. American Journal of Science 302, 169-190.

Waitt, R. B., Jr., 1975. Late Pleistocene alpine glaciers and the Cordilleran Ice Sheet at Washington Pass, north Cascade Range, Washington. Arctic and Alpine Research 7, 25-32.

Waitt, R. B., Jr., and Thorson, R. M., 1983. The Cordilleran ice sheet in Washington, Idaho and Montana. In Porter, S.C. (Ed.), Late Quaternary Environments of the United States, University of Minnesota Press, Minneapolis. 53-70.

Weissenborn, A.E., 1969. Geologic Map of Washington. USGS Miscellaneous Geologic Investigations Map I-583.

Whipple, K.X., Kirby, E., and Brocklehurst, S.H., 1999. Geomorphic limits to climate-induced increases in topographic relief. Nature 401, 39-43.

Willis, B., 1903. Physiography and deformation of the Wenatchee-Chelan district Cascade Range. USGS Professional Paper 19, 47-97.

CHAPTER 4

Contribution of Isostatic Response due to Valley Incision to Altitude Trends of the Cascade Range, Washington State

Summary

Peaks in the Cascade Range in northern Washington are on average ~1000 m higher than in southern Washington. The degree to which this difference in altitude is a result of: A) differential valley excavation, or B) variations in hillslope length and average slope, was tested using a 3-dimensional model for isostatic rock uplift and calculations of hillslope length and slope, respectively. The magnitude of potential rock uplift determined by the model is highly dependent on the flexural rigidity (D) and the related effective elastic thickness (T_e) of the crust of this region (see Table 4.1 for list of symbols). The rigidity of the crust was constrained using published estimates and by estimating the depth of the seismogenic zone in the area ($D > 10^{23}$ Nm and $T_e > 24$ km). With these constraints, isostatic compensation due to differential erosion could have added a maximum of ~700 m and 400 m of height to peaks in the northern and southern Cascades, respectively; the actual effect was probably significantly less. Deeper valley incision, glacial or fluvial, in the northern Cascades can account at most for ~300 m of the 800 m difference in peak altitudes between north and south. Similarly, variation in valley spacing and slope has only a modest (< 350 m) effect on the difference in mean altitude between northern and southern regions. Thus, much of the difference in altitude between the northern and southern regions of the Cascades in Washington must be due to the topographic influence of tectonics, geology and crustal thickness rather than purely geomorphic effects like valley incision and geometry.

Introduction

How valley incision and the creation of relief influences the peak altitudes of mountain ranges has been a topic of considerable interest over the past several decades (e.g., Molnar and England, 1990; Gilchrist et al., 1994; Montgomery, 1994; Small and Anderson, 1998; Whipple et al., 1999; Montgomery and Greenberg, 2000). Incision of valleys at rates higher than the erosion of adjacent peaks causes spatially non-uniform unloading which, when isostatically compensated at depth, causes some amount of peak uplift (Wager, 1933; Holmes, 1945). Molnar and England (1990) hypothesized a feedback system wherein increased valley incision brought on by global cooling could effectively raise the crests of mountain ranges, thereby influencing local and global climate patterns and further enhance relief development. However, because the volume of crust removed is replaced by a smaller volume of denser mantle, the average altitude of the area will be lower than it was originally (Holmes, 1945; Molnar and England, 1990). The influence of this feedback is limited by how much altitude neighboring peaks can realistically gain via valley incision.

Rigidity of the Crust

The extent to which peaks rise due to valley incision is a direct function of the flexural strength of the crust in that location (Turcotte and Schubert, 1982); however, the strength of the crust in geologically and tectonically complex regions such as orogenic belts and subduction zones is difficult to estimate (Miller and Paterson, 2000; Lowry et al., 2000; Flück et al., 2003; Burov and Watts, 2006). In this investigation, I used several estimates for crustal thickness and/or flexural rigidity to constrain the maximum possible isostatic response of the Cascade landscape, and thus the degree to which this response contributes to the general altitude trends of the range.

The strength of the crust is generally expressed either in terms of flexural rigidity (D) or effective elastic thickness (T_e), which relate to each other by:

$$D = \frac{ET_e^3}{12\left(1-\nu^2\right)} \qquad \text{Eq. 1}$$

where E is the modulus of elasticity (8.35×10^{10} N m^{-2}) and v is Poisson's ratio (0.25) (Figure 4.1). Although valley incision can be constrained using geographic information system (GIS) techniques, and the densities of the crust and mantle can be estimated with reasonable accuracy, it remains difficult to constrain the strength of the crust (Burov and Watts, 2006). While Airy isostasy, a hypothetical condition in which the crust has no strength and isostatic effects are purely local, is often used as an endmember in uplift calculations (e.g., Small and Anderson, 1998; Montgomery and Greenberg, 2000), substantial uncertainty remains in constraining a realistic crustal strength.

T_e is highly variable in continental settings, ranging between 0 and 100 km depending on the age, temperature, and thickness of the crust (Burov and Watts, 2006). Many techniques have been used to estimate T_e (and thus D) for different tectonic and lithospheric environments. Maggi et al. (2000), for example, argued that the primary strength in the crust was contained within the brittle seismogenic zone, and thus the thickness of the seismogenic zone (T_s) is equivalent to T_e. Adopting this logic, one may constrain T_e through earthquake focal depths. In contrast, Watts and Burov (2003) argued that T_e should instead represent the combined brittle, ductile, and elastic strength of the crust and therefore $T_s < T_e$ in most continental settings. Constraints on T_e are also estimated via modeling from topography and Bouguer anomalies (e.g., Fluck et al., 2003; Perez-Gussinye et al., 2004) and thermomechanical and viscoelastic properties (Burov and Watts, 2006; Cohen and Darby, 2003). Perhaps some of the most reliable T_e estimates on timescales relevant to isostatic peak uplift come from measured deformation due to other isostatic effects such as glacial unloading (e.g., James et al., 2000).

Nearly all previous studies on peak uplift due to valley incision acknowledge the importance of constraining D or T_e and the resulting uncertainty in the uplift calculations. Montgomery (1994) estimated the maximum peak uplift of the Himalaya, Sierra Nevada, and Tibetan Plateau assuming purely local (Airy) isostatic compensation, and then assessed the percentage of local (maximum) compensation that would occur given a range of D from 10^{20} to 10^{25} N m. Gilchrist et al. (1994)

acknowledged that their estimate for uplift of the European Alps based on Airy isostasy by definition provides a maximum constraint. Small and Anderson (1998) estimated isostatic uplift of Laramide mountain ranges to be ~290 m using Airy isostasy, but ~90 m using a minimum plausible T_e estimate of 16 km. Montgomery and Greenberg (2000) similarly use a range of T_e of 5 to 24 km to calculate ~500-700 m of superelevation in the Olympic Mountains of Washington State. Most recently, Stern et al. (2005) used isostasy to constrain the rheology of the Transantarctic Mountains. They modeled the isostatic uplift of the range using four different rheological models and identified the flexural rigidity that resulted in uplift that best fit observed deformation of erosion surfaces. Using this model, they showed that isostasy may account for 25% of peak elevation of the Transantarctic Mountains, a percentage comparable to those reached by previous studies in other areas (Montgomery, 1994; Gilchrist et al., 1994).

Study Area

I used similar techniques to investigate the effects of valley incision on the topography of the Cascade Range in Washington State. The Cascade Range forms a ~150- to 220-km-wide topographic high in Washington State and bisects the state from south to north (Figure 4.2). Although recent subduction arc volcanism has created five large and currently active stratovolcanoes, the range itself is an antiform and many of the peaks in the range, particularly in the north, consist of uplifted sedimentary rocks and exhumed plutonic and metamorphic rocks (Schuster, 2005). While the "Cascade Range" as a physiographic entity extends many hundreds of kilometers through Oregon and south to California, in this chapter I use the phrase "North Cascades" to refer to the range located between ~ 47° 30' N and 49° N latitude; the term "southern Cascades" refers to the range between ~ 47° 30' N latitude and the Washington-Oregon border (Figure 4.2A). I chose these boundaries because previous work has suggested that the Cascade Range experienced significantly different geologic, tectonic, and thus geomorphic histories in northern and southern Washington. According to the interpretations of Mackin and Cary (1965) and Mitchell and Montgomery (accepted

pending revisions), the North Cascades existed as high topography prior to the middle Miocene, whereas the southern Cascades were uplifted after the middle Miocene. In central Washington, Quaternary glacial erosion removed rock preferentially at and above the Quaternary average glacial equilibrium line altitude (ELA) independent of large W-E gradients in rock uplift rate, thereby masking major differences in relief history between the Cascades in northern and southern Washington (Mitchell and Montgomery, 2006).

I model the spatial distribution of superelevation using a range of flexural rigidities. Using independent constraints on *D*, I then determine the maximum possible elevation that the Cascades could have gained through this process, and the degree to which isostatic effects control N-S relief trends in the Washington Cascades. Because peak uplift due to valley incision should reduce mean altitudes in areas undergoing the most incision and most peak uplift, I also explore the extent to which systematic variation in the topographic parameters of slope and valley spacing contribute to spatial variation in mean altitudes of the range.

Methods

I use GIS techniques to analyze topographic trends of the Cascade Range, quantify potential isostatic effects from valley incision, and constrain the role of valley spacing and slope on range-scale altitudinal gradients. All GIS work was conducted using a 10-m-grid-size digital elevation model (DEM) of the Cascade physiographic province, as defined by Haugerud (2004). The base DEM was constructed by merging DEMs made from digitization of 7.5-minute USGS topographic quadrangles. The vertical resolution of the DEM is 0.1 m.

Mean and Maximum Altitude

I analyzed large-scale, N-S trends in mean and maximum altitude by dividing the DEM of the Cascade physiographic province into nineteen 20-km wide, W-E trending “swaths” (Figure 4.2B). Within each topographic swath I determined the mean

and maximum altitude for each row, calculated one 10-m column at a time. I then determined the average of all the mean and maximum altitudes for each swath within the Cascade province. Note that the "average maximum altitude" is not the average of all summit altitudes; rather, it is the average of all the maximum altitudes for each 10-m by 20-km column of DEM grid cells. Because the high-altitude Quaternary volcanoes influence these calculations, I determined the mean and maximum average altitudes excluding the volcanoes from the analysis. I then subtracted the mean altitude from the average of all maximum altitudes in each swath to find the average relief above the mean altitude (ARAMA). ARAMA thus represents the trend in maximum altitude with the trend in mean altitudes removed. To get a sense of the range height as seen by climate conditions, I also determined the altitude of the five highest peaks in each swath, excluding volcanoes (which stand well above the surrounding topography and form less of a barrier to prevailing winds than the crest of the range as a whole).

Isostatic Compensation

Using the methods of Montgomery and Greenberg (2000) and with the assistance of Harvey Greenberg, I calculated the potential rock uplift resulting from the creation of relief in the Cascades. We first determined the amount and location of "missing mass" below the peaks in the range, and then calculated the amount of isostatic uplift resulting from the mantle replacing that missing mass by summing the flexural response for the resulting negative load at each grid point. This method assumes that all relief is created by differential erosion.

To create a grid of missing mass, I chose an analysis window that contains the Cascades physiographic province in Washington State, plus a 100 km buffer to the north to remove edge effects of the uplift calculation. This buffer was not extended to the south. We then compiled a 90-m-grid-size DEM for this region using a resampled 10-m DEM, bathymetric data for Puget Sound, and DTED 3-arc-second data for Canada. Next, we created a grid of the maximum elevation within a 6.6 km radius, a length scale large enough to span major valleys but small enough not to exclude many

mountain peaks (Montgomery and Greenberg, 2000). This grid of maximum elevations was then used to create a triangular irregular network (TIN) of 5428 local maxima, creating a reference surface by connecting the highest peaks. The Quaternary volcanoes were removed from this surface, assigning the areas within 15 km of the summit of each large volcano the average elevation of points located between 15 and 25 km. Then I subtracted the modern elevations from the 90-m DEM from this surface to create a grid showing the thickness of "missing" rock from below the reference surface for each cell.

Using the grid of missing rock mass, we calculated the vertical deflection resulting from the unloading (or loading, in the areas of the Quaternary volcanoes which add mass to the crust) of each grid cell (w):

$$w = \left(\frac{r}{\alpha}\right)\left(\frac{q}{2\pi\rho_m g\alpha^2}\right) Kel\left(\frac{r}{\alpha}\right) \qquad \text{Eq. 2}$$

where (r/α) is the non-dimensional distance from the point load, g is the acceleration due to gravity (9.81 m s^{-2}), ρ_m is the density of the mantle (3300 kg/m^3), and Kel is the Kelvin function (Abramowitz and Stegun, 1965). The flexural rigidity parameter α is given by:

$$\alpha = (D/\rho_c g)^{1/4} \qquad \text{Eq. 3}$$

where D is the flexural rigidity (see Eq. 1) and ρ_c is the density of the crust (2800 kg m^{-3}). Finally, q is the point load:

$$q = zg\rho_c\, dx\, dy \qquad \text{Eq. 4}$$

where z is the equivalent eroded thickness and dx and dy are the grid cell dimensions (in this study, both dx and dy are 90 m). The overall vertical movement at any given point is affected by the amount of mass either lost or gained at that point and at all points near enough to also affect it. The flexural rigidity controls how far out and to what extent neighboring cells affect the uplift of each cell. I calculated w for each cell using the range of D observed in continental crust: from 10^{19} to 10^{24} N m (Burov and Watts, 2006).

While I used the full range of rigidities in the model, there are independent estimates for both D and T_e. For example, James et al. (2000) used postglacial isostatic rebound rates to constrain the T_e of the Puget Lowland, adjacent to the northern Cascade region, to be between 30 and 40 km, equivalent to $D = 2$ to 5 x 10^{23} Nm. Clague and James (2002) use similar methods to show that $T_e \sim 35$ km ($D \sim 3.2$ x 10^{23}) along the British Columbia coast, a few tens of km north of the Cascades in Washington. Using an entirely different technique, Lowry et al. (2000) use gravity anomaly and topographic data to model T_e for the entire Cordillera of the United States. For the Cascade region of Washington, Lowry et al. (2000) calculate an average T_e of 26 ± 6.5 km, with minimum and maximum constraints of 16 km and 40 km respectively.

Because the depth of the seismogenic zone (T_s) for an area provides a minimum constraint on T_e (e.g., Maggi et al., 2000; Watts and Burov, 2003), I estimated T_s using earthquake data retrieved from the Pacific Northwest Seismograph Network, a service run by the Advanced National Seismic System run by the Northern California Earthquake Data Center (http://www.ncedc.org/anss/catalog-search.html, March 2006). These data include the date, magnitude, focus location, and focus depth for M > 1 earthquakes occurring between 125º W and 117º W longitude, 45º N and 49º N latitude and happening between 1970 and 2006.

Hillslope Length and Slope

While isostatic compensation from valley incision may increase peak altitudes and the relief above the mean, other geomorphic factors may also influence trends in relief and altitude in the Cascades. One possible control on mean altitudes is the average hillslope length and slope of the area; on average, areas with long or steep hillslopes will have higher mean altitudes than areas with short or gentle hillslopes. In other words, are the North Cascades higher simply because they have more widely spaced main drainages and/or steeper slopes than the southern Cascades? I have therefore determined the extent to which observed N-S differences in mean altitudes are attributable to systematic variation in average hillslope lengths and slopes. I calculated

average hillslope length using two methods: 1) using drainage density, and 2) using flowdirection algorithms to calculate the mean downstream distance between ridges and the channel network. For both of these methods, I divided the range by major watershed boundaries rather than by swath; I used the centroid of each drainage basin to compare relative north-south positions (Figure 4.2C). Because drainage density and hillslope length are scale dependent, I defined two resolutions of the channel network: cells containing ≥ 1 km^2 and ≥ 10 km^2 of flow accumulation area. To calculate drainage density (*DD*), I measured the length of channel per unit area for each watershed. The relationship between average hillslope length (l_s) and *DD* is given by Horton (1945):

$$l_s = \frac{1}{2DD} \qquad \text{Eq. 5}$$

The second method for determining hillslope lengths was to measure directly the distance between ridges (areas with accumulation area = 1 cell) and channels (accumulation area ≥ 1 and ≥ 10 km^2) as measured down the steepest descent (Figure 4.3A). I then calculated the mean and standard deviation of these distances within each watershed. Finally, the slope of each 10 m by 10 m grid cell was determined using the steepest descent angle defined by each cell's eight nearest neighbors. I then calculated the mean and standard deviation of slope for each drainage basin.

The slopes and the different measures of hillslope length were then used to quantify the extent to which differences in the mean altitude of each drainage basin are due to differences in mean hillslope length $\left(\overline{l_s}\right)$ and slope (θ) (Figure 4.3). For each drainage basin, I used the following equation to determine mean altitude ($\overline{Z_m}$) above the local datum of the valley floor:

$$\overline{Z_m} = \frac{1}{2}\overline{l_s}\tan(\theta) \qquad \text{Eq. 6}$$

Finally, I calculated ΔZ_m as the difference in Z_m between each basin and the lowest Z_m. This ΔZ_m is the degree to which the difference in measured mean N-S altitude could be attributable to the geomorphic parameters of slope and valley spacing.

Results

The northern Cascades are "higher" than the southern Cascades in every measure. Mean altitudes in the Cascades range from < 800 m in southernmost swaths to to ~1300 m in northernmost Washington (Figure 4.4A). Similarly, average maximum altitudes increase from ~950 m in the south to over 1800 m in the north (Figure 4.4A). The average altitude of the five highest peaks in each swath also increases to the north, ranging from < 1800 m in swaths 2-5, averaging ~2200 m in swaths 5-14, and averaging ~2700 m in the northernmost 5 swaths (Figure 4.4A). Because the average maximum altitude increases at a steeper gradient towards the north than the mean altitudes, there is a northerly increase in the average relief above the mean altitude (ARAMA). The ARAMA is ~350 to 450 m in southern Washington and increases northward to 550 to 750 m. As a percentage of the average altitude of the highest five summits, ARAMA is essentially constant across all swaths, averaging 22 ± 3 % (Figure 4.4B).

The general depth of the seismogenic zone (T_s) beneath the Cascade Range is comparable to other constraints of T_e for this region. Over 26,000 earthquakes have occurred in this region and time period, the majority of which had a magnitude between 1 and 2 (Figure 4.5). While T_s interpreted from the earthquake foci is complex due to the presence of the subducting slab of the Juan de Fuca plate, T_s determined with earthquake foci from just the North American Plate is ~ 30 to 35 km in the western area of the Cascade region of Washington, and ~ 20-30 km in the eastern area (Figure 4.5).

Spatial analysis of the topography shows that a greater amount of mass is "missing" between peaks in the northern part of the range, where deep valleys extensively dissect the high-relief topography. As a result, there is greater potential for superelevation in the North Cascades than in the southern Cascades. As expected, both the magnitude of superelevation in a given area and the difference in superelevation between north and south are highly dependent on the flexural rigidity used in the calculation (Figure 4.6). The mean and maximum superelevations within each swath increase from south to north for all modeled flexural rigidities (Figure 4.7). For

example, using the Airy endmember ($D = 10^{19}$ N m), the mean superelevations in the north and south are ~900 and 400 m respectively, contributing on average ~500 m more altitude to peaks in the north compared to the south.

However, limiting D to $< 10^{23}$ N m ($T_e > 24$ km) limits the mean superelevation to ~575 and 275 m in swaths 2-5 and 15-19, respectively. Considering the altitude of the highest peaks in those swaths, 2700 m and 1900 m, respectively, superelevation accounts for < 25% of peak altitudes. Furthermore, the contribution of isostatic uplift to the overall altitude difference between north and south is < 300 m of the observed 800 m altitude difference (Table 4.2).

It is not surprising that as the average relief above the mean increases towards the north, meaning more mass is missing in a swath relative to the peak altitudes, so does superelevation (Figure 4.7). What is intriguing, however, is that ARAMA is essentially equivalent to superelevation for the case where $D = 10^{23}$ N m, particularly for the northernmost swaths (Figure 4.7). This relationship may suggest that when D is properly constrained, superelevation (at least when averaged over a large area) should not generally exceed the average relief above the mean for that area.

Mean hillslope lengths calculated from individual drainage basins using drainage density and mean downstream distances from ridges to streams are similar for most basins, ranging from ~550-900 m using the 1 km^2 stream network and ~1900-2500 m using the 10 km^2 stream network (Table 4.3, Figure 4.8A). The method used to determine hillslope length has a slight effect on the trends; mean hillslope lengths tend to be somewhat longer using the downslope method than the drainage density method, particularly in southern drainages. As a result, mean hillslope lengths increase slightly towards the north when determined using drainage density; however, hillslope lengths do not have much latitude dependence when determined using the downslope distance calculation.

In contrast, mean slope angles are 11º to 22º in the southern half of the range and increase to 20º - 27º in the northern half, although standard deviations for all overlap (Figure 4.8B). As a result, the calculated mean altitude above the valley floor

based on mean slope angles is higher in the northern basins than in the southern basins (Figure 4.9). The modeled mean altitudes from the 1 km^2 stream network are at most 135 m higher in the north than south. The mean altitude above the valley floor using the 10 km^2 stream network is about 350 m higher in the north than in the south (Figure 4.9).

Discussion

Molnar and England (1990) suggested that the onset of glaciation and the resulting valley incision could have triggered enough peak uplift to affect Cenozoic climate conditions, both through increased weathering and the physical effects of the peaks on atmospheric circulation patterns. Based on constraints of *D*, I can determine the maximum possible superelevation and thus additional peak altitude that could have been created in the Cascades as a result of valley incision and relief creation. The maximum possible superelevation that can be achieved at a single spot in the Cascades is 700 m in the northern region (Table 4.2, Figure 4.7). When averaged over swaths, the upper limit on average superelevation ranges from 575 m in the North Cascades to < 300 m in the southern Cascades. This amount of superelevation represents < 25% of the observed highest summit altitudes. Furthermore, as many of these valleys must have existed prior to glaciation, and erosion from valley glaciers have been shown to about double the volume of valleys (Montgomery, 2002; Amerson, 2005), I suggest that the effect of global cooling and the onset of glaciation could have accounted for perhaps half the overall superelevation. Therefore, glaciation could have increased the highest summit altitudes by at most 350 m, probably insufficient to create a high orographic barrier from a low- or modest-relief landscape or trigger a large-scale change in climate.

Greater incision of the Cascades in northern Washington gives that area more potential for isostatic peak uplift than in southern Washington. Based on my constraints of *D*, the maximum difference between maximum and mean superelevation between northern and southern regions is ~500 and 300 m, respectively. However, the highest peaks in the northern Cascades are ~1000 m higher than those in southern Washington, and the average maximum altitudes are ~800 m higher in the north than south. Thus, at

most, differences in incision between north and south can account for only about half (and probably a lot less) of the total difference in the altitude of the peaks. In addition, average ridge-to-valley lengths are relatively constant between north and south, the generally higher slopes in the north Cascades give that region average altitudes about 350 m farther above the valley floors than in the south (Figure 4.8). Again, while this effect is measurable, it cannot account for the entire difference in mean and maximum altitudes between the northern and southern Cascades. I conclude that tectonic or geologic distinctions, whether a long-term difference in rock uplift rate or difference in crustal thickness between north and south, must contribute to the higher altitudes in the Cascades of northern Washington. This result is consistent with the interpretation first presented by Mackin and Cary (1965) and recently supported by Mitchell and Montgomery (accepted pending revisions) that the northern and southern Cascade Range in Washington have had strikingly different geologic, tectonic, and geomorphic histories since the Miocene. For example, Mitchell and Montgomery (accepted pending revisions) show that the Cascades in northern Washington have had significant relief since before the initial eruption of the 15 My-old Columbia River Basalts, and that the crystalline core of the northern part of the range may be acting as a relatively immobile, rigid tectonic barrier. Conversely, the Cascades of southern Washington likely had relatively low relief until after the eruption of the basalts, whereupon they rose likely due to north-south compression.

Conclusions

Using plausible crustal strength constraints, the maximum possible superelevation of the Cascade Range due to isostatic response from valley incision is 700 m, with an average of 575 m in the north and 300 m in the south. In the Cascades, the average amount of superelevation is comparable to the average relief above the mean in that same area. The overall magnitude of uplift is relatively minor; < 25% of the altitudes of the highest peaks in their respective areas. As glacial erosion likely accounts for only about half of that superelevation, glacial widening and deepening of

valleys can not be responsible for creating the Cascade Range rainshadow or having significant effects on global cooling.

Peak uplift due to isostatic effects from valley incision can account for at most ~300 m of the difference in peak altitudes between the northern and southern Cascades. Because peak altitudes are 800 - 1000 m higher in the northern than southern Cascades (Figure 4.3), some other factor must be responsible for higher peaks in the north. Higher slopes in the Cascades of northern Washington could be responsible for raising mean altitudes above valley bottoms up to 350 m higher than those in southern Washington. While these parameters are not directly comparable, measured mean altitudes are up to 1000 m higher in the northern Cascades than in the southern Cascades. Therefore, a significant amount of the difference in mean and maximum altitudes between the northern and southern Cascades in Washington is largely due to geologic or tectonic differences between the two regions. This conclusion is consistent with previous interpretations regarding the topographic histories of the two regions (e.g., Mackin and Cary, 1965; Mitchell and Montgomery, accepted pending revisions).

Table 4.1: List of Symbols

T_e	Effective elastic thickness (km)
D	Flexural rigidity (N m)
E	Modulus of elasticity (8.35 x 1010 Nm^{-2})
v	Poisson's ratio (0.25)
N m	Newton-meters
w	"Superelevation," vertical deflection of the landscape due to rebound
ρ/α	Non-dimensional distance from point load
α	Flexural rigidity parameter
z	Equivalent eroded thickness (m)
q	Point load used in isostasy calculation
π	3.1415
ρ_m	Density of the mantle (3300 kg/m^3)
ρ_c	Density of the crust (2800 kg/m^3)
g	Acceleration due to gravity (9.81 m s-2)
Kel	Kelvin function
dx, dy	Grid cell dimensions (m)
l_s	Hillslope length (m)
ls	Mean hillslope length (m)
DD	Drainage density
θ	Slope angle
Z_m	Mean altitude above valley floor (m)
ΔZ_m	Difference in mean altitude above valley floor (m)

Table 4.2. Mean Superelevation and ARAMA in Swaths.

			Mean w (m)						w as % of ARAMA						Maximum w (m)	
Swath	Swath UTM	ARAMA	*19	20	21	22	23	24	19	20	21	22	23	24	23	24
1	5065965	450	160	169	167	187	165	86	36	37	37	41	37	19	172	90
2	5085975	346	397	344	281	247	182	89	115	99	81	71	52	26	238	118
3	5105985	340	384	378	364	334	229	107	113	111	107	98	67	32	301	146
4	5125995	344	388	398	431	417	284	133	113	115	125	121	83	39	357	172
5	5146005	462	620	595	552	490	335	158	134	129	120	106	72	34	404	196
6	5166015	438	630	605	561	505	358	172	144	138	128	115	82	39	436	213
7	5186025	428	466	479	504	513	382	186	109	112	118	120	89	44	469	229
8	5206035	428	559	548	555	575	433	212	131	128	130	134	101	49	497	241
9	5226045	433	698	678	652	633	468	228	161	157	151	146	108	53	521	250
10	5246055	547	697	701	704	671	487	236	127	128	129	123	89	43	550	263
11	5266065	579	841	807	770	726	524	253	145	139	133	125	91	44	584	282
12	5286075	478	800	785	765	742	546	265	167	164	160	155	114	56	617	300
13	5306085	568	774	758	754	751	560	274	136	134	133	132	99	48	651	318
14	5326095	635	830	815	796	777	573	278	131	128	125	122	90	44	681	331
15	5346105	582	873	848	833	798	579	280	150	146	143	137	99	48	703	340
16	5366115	612	887	870	852	805	578	278	145	142	139	132	94	45	712	343
17	5386125	601	916	879	837	794	574	277	152	146	139	132	95	46	713	343
18	5406135	565	791	787	791	780	575	279	140	139	140	138	102	49	709	341
19	5426145	496	779	759	754	753	562	275	157	153	152	152	113	55	704	340

*Numbers in this row represent the power of D, for $D = 10^{19}$

Table 4.3: Drainage Basin Characteristics.

Drainage	UTM northing of drainage centroid (m)	Basin area* (km2)	Mean ± 1σ slope (degrees)	Pourpoint altitude (m)	Mean altitude (m)	Basin relief (m)	Drainage density 1 km^2 (10^{-4} m)	Drainage density 10 km^2 (10^{-4} m)
Similkameen	5464591	1572.1	19.51 ±10.84	349	1570	2310	6.954	2.387
Nooksack	5406495	1620.6	21.43 ± 12.48	21	839	3262	7.133	2.504
Skagit	5385139	6969.7	26.93 ± 14.09	5	1094	3277	6.460	2.427
Methow	5378138	4712.3	22.23 ± 11.35	237	1416	2487	6.702	3.717
Stillaguamish	5341494	1156.4	20.90 ± 13.74	31	691	2058	6.959	2.516
Chelan	5340391	2413.0	27.21 ± 13.61	216	1346	2677	6.579	2.410
Entiat	5304868	1082.7	23.97 ± 10.52	216	1288	2603	7.018	2.327
Wenatchee	5286537	3440.0	25.20 ± 12.16	190	1200	2678	6.640	2.464
Snohomish	5284847	3518.7	26.38 ± 13.49	0.2	827	2428	6.873	2.540
Cedar-Green	5236433	903.4	22.00 ± 11.07	238	860	1510	6.676	2.254
Yakima	5217881	5538.6	17.45 ± 11.64	329	966	2100	8.382	2.545
Puyallup	5207331	2020.2	21.88 ± 12.64	61	1070	4332	7.225	2.009
Naches	5183251	2861.8	19.07 ± 11.09	329	1249	2167	7.262	2.530
Nisqually	5180140	1155.1	17.88 ± 11.89	137	816	4256	7.513	2.921
Cowlitz	5145060	5702.1	18.74 ± 12.15	3	778	4263	7.194	2.624
Klickitat	5099823	3500.4	11.73 ± 9.56	23	912	3725	8.532	2.736
Lewis	5096477	2691.6	15.72 ± 11.11	0.6	682	3666	7.605	2.535
South Columbia	5080864	2346.7	14.77 ± 10.87	20	786	3725	7.639	2.543

*Within analysis area

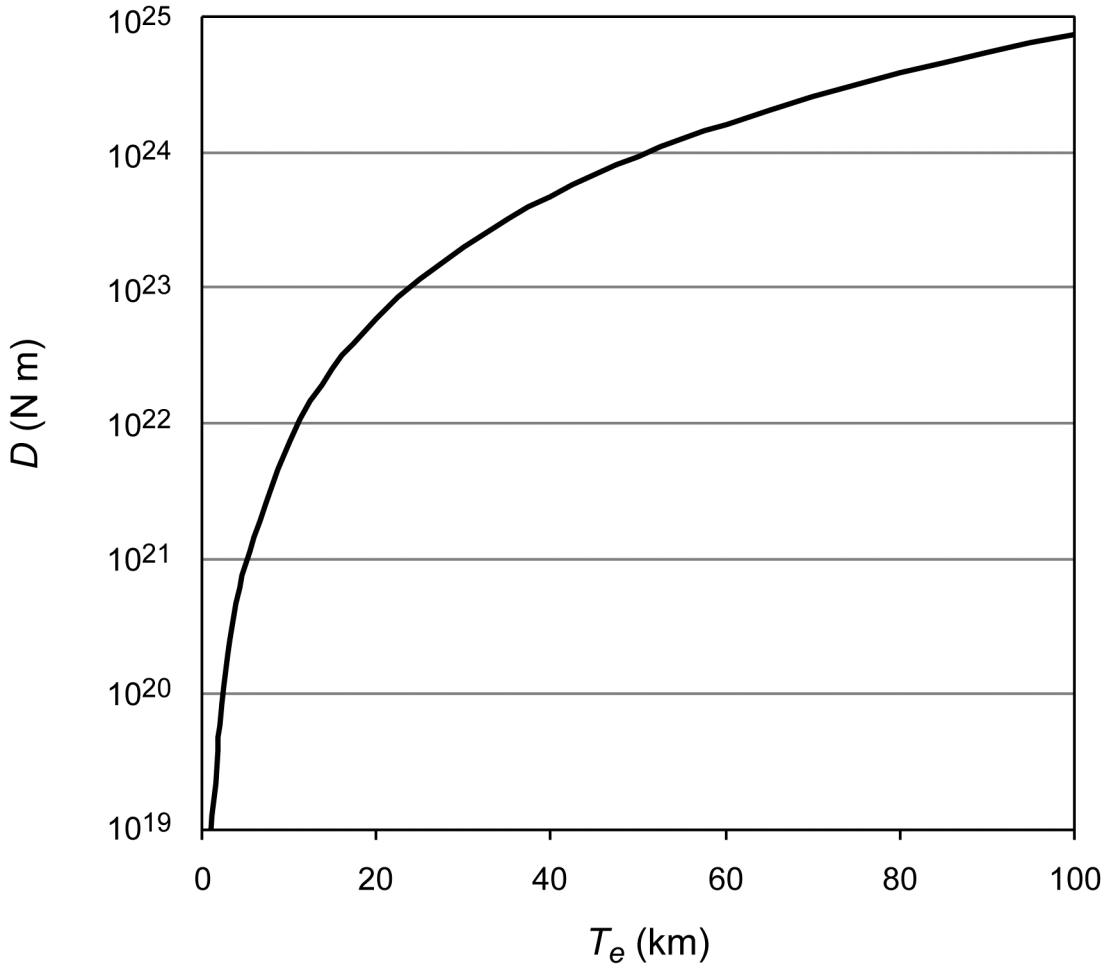

Figure 4.1: Relationship between effective elastic thickness (T_e) and flexural rigidity (D).

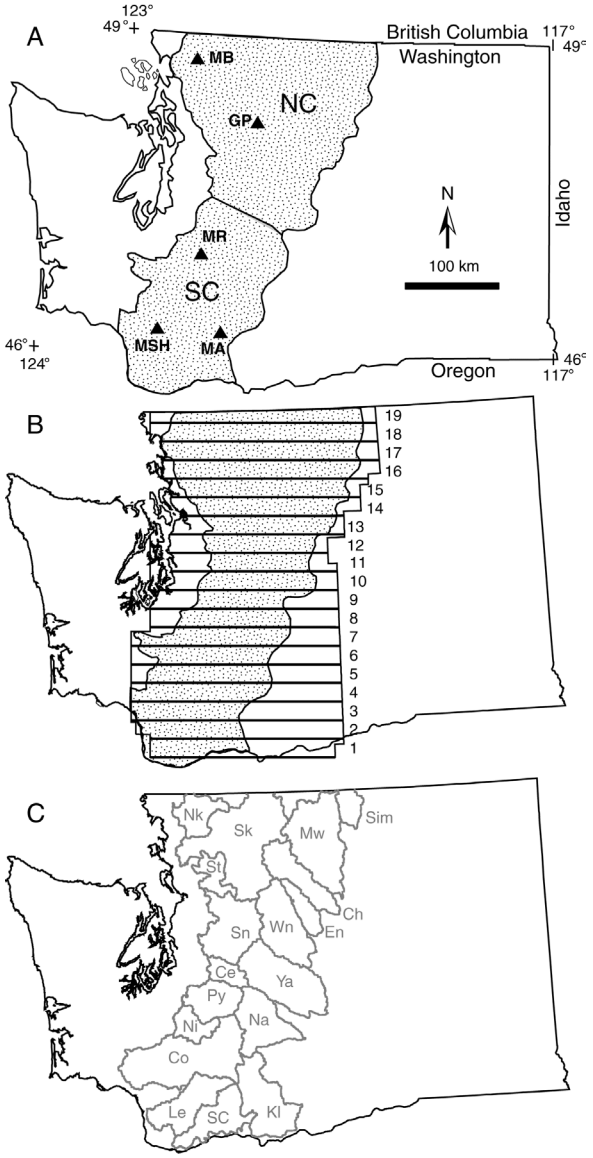

Figure 4.2: A. Location of Cascade Range (stippled region) and Quaternary volcanoes (triangles) in Washington State. North Cascades = NC, southern Cascades = SC; the division is formed by the Snoqualmie and Yakima rivers. Quaternary volcanoes are: MB = Mount Baker, GP = Glacier Peak, MR = Mt. Rainier, MA = Mount Adams, MSH = Mount St. Helens. B. Location of analysis swaths (horizontal bars) numbered 1 – 19. C. Location of drainage basins: Sim = Similkameen, Nk = Nooksack, Sk = Skagit, Mw = Methow, St = Stilliguamish, Ch = Chelan, En = Entiat, Wn = Wenatchee, Sn = Snoqualmie, Ce = Cedar-Green, Ya = Yakima, Py = Puyallup, Na = Naches, Ni = Nisqually, Co = Cowlitz, Kl = Klickitat, Le = Lewis, SC = South Columbia. Drainage basin characteristics are shown in Table 4.3.

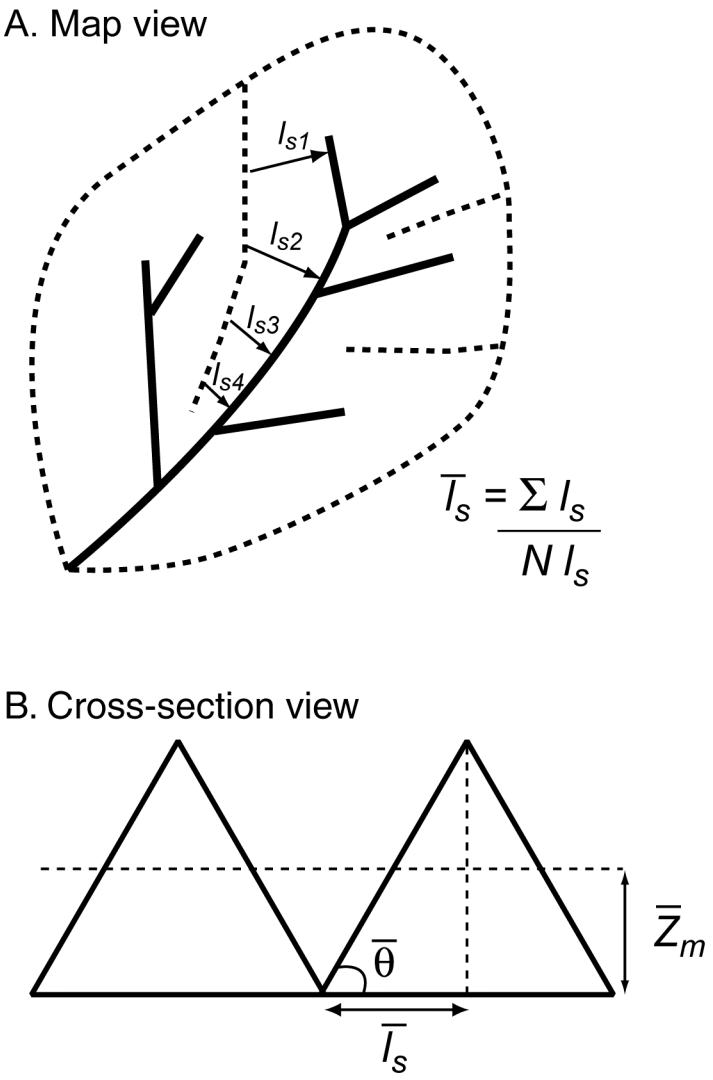

Figure 4.3: Diagrams of hillslope length (l_s) and mean altitude above the valley bottom ($\overline{Z}_m$). A. Map view of a hypothetical drainage basin; streams are solid bold lines, dashed lines are ridges (accumulation area = 1 cell). The first method for getting $\overline{l}_s$ was to determine the drainage density of each basin from stream length and basin area and use Eq. 5 to calculate mean hillslope length. The second method was to find the average steepest downslope distance between ridges and streams (l_{s1}, l_{s2}, l_{s3}...). B. Cross-section view of hypothetical drainage basin. Once the average hillslope length and slope of each basin was determined, I use Eq. 6 to find the average altitude above the valley bottoms for each basin.

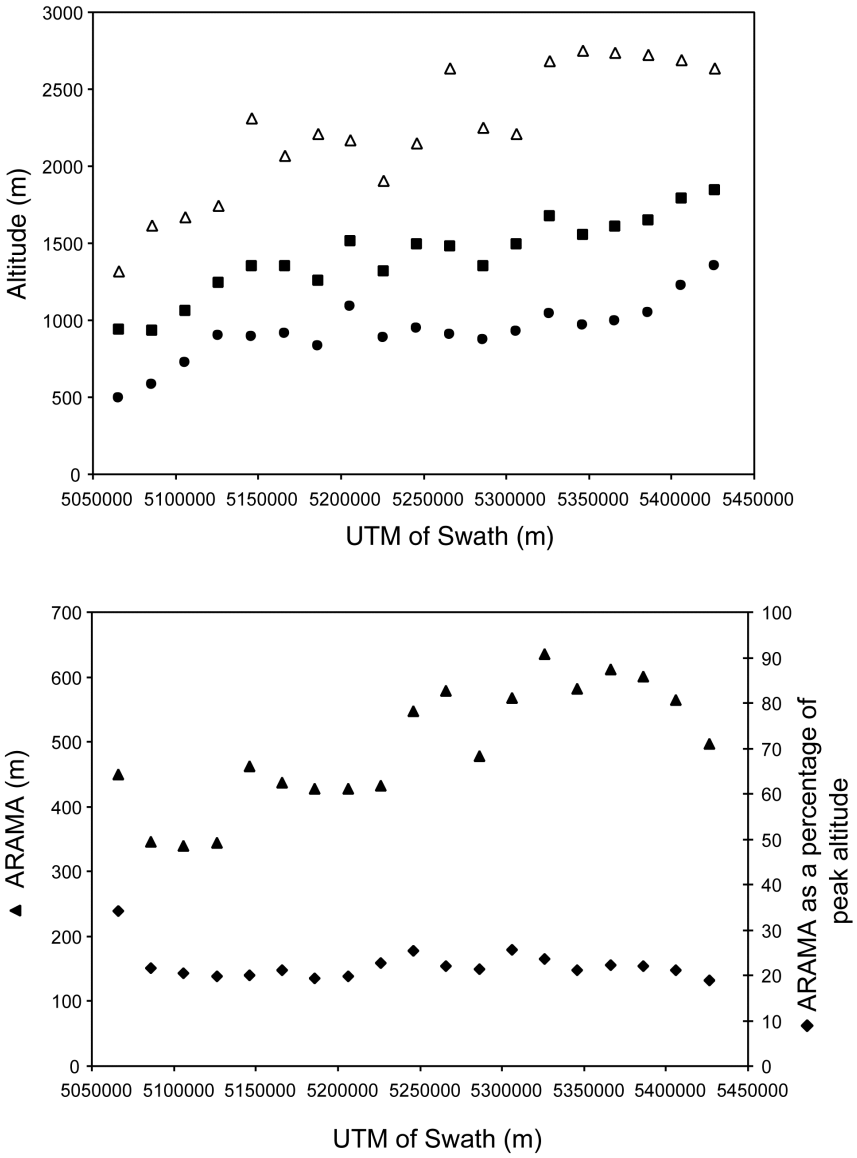

Figure 4.4: Average altitude of the five highest non-volcanic summits (open triangles), average altitude of the maximum topography profile (squares) and mean altitude (circles) in each swath shown in Figure 4.2. B. Average relief above mean altitude (ARAMA) (triangles), calculated by subtracting the mean altitude from the average maximum altitude in each swath; this value is equivalent to one-half the local relief. ARAMA as a percentage of the average altitude of the five highest peaks in each swath (diamonds).

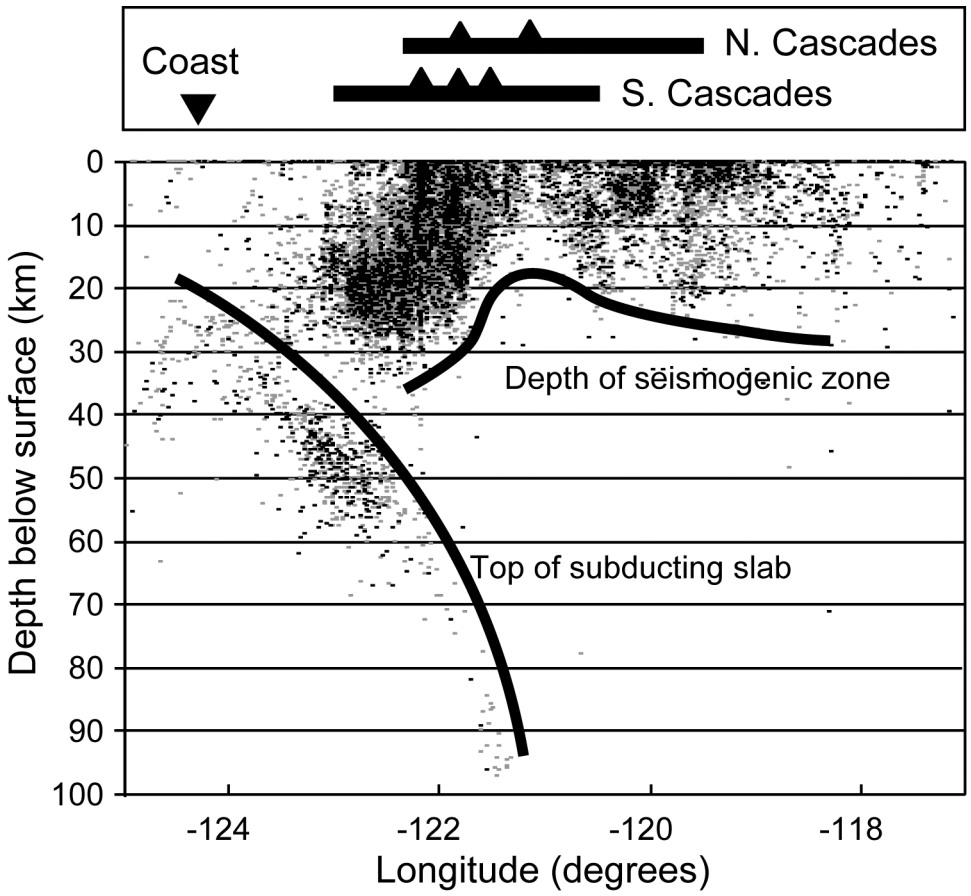

Figure 4.5: Earthquake focal depths (in km) between 45° N and 49° N latitude as a function of longitude (decimal degrees) in Washington State, 1965-2006 (data from Pacific Northwest Seismograph Network). Earthquakes with M > 2 (N = 8,910) are shown as black dots, earthquakes with 1 < M < 2 (N = 17,387) are shown as gray dots. Top panel shows approximate longitude of the coast (downward triangle), the western and eastern limits of the Cascades (horizontal bars), and the Quaternary volcanoes (triangles).

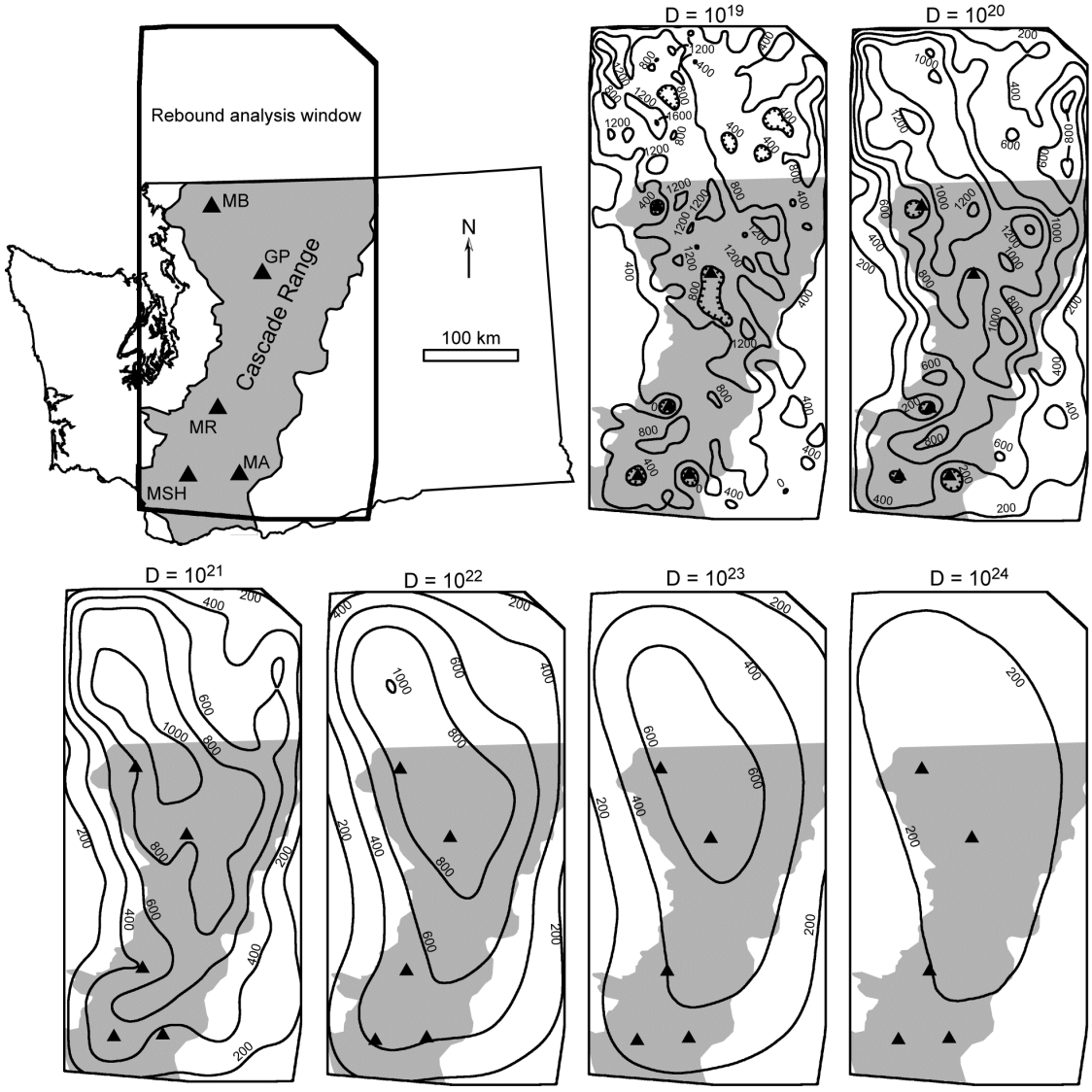

Figure 4.6: Contour maps of vertical deflection (superelevation) due to valley incision (w, see Equation 2). Upper left shows relationship between rebound analysis window, Cascade region, and Washington State borders. Quaternary volcanoes are indicated with triangles and Cascade region is shaded. The six panels represent superelevation (w from Eq. 2) calculated using different flexural rigidities (D), noted above each panel. Note that the contour interval for $D = 10^{19}$ panel is 400 m; contour interval = 200 m for all other panels.

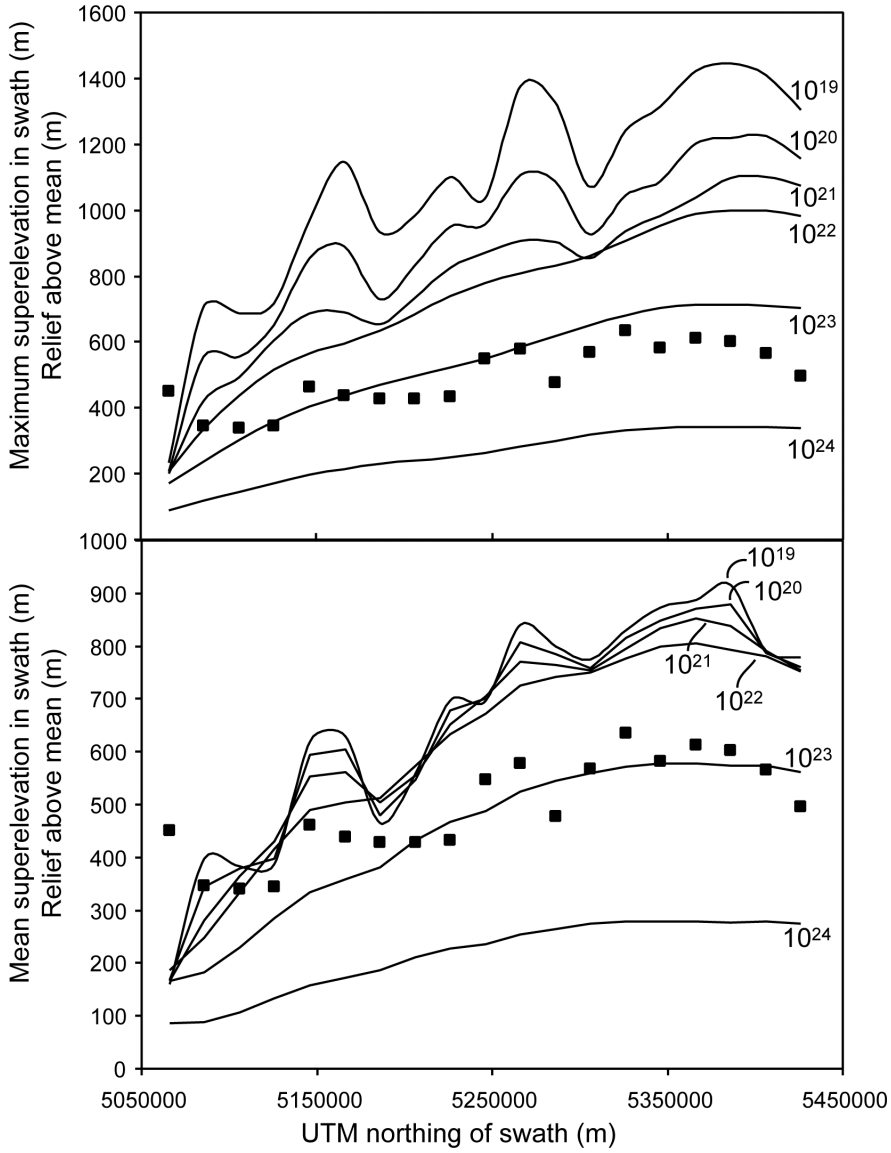

Figure 4.7: Maximum (top panel) and mean (bottom panel) superelevation in each swath (Figure 4.2) for flexural rigidities of $D = 10^{19}$, 10^{20}, 10^{21}, 10^{22}, 10^{23}, and 10^{24} N m. Squares show ARAMA for each swath.

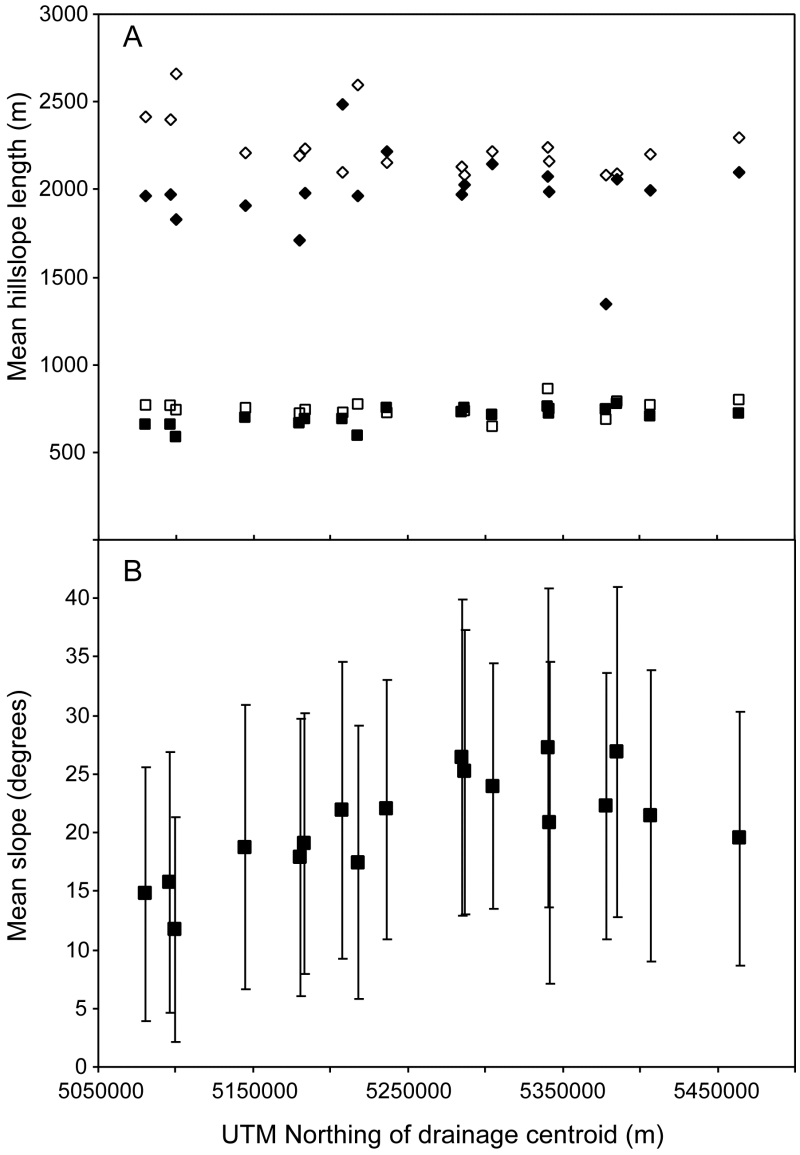

Figure 4.8: A. Mean hillslope lengths calculated for drainage basins (Figure 4.2C). Diamonds are values calculated from 10 km^2 accumulation area: open = downslope method, filled = drainage density method. Squares are values calculated from 1 km^2 accumulation area: open = downslope method, filled = drainage density method. B. Mean slope angle of all cells in each basin; error bars represent 1σ.

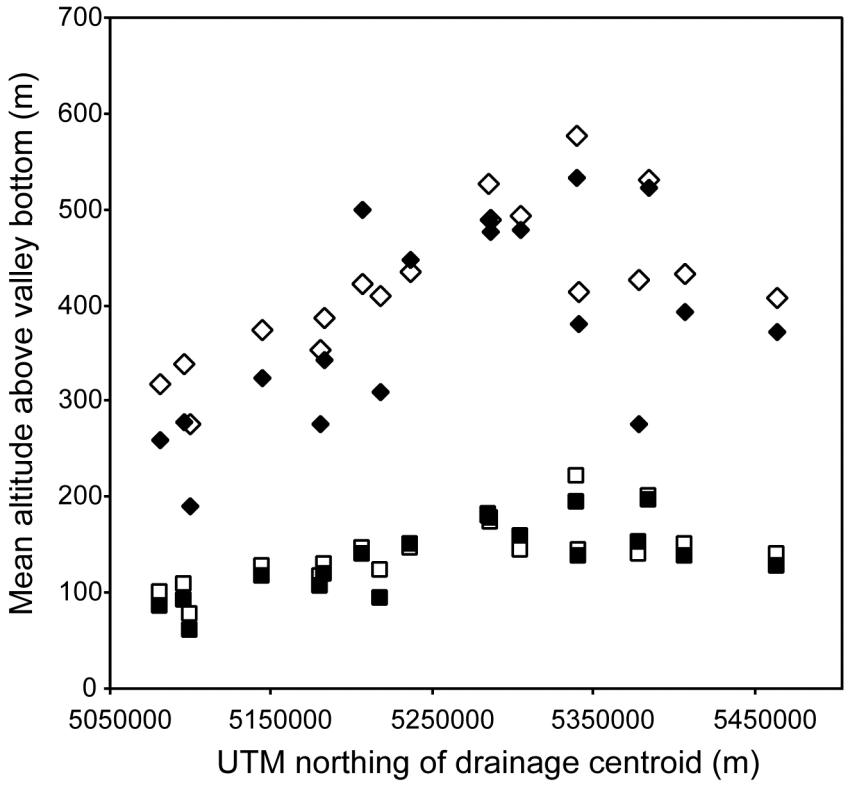

Figure 4.9: Modeled mean altitude above valley bottoms for Cascade drainage basins (Figure 4.2C, Table 4.3). Diamonds are values calculated from 10 km^2 accumulation area: open = downslope method, filled = drainage density method. Squares are values calculated from 1 km^2 accumulation area: open = downslope method, filled = drainage density method.

Notes to Chapter 4

Abramowitz, M. and Stegun, I.A., 1965, Handbook of Mathematical Functions, Dover Publications, New York.

Amerson, B., 2005, Morphometry of glacial and fluvial valleys in central Idaho [M.S. thesis]: Seattle, University of Washington, 49 p.

Burov, E.B., Diament, M., 1995, The effective elastic thickness (T_e) of continental lithosphere: What does it really mean?: Journal of Geophysical Research, v. 100, 3905-3927.

Burov, E.B., Watts, A.B., 2006, The long-term strength of the continental lithosphere: "jelly sandwich" or "crème brûlée"?: GSA Today v. 16, p. 4-10.

Clague, J.J. and James, T.S., 2002, History and isostatic effects of the last ice sheet in southern British Columbia: Quaternary Science Reviews, v. 21, p. 71-87.

Cohen, S.C. and Darby, D.J., 2003, Tectonic plate coupling and elastic thickness derived from the inversion of a steady state viscoelastic model using geodetic data: Application to southern North Island, New Zealand: Journal of Geophysical Research, v. 108, no. B3, 2164, doi:10.1029/2001JB001687.

Fluck, P., Hyndman, R.D., and Lowe, C., 2003, Effective elastic thickness T_e of the lithosphere in western Canada: Journal of Geophysical Research, v. 108, no. B9, 2430, doi:10.1029/2002JB002201.

Gilchrist, A.R., Summerfield, M.A., Cockburn, H.A.P., 1994, Landscape dissection, isostatic uplift, and the morphologic development of orogens: Geology, v. 22, no. 11, p. 963-966.

Haugerud, R.A., 2004, Cascadia—Physiography: USGS Miscellaneous Investigations Map I-2689.

Holmes, A., 1945, *Principles of Physical Geology*. Ronald Press, New York, 532 p.

Horton, R.E., 1945, Erosional development of streams and their drainage basins, hydrophysical approach to quantitative morphology: Geological Society of America Bulletin, v. 56, p. 275-370.

James, T.S., Clague, J.J., Wang, K., Hutchinson, I., 2000, Postglacial rebound at the northern Cascadia subduction zone: Quaternary Science Reviews v. 19, p. 1527-1541.

Lowry, A.R., Ribe, N.M., Smith, R.B,. 2000, Dynamic elevation of the Cordillera, western United States: Journal of Geophysical Research, v. 105, no. B10, p. 23,372-23,390.

Mackin, J.H., and Cary, A.S., 1965, Origin of Cascade landscapes: Washington Division of Mines and Geology Information Circular 41, 35 p.

Maggi, A., Jackson, J.A., McKenzie, D., Priestley, K. 2000, Earthquake focal depths, effective elastic thickness, and the strength of the continental lithosphere: Geology v. 28: no. 6, 485-498.

Miller, R.B., and Paterson, S.R., 2001, Influence of lithological heterogeneity, mechanical anisotropy, and magmatism on the rheology of an arc, North Cascades, Washington: Tectonophysics, v. 342, p. 351-370.

Mitchell, S.G. and Montgomery, D.R., 2006, Influence of a glacial buzzsaw on the height and morphology of the Cascade Range in central Washington State, USA: Quaternary Research, v. 65, p. 96-107.

Molnar, P., England, P.C., 1990, Late Cenozoic uplift of mountain peaks: Chicken or egg?: Nature, v. 346, p. 29-34.

Montgomery, D.R., 2002, Valley formation by fluvial and glacial erosion: Geology, v. 30, no. 11, p. 1047-1050.

Montgomery, D.R. and Greenberg, H.M., 2000, Local relief and the height of Mt. Olympus: Earth Surface Processes and Landforms, v. 25, p. 385-396.

Montgomery, D.R., 1994, Valley incision and the uplift of mountain peaks: Journal of Geophysical Research, v. 99, no. B7, p. 13,913-13,921.

Pelletier, J.D., 2004, Estimate of three-dimensional flexural-isostatic response to unloading: Rock uplift due to late Cenozoic glacial erosion in the western United States: Geology, v. 32, no. 2, p. 161-164.

Perez-Gussinye, M., Lowry, A.R., Watts, A.B., Velicogna, I.. 2004, On the recovery of effective elastic thickness using spectral methods: Examples from synthetic data and from the Fennoscandian Shield: Journal of Geophysical Research, v. 109, no. B10, B10409. DOI: 10.1029/2003JB002788.

Schuster, J.E., 2005, Geologic map of Washington State: Washington Division of Geology and Earth Resources GM 53, 1 sheet, scale 1:500,000, 44 p. text.

Small, E.E., Anderson, R.S., 1998, Pleistocene relief production in Laramide mountain ranges, western United States: Geology v. 26, no. 2, 123-126.

Small, E.E. and Anderson, R.S., 1995, Geomorphically driven late Cenozoic rock uplift in the Sierra Nevada, California: Science, v. 270, p. 277-280.

Stern, T.A, Baxter, A.K., Barrett, P.J., 2005, Isostatic rebound due to glacial erosion within the Transantarctic Mountains: Geology v. 33, no. 3, p. 221-224.

Turcotte, D.L., Schubert, G., 1982, Geodynamics: Applications of continuum physics to geological problems: Wiley: New York, 450 p.

Wager, L.R., 1933, The rise of the Himalaya: Nature, v. 132, p. 28.

Watts, A.B. and Burov, E.B., 2003, Lithospheric strength and its relationship to the elastic and seismogenic layer thickness: Earth and Planetary Science Letters, v. 213, p. 113-131.

LIST OF REFERENCES

Abramowitz, M. and Stegun, I.A., 1965, Handbook of Mathematical Functions, Dover Publications, New York.

Amerson, B., 2005. Morphometry of fluvial and glacial valleys in central Idaho. Unpublished M.S. thesis, University of Washington, 43 p.

Anderson, J.L., and Vogt, B.F, 1987, Intracanyon flows of the Columbia River Basalt group in the southwest part of the Columbia Plateau and adjacent Cascade Range, Oregon and Washington, in, Schuster, J.E., editor, Selected papers on the geology of Washington: Bulletin of the Washington Department of Natural Resources, Division of Geology and Earth Resources, v. 77, p. 249-267.

Bagnold, R.A., 1960. Flow resistance in sinuous or irregular channels: part 2, A theoretical model of energy loss in curved channels. USGS Professional paper, 122-130.

Ballantyne, C.K., 2002. Paraglacial geomorphology. Quaternary Science Reviews 21, 1935-2017.

Bates, R.G., Beck, M.E., Jr., and Burmester, R.F., 1981, Tectonic rotations in the Cascade Range of southern Washington: Geology, v. 9, no. 4, p. 184-189.

Beck, G.F., 1945, Ancient forest tress of the sagebrush area in central Washington: Journal of Forestry, v. 43, no. 5, p. 334-338.

Beeson, M.H., and Tolan, T.L., 1989, The Columbia River Basalt Group in the Cascade Range—a middle Miocene reference datum for structural analysis: *in* Muffler, L.J.P., Weaver, C.S., Blackwell, D.D. editors, Proceedings of workshop XLIV—Geological, geophysical and tectonic setting of the Cascade Range: US Geological Survey Open File Report 89-178, p. 257-290.

Benn, D.I. and Lehmkuhl, F., 2000. Mass balance and equilibrium-line altitudes of glaciers in high-mountain environments. Quaternary International 65/66, 15-29.

Bennett, M.R., Huddart, D., Glasser, N.F., 1999, Large-scale bedrock displacement by cirque glaciers: Arctic, Antarctic, and Alpine Research, v. 31, p. 99-107.

Booth, D.B., Troost, K.G., Clague, J.J., and Waitt, R.B., 2004. The Cordilleran Ice Sheet, In: Gillespie, A.R., Porter, S.C., and Atwater, B.F., eds., The Quaternary period in the United States, Developments in Quaternary Science 1, 17-43.

Brandon, M.T., Roden-Tice, M.K., and Garver, J.I., 1998, Late Cenozoic exhumation of the Cascadia accretionary wedge in the Olympic Mountains, Northwest

Washington State: Geological Society of America Bulletin, v. 110, no. 8, p. 985-1009.

Brocklehurst, S.H., and Whipple, K.X., 2002. Glacial erosion and relief production in the eastern Sierra Nevada, California. Geomorphology 42, 1-24.

Brocklehurst, S.H., and Whipple, K.X., 2004. Hypsometry of glaciated landscapes. Earth Surface Processes and Landforms 29, 907-926.

Brozovic, N., Burbank, D.W., and Meigs, A.J., 1997. Climatic limits on landscape development in the northwestern Himalaya. Science 276, 571-574.

Bunning, B.B., 1990, Geologic map of the east half of the Twisp 1:100,000 quadrangle, Washington: Washington Division of Geology and Earth Resources Open File Report 90-9, 51 p., 1 plate.

Burbank, D.W., 2002, Rates of erosion and their implications for exhumation: Mineralogical Magazine, v. 66, no. 1(434), p. 25-52.

Burbank, D.W., Leland, J., Fielding, E., Anderson, R.S., Brozovic, N., Reid, M.R., and Duncan, C., 1996. Bedrock incision, rock uplift and threshold hillslopes in the northwestern Himalayas. Nature 379, 505-510.

Burov, E.B., Diament, M., 1995, The effective elastic thickness (T_e) of continental lithosphere: What does it really mean?: Journal of Geophysical Research, v. 100, 3905-3927.

Burov, E.B., Watts, A.B., 2006, The long-term strength of the continental lithosphere: "jelly sandwich" or "crème brûlée"?: GSA Today v. 16, p. 4-10.

Campbell, N.P., 1988, Structural geology along the northwestern Columbia River basalt margin, Washington: Washington Division of Geology and Earth Resources Open File Report 88-5, 108 p., 8 plates.

Chamberlain, C.P., and Poage, M.A., 2000, Reconstructing the paleotopography of mountain belts from the isotopic composition of authigenic minerals: Geology v. 28, no 2, p. 115-118.

Chaney, R.W., 1938, Paleoecological interpretations of Cenozoic plants in western North America: Botanical Review, v. 4, p. 371-396.

Chaney, R.W., 1959, Miocene floras of the Columbia Plateau—Part 1, Composition and interpretation: Carnegie Institution of Washington Publication, v. 617, p. 1-34.

Cheney, E.S., 1997, What is the age and extent of the Cascade magmatic arc?: Washington Geology, v. 25, no. 2, p. 28-32.

Charlesworth, J.K., 1957. The Quaternary Era. Arnold, London.

Christiansen, R.L., Yeats, R.S., Graham, S.A., Niem, W.A., Niem, A.R., and Snavely, P.D. Jr., 1992, Post-Laramide geology of the U.S. Cordilleran region, *in* Burchfiel, B.C., Lipman, P.W., and Zoback, M.L., editors, The Cordilleran Orogen; conterminous U.S.: The Geology of North America v. G-3, Geological Society of America, p. 261-406.

Clague, J.J. and James, T.S., 2002, History and isostatic effects of the last ice sheet in southern British Columbia: Quaternary Science Reviews, v. 21, p. 71-87.

Cohen, S.C. and Darby, D.J., 2003, Tectonic plate coupling and elastic thickness derived from the inversion of a steady state viscoelastic model using geodetic data: Application to southern North Island, New Zealand: Journal of Geophysical Research, v. 108, no. B3, 2164, doi:10.1029/2001JB001687.

Daly, R.A., 1905. The accordance of summit levels among alpine mountains; the fact and its significance. Journal of Geology, 105-125.

Dragovich, J.D., Logan, R.L., Schasse, H.W., Walsh, T.J., Lingley, W.S., Norman, D.K., Gerstel, W.J., Lapen, T.J., Schuster, J.E., and Meyers, K.D., 2002, Geologic map of Washington; northwest quadrant: Washington Division of Geology and Earth Resources Geologic Map GM-50, 3 sheets, scale 1:250,000, with 72 p. text.

Dragovich, J.D., and Norman, D.K., 1995, Geologic map of the west half of the Twisp 1:100,000 quadrangle, Washington: Washington Division of Geology and Earth Resources Open File Report 95-3, 63 p., 1 pl.

England, P.C., and Molnar, P., 1990, Surface uplift, uplift of rocks, and exhumation of rocks: Geology, v. 18, no 12, p. 1173-1177.

England, P.C., and Wells, R.E., 1991, Neogene rotations and quasicontinuous deformation of the Pacific Northwest continental margin: Geology, v. 19, p. 978-981.

Evarts, R.C., and Swanson, D.A., 1994, Geologic transect across the Tertiary Cascade Range, southern Washington, *in* Swanson, D. A.; Haugerud, R. A., editors, Geologic field trips in the Pacific Northwest: University of Washington Department of Geological Sciences, v. 2, p. 2H 1 - 2H 31.

Farley, K.A., 2002, (U-Th)/He dating: Techniques, calibrations, and applications *in*: Noble Gases in Geochemistry and Cosmochemistry, Reviews in Mineralogy and Geochemistry, v. 47, p. 819-844.

Finlayson, D.P. and Montgomery, D.R., 2003. Modeling large-scale fluvial erosion in geographic information systems. Geomorphology 53, 147-164.

Foster, R.J., 1960, Tertiary geology of a portion of the central Cascade Mountains, Washington: Bulletin of the Geological Society of America, v. 71, p. 99-126.

Fluck, P., Hyndman, R.D., and Lowe, C., 2003, Effective elastic thickness T_e of the lithosphere in western Canada: Journal of Geophysical Research, v. 108, no. B9, 2430, doi:10.1029/2002JB002201.

Frizzell, V.A., Jr., Tabor, R.W., Booth, D.B., Ort, K.M., and Waitt, R.B., 1984, Preliminary geologic map of the Snoqualmie Pass 1:100,000 quadrangle, Washington: U.S. Geological Survey Open-File Report 84-693, 43 p., 1 plate, scale1:100,000.

Gilchrist, A.R., Summerfield, M.A., and Cockburn, H.A.P., 1994, Landscape dissection, isostatic uplift, and the morphologic development of orogens: Geology, v. 22, p. 963-966.

Gulick, C. W., and Korosec, M.A., 1990a, Geologic map of the Banks Lake 1:100,000 quadrangle, Washington: Washington Division of Geology and Earth Resources Open File Report 90-6, 20 p., 1 plate.

Gulick, C.W., and Korosec, M.A., 1990b, Geologic map of the Omak 1:100,000 quadrangle, Washington: Washington Division of Geology and Earth Resources Open File Report 90-12, 52 p., 1 plate.

Gresens, R.L., 1980, Deformation of the Wenatchee Formation and its bearing on the tectonic history of the Chiwaukum Graben, Washington, during Cenozoic time: Geological Society of America Bulletin, v. 91, no. 1, p. ?

Hagstrum, J.T., Swanson, D.A., and Evarts, R.C., 1999, Paleomagnetism of an east-west transect across the Cascade arc in southern Washington--Implications for regional tectonism: Journal of Geophysical Research, v. 104, no. B6, p. 12,853-12,863.

Hallet, B., Hunter, L., and Bogen, L., 1996. Rates of erosion and sediment evacuation by glaciers; a review of field data and their implications. Global and Planetary Change 12, 213-235.

Hammond, P.E., 1998, Tertiary andesitic lava-flow complexes (stratovolcanoes) in the southern Cascade Range of Washington—observations on tectonic processes within the Cascade arc: Washington Geology, v. 26, no. 1, p. 20-30.

Hammond, P.E., Brunstad, K.A., Hooper, P.R., and Cole, S.F., 1992, Isolated occurrences of Columbia River basalt flows at Steamboat Mountain, southern Washington Cascade Range--Indication of yet greater westward extent of these flood-basalt flows: Oregon Academy of Sciences, Proceedings--Volume XXVIII: Oregon Academy of Science, p. 38.

Hammond, P.E., 1988, The Cascade paleosurface: Geological Society of America Abstracts with Programs, v. 20, no. 7, p. A284.

Harbor, J.M., 1992, Numerical modeling of the development of U-shaped valleys by glacial erosion: Geological Society of America Bulletin, v. 104, p. 1364-1375.

Harbor, J.M. and Warburton, J., 1993, Relative rates of glacial and nonglacial erosion in alpine environments: Arctic and Alpine Research, v. 25, p. 1-7.

Haugerud, R.A., 2004, Cascadia—Physiography: USGS Miscellaneous Investigations Map I-2689.

Haugerud, R.A., van der Heyden, P., Tabor, R.W., Stacey, J.S., and Zartman, R.E., 1991, Late Cretaceous and early Tertiary plutonism and deformation in the Skagit Gneiss Complex, North Cascade Range, Washington and British Columbia: Geological Society of America Bulletin, v. 103, p. 1297-1307.

Holmes, A., 1944, *Principles of Physical Geology*, Thomas Nelson and Sons, London, 532 p.

Horton, R.E., 1945, Erosional development of streams and their drainage basins, hydrophysical approach to quantitative morphology: Geological Society of America Bulletin, v. 56, p. 275-370.

House, M.A., Wernicke, B.P., Farley, K.A., 1997. Dating topography of the Sierra Nevada, California, using apatite (U-Th)/He ages. Nature 396, 66-69.

Hunting, M.T., Bennett, W.A., Livingston, V.E., Jr., and Moen, W.S., 1961, Geologic Map of Washington: Washington Department of Conservation, Division of Mines and Geology, 1 plate, scale 1:500,000.

James, A.L., 2003. Glacial erosion and geomorphology in the northwest Sierra Nevada, CA. Geomorphology, 55, 283-303.

James, T.S., Clague, J.J., Wang, K., and Hutchinson, I. 2000, Postglacial rebound at the northern Cascadia subduction zone: Quaternary Science Reviews, v. 19, p. 1527-1541.

Johnson, S.Y., 1984, Stratigraphy, age, and paleogeography of the Eocene Chuckanut Formation, Northwest Washington: Canadian Journal of Earth Sciences, v. 21, no. 1, p. 92-106.

Kaufman , D.S., Porter, S.C., and Gillespie, A.R., 2004, Quaternary alpine glaciation in Alaska, the Pacific Northwest, Sierra Nevada, and Hawaii: in Gillespie, A.R., Porter, S.C., and Atwater, B.F., eds., *The Quaternary Period in the United States*, Amsterdam, Elsevier, p. 77-103.

Korosec, M.A., 1987a, Geologic map of the Hood River quadrangle, Washington and Oregon: Washington Division of Geology and Earth Resources Open File Report 87-6, 40 p., 1 plate, scale 1:100,000.

Korosec, M.A., 1987b, Geologic map of the Mount Adams quadrangle, Washington: Washington Division of Geology and Earth Resources Open File Report 87-5, 39 p., 1 plate, scale 1:100,000.

Leopold, E.B., and Denton, M.F., 1987, Comparative age of grassland and steppe east and west of the northern Rocky Mountains: Annals of the Missouri Botanical Garden, v. 74, p. 841-867.

Logan, R.L., 1987, Geologic map of the Chehalis River and Westport quadrangles, Washington: Washington Division of Geology and Earth Resources Open File Report 87-8, 16 p., 1 plate, scale 1:100,000.

Long, W. A., 1951. Glacial geology of the Wenatchee-Entiat area, Washington. Northwest Science, 25, 3-16.

Lowry, A.R., Ribe, N.M., and Smith, R.B., 2000, Dynamic elevation of the Cordillera, western United States: Journal of Geophysical Research, v. 105, no B10, p. 23,371-23,390.

MacGregor, K.R., Anderson, R.S., Anderson, S.P., and Waddington, E.D., 2000. Numerical simulations of glacial-valley longitudinal profile evolution. Geology 28, 1031-1034.

Mackin, J. H., 1941. Glacial geology of the Snoqualmie-Cedar area, Washington. Journal of Geology 49, 449-481.

Mackin, J.H., and Cary, A.S., 1965, Origin of Cascade landscapes: Washington Division of Mines and Geology Information Circular 41, 35 p.

Maggi, A., Jackson, J.A., McKenzie, D., Priestley, K. 2000, Earthquake focal depths, effective elastic thickness, and the strength of the continental lithosphere: Geology v. 28: no. 6, 485-498.

Martin, Y., 2000. Modelling hillslope evolution: linear and nonlinear transport relations. Geomorphology 34, 1-21.

Martin, Y., and Church, M., 1997. Diffusion in landscape development models: on the nature of basic transport relations. Earth Surface Processes and Landforms 22, 273-279.

Mathews, W.H., 1981, Early Cenozoic resetting of potassium-argon dates and geothermal history of North Okanagan area: British Columbia. Canadian Journal of Earth Sciences, v. 18, no. 8, p. 1310-1319.

Matsuoka, N. and Sakai, H. 1999, Rockfall activity from an alpine cliff during thawing periods: Geomorphology, v. 28, p. 309-328.

Mazzotti, S., Dragert, H., Henton, J., Schmidt, M., Hyndman, R., James, T., Lu, Yuan and Craymer, M., 2003, Current tectonics of northern Cascadia from a decade of GPS measurements: Journal of Geophysical Research, v. 108, no. B12, doi: 10.1029/2003JB002653.

McDaniel, P.A., Othberg, K.L., and Breckenridge, R.M., 1998, Paleogeomorphic evolution of the Columbia River basalt embayments, western margin of the northern Rocky Mountains—Part II, Miocene paleosols: Geological Society of America Abstracts with Programs, v. 30, no. 6, p. 15.

McGroder, M.F., 1991, Reconciliation of two-sided thrusting, burial metamorphism, and diachronous uplift in the Cascades of Washington and British Columbia: Geological Society of America Bulletin, v. 103, no. 2, p. 189-209.

Meigs, A., and Sauber, J., 2000. Southern Alaska as an example of the long-term consequences of mountain building under the influence of glaciers. Quaternary Science Reviews 19, 1543-1562.

Miller, R.B., 1989, The Mesozoic Rimrock Lake inlier, southern Washington Cascades: Implications for the basement to the Columbia Embayment: Geological Society of America Bulletin, v. 101, p. 1289-1305.

Miller, R.B., and Paterson, S.R., 2001, Influence of lithological heterogeneity, mechanical anisotropy, and magmatism on the rheology of an arc, North Cascades, Washington: Tectonophysics, v. 342, p. 351-370.

Mills, J.E., 1892. Stratigraphy and succession of the rocks of the Sierra Nevada of California. Geological Society of America Bulletin, 413-444.

Mitchell, S.G. and Montgomery, D.R., 2006, Influence of a glacial buzzsaw on the height and morphology of the Cascade Range in central Washington State, USA: Quaternary Research, v. 65, p. 96-107.

Mitchell, S.G., Matmon, A, Bierman, P. R., Enzel, Y., Caffee, M., and Rizzo, D., 2001, Displacement history of the Nahef East fault, northern Israel, using cosmogenic ^{36}Cl: Journal of Geophysical Research, v. 106, no. B3, p. 4247-4264.

Molnar, P. and England, P.C., 1990. Late Cenozoic uplift of mountain ranges and global climate change: Chicken or egg?: Nature, v. 346, p. 29-34.

Montgomery, D.R., 1994, Valley incision and the uplift of mountain peaks: Journal of Geophysical Research, v. 99, no. B7, p. 13,913-13,921.

Montgomery, D.R., Balco, G., and Willett, S.D., 2001. Climate, tectonics, and the morphology of the Andes. Geology 29, 579-582.

Montgomery, D.R., 2001. Slope distributions, threshold hillslopes, and steady-state topography. American Journal of Science 301, 432-454.

Montgomery, D.R., 2002. Valley formation by fluvial and glacial erosion. Geology 30, 1047-1050.

Montgomery, D.R. and Brandon, M.T., 2002. Topographic controls on erosion rates in tectonically active mountain ranges. Earth and Planetary Science Letters 201, 481-489.

Montgomery, D.R. and Greenberg, H.M., 2000, Local relief and the height of Mt. Olympus: Earth Surface Processes and Landforms, v. 25, p. 385-396.

Mullineaux, D.R., Gard, L.M., and Jr., Crandell, D.R., 1959, Continental sediments of Miocene age in Puget Sound lowland, Washington: American Association of Petroleum Geologists Bulletin, v. 43, no. 3, pt. 1, p. 688-696.

Mustoe, G.E., 2001, Washington's fossil forests: Washington Geology, v. 29, p. 10-20.

Oskin, M., Burbank, D.W., 2005, Alpine landscape evolution dominated by cirque retreat: Geology, v. 33, no. 12, p. 933-936.

Page, B.M., 1939. Multiple alpine glaciation in the Leavenworth area, Washington. Journal of Geology 47, 785-815.

Pelletier, J.D., 2004, Estimate of three-dimensional flexural-isostatic response to unloading: Rock uplift due to late Cenozoic glacial erosion in the western United States: Geology, v. 32, no. 2, p. 161-164.

Perez-Gussinye, M., Lowry, A.R., Watts, A.B., Velicogna, I.. 2004, On the recovery of effective elastic thickness using spectral methods: Examples from synthetic data and from the Fennoscandian Shield: Journal of Geophysical Research, v. 109, no. B10, B10409. DOI: 10.1029/2003JB002788.

Phillips, W.M., and Walsh, T. J., 1987, Geologic map of the northwest part of the Goldendale quadrangle, Washington: Washington Division of Geology and Earth Resources Open File Report 87-13, 7 p., 1 pl., scale 1:100,000.

Phillips, W.M., 1987a, Geologic map of the Mount St. Helens quadrangle, Washington and Oregon: Washington Division of Geology and Earth Resources Open File Report 87-4, 59 p., 1 plate, scale 1:100,000.

Phillips, W.M., 1987b, Geologic map of the Vancouver quadrangle, Washington [and Oregon]: Washington Division of Geology and Earth Resources Open File Report 87-10, 27 p., 1 plate, scale 1:100,000.

Porter, S.C., 2001. Snowline depression in the tropics during the Last Glaciation. Quaternary Science Reviews 20, 1067-1091.

Porter, S.C., 1989. Some geological implications of average Quaternary glacial conditions. Quaternary Research 32, 245-261.

Porter, S.C., 1977. Present and past glaciation threshold in the Cascade Range, Washington, U.S.A.: topographic and climatic controls, and paleoclimate implications. Journal of Glaciology 18, 101-116.

Porter, S. C., 1976a. Pleistocene glaciation on the southern part of the North Cascade Range, Washington. Geological Society of America Bulletin 87, 61-75.

Porter, S. C., 1976b. Geomorphic evidence of post-Miocene deformation of the eastern North Cascade Range. Geological Society of America Abstracts with Programs, 8, 402-403.

Porter, S.C., 1964. Composite Pleistocene snow line of Olympic Mountains and Cascade Range, Washington. Geological Society of America Bulletin 75, 477-482.

Power, S.G., Field, C.W., Armstrong, R.L., and Harakal, J.E., 1981, K-Ar ages of plutonism and mineralization, western Cascades, Oregon and southern Washington: Isochron/West, no. 31, p. 27-29.

Reidel, S.P., Tolan, T.L., Hooper, P.R., Beeson, M.H., Fecht, K.R., Bentley, R.D., and Anderson, J.L., 1989, The Grande Ronde Basalt, Columbia River Basalt Group; Stratigraphic descriptions and correlations in Washington, Oregon, and Idaho, *in* Reidel, S. P.; Hooper, P. R., editors, Volcanism and tectonism in the Columbia River flood-basalt province: Geological Society of America Special Paper 239, p. 21-53.

Reiners, P.W., Ehlers, T.A., Mitchell, S.G., and Montgomery, D.R., 2003. Coupled spatial variations in precipitation and long-term erosion rates across the Washington Cascades. Nature 426, 645-647.

Reiners, P.W., Ehlers, T.A., Garver, J.I., Mitchell, S.G., Montgomery, D.R., Vance, J.A., and Nicolescu, S., 2002. Late Miocene exhumation and uplift of the Washington Cascade Range. Geology 30, 767-770.

Roe, G.H., Montgomery, D.R., and Hallet, B., 2002. Effects of orographic precipitation variations on the concavity of steady-state river profiles. Geology 30, 143-146.

Roering, J.J., Kirchner, J.W., and Dietrich, W.E., 1999. Evidence for nonlinear, diffusive sediment transport on hillslopes and implications for landscape morphology. Water Resources Research 35, 853-870.

Rudberg, S., 1984. Fossil glacial cirques or cirque problematica at lower levels in northern and central Sweden. Geografiska Annaler 66A, 29-39.

Russell, I.C., 1900. A preliminary paper on the geology of the Cascade Mountains in northern Washington. USGS Annual Report 20, pt. 2, 83-210.

Saleeby, J.B., Busby, S.C., Oldow, J.S., Dunne, G.C., Wright, J.E., Cowan, D.S., Walker, N.W., and Allmendinger, R.W., 1992, Early Mesozoic tectonic evolution of the Western U.S. Cordillera, *in* Burchfiel, B.C., Lipman, P.W., and Zoback, M.L., editors, The Cordilleran Orogen; conterminous U.S.: The Geology of North America v. G-3, Geological Society of America, p. 107-168.

Saltus, R.W., 1993, Upper-crustal structure beneath the Columbia River Basalt Group, Washington--Gravity interpretation controlled by borehole and seismic studies: Geological Society of America Bulletin, v. 105, no. 9, p. 1247-1259.

Schasse, H.W., 1987a, Geologic map of the Mount Rainier quadrangle, Washington: Washington Division of Geology and Earth Resources Open File Report 87-16, 43 p., 1 plate, scale 1:100,000.

Schasse, H.W., 1987b, Geologic map of the Centralia quadrangle, Washington: Washington Division of Geology and Earth Resources Open File Report 87-11, 28 p., 1 plate, scale 1:100,000.

Schmidt, K.M., and Montgomery, D.R., 1995. Limits to relief. Science 270, 617-620.

Schmincke, H.U., ms, 1964, Petrology, paleocurrents, and stratigraphy of the Ellensburg Formation and interbedded Yakima Basalt flows, south-central Washington [Ph.D. thesis]: Baltimore, Johns Hopkins University, 426 p.

Schuster, J.E., 2005, Geologic map of Washington State: Washington Division of Geology and Earth Resources GM 53, 1 sheet, scale 1:500,000, 44 p. text.

Schuster, J.E., 1994a, Geologic maps of the east half of the Washington portion of the Goldendale 1:100,000 quadrangle and the Washington portion of the Hermiston 1:100,000 quadrangle: Washington Division of Geology and Earth Resources Open File Report 94-9, 17 p., 1 pl.

Schuster, J.E., 1994b, Geologic map of the east half of the Toppenish 1:100,000 quadrangle, Washington: Washington Division of Geology and Earth Resources Open File Report 94-10, 15 p., 1 pl.

Schuster, J.E., 1994c, Geologic map of the east half of the Yakima 1:100,000 quadrangle, Washington: Washington Division of Geology and Earth Resources Open File Report 94-12, 19 p., 1 pl.

Schuster, J.E., 1992, Geologic map of Washington: Washington State Department of Natural Resources, Division of Geology and Earth Resources, scale, 1:2,250,000. 1 p. with 1 p. text.

Searle, M.P., and Treloar, P.J., 1993, Himalayan Tectonics—an introduction, *in* Searle, M.P. and Treloar, P.J., editors, Himalayan Tectonics: Geological Society of America Special Publication, no. 74, p. 1-7.

Small, E.E., Anderson, R.S., 1998, Pleistocene relief production in Laramide mountain ranges, western United States: Geology v. 26, no. 2, p. 123-126.

Small, E.E., Anderson, R.S., 1995, Geomorphically driven late Cenozoic rock uplift in the Sierra Nevada: Science, v. 270, no. 5234, p. 277-280.

Smiley, C.J., 1963, The Ellensburg flora of Washington: University of California Publications in Geological Sciences: v. 35, no. 3, p. 159-276.

Smith, G.A., Bjornstad, B.N., and Fecht, K.R., 1989, Neogene terrestrial sedimentation on and adjacent to the Columbia Plateau; Washington, Oregon and Idaho, *in* Reidel, S. P. and Hooper, P. R., editors., Volcanism and tectonism in the Columbia River flood-basalt province: Geological Society of America, Special Paper 239, p. 187-198.

Smith, G.A., 1988, Neogene synvolcanic and syntectonic sedimentation in central Washington: Geological Society of America Bulletin, v. 100, no. 9, p. 1479-1492.

Smith, G.O., 1903. Geology and Physiography of Central Washington. USGS Professional Paper 19, 1-46.

Smith, J.G., 1993, Geologic map of upper Eocene to Holocene volcanic and related rocks in the Cascade Range, Washington: U.S. Geological Survey Miscellaneous Investigation, Map I-2005, scale 1:500,000.

Spotila, J.A., Buscher, J.T., Meigs, A.J., and Reiners, P.W., 2004. Long-term glacial erosion of active mountain belts: example from the Chugach-St. Elias Range, Alaska. Geology 32, 501-504.

Stanley, W.D., Johnson, S.Y., Qamar, A.I., Weaver, C.S., and Williams, J. M., 1996, Tectonics and seismicity of the southern Washington Cascade Range: Seismological Society of America Bulletin, v. 86, no. 1A, p. 1-18.

Stern, T.A., Baxter, A.K., and Barrett, P.J., 2005, Isostatic rebound due to glacial erosion within the Transantarctic Mountains: Geology, v. 33, no. 3, p. 221-224.

Stoffel, K.L. and McGroder, M.F., 1990, Geologic map of the Robinson Mtn. 1:100,000 quadrangle, Washington: Washington Division of Geology and Earth Resources Open File Report 90-5, 39 p., 1 plate.

Svarc, J.L., Savage, J.C., Prescott, W.H., and Murray, M.H., 2002, Strain accumulation and rotation in western Oregon and southwestern Washington: Journal of Geophysical Research, v. 107, no. B5, 2087, 10.1029/2001JB000625.

Swanson, D.A., 1997, Uplift of the southern Washington Cascades in the past 17 million years: Geological Society of America Abstracts with Programs, v. 29, no. 5, p. 68.

Summers, K.V., ms, 1976, Palagonite and pillow basalts of the Columbia River group: MSc. thesis, Washington State University, Pullman, 99 p.

Tabor, R.W., Waitt, R.B., Frizzell, V.A. Jr., Swanson, D.A., Byerly, G.R., and Bentley, R.D., 1982. Geologic map of the Wenatchee 1:100,000 quadrangle, central Washington. USGS Miscellaneous Investigations Series Map 1-1311, 26 p.

Tabor, R.W., Frizzell, V.A. Jr., Waitt, R.B., Swanson, D.A., Byerly, G.R., Booth, D.B., Hetherington, M.J., and Zartman, R.E., 1987. Geologic map of the Chelan 30- by 60-minute quadrangle, Washington. USGS Miscellaneous Investigations Series Map I-1661, scale 1:100,000, 29 p.

Tabor, R.W., Frizzell, V.A. Jr., Booth, D.B., Waitt, R.B., Whetten, J.T., and Zartman, R.E., 1993. Geologic map of the Skykomish River 30- by 60-minute quadrangle, Washington. USGS Miscellaneous Investigations Series Map I-1963, scale 1:100,000, 42 p.

Tabor, R.W., Frizzell, V.A. Jr., Booth, D.B., Waitt, R.B., 2000. Geologic map of the Snoqualmie Pass 30 x 60 minute quadrangle, Washington. USGS Geologic Investigations Series Map I-2538, scale 1:100,000, 57 p.

Tabor, R.W., Haugerud, R.A., Hildreth, W., and Brown, E.H., 2003, Geologic map of the Mount Baker 30- by 60-minute quadrangle, Washington: U.S. Geological Survey Geologic Investigations Series I-2660, 2 sheets, scale 1:100,000, with 73 p. text.

Tabor, R.W., Haugerud, R.A., Booth, D.B. and Brown, E.H., 1994, Preliminary geologic map of the Mount Baker 30- by 60-minute quadrangle, Washington: U.S. Geological Survey Open-File Report 94-403, 55p., 2 pl.

Tabor, R.W., Frizzell, V.A., Jr., Booth, D.B., Waitt, R.B., Whetten J.T., and Zartman, R.E., 1993, Geologic map of the Skykomish River 30- by 60-minute quadrangle, Washington: U.S. Geological Survey Miscellaneous Investigations Series Map I-1963, 1 sheet, scale 1:100,000, with 42 p. text.

Tabor, R.W., Booth, D.B., Vance, J.A., Ford, A.B., and Ort, M.H., 1988, Preliminary geologic map of the Sauk River 30 by 60 minute quadrangle, Washington: U.S. Geological Survey Open-File Report 88-692, 50p., 2 pl.

Tabor, R.W., Frizzell, V.A., Jr., Whetten, J.T., Waitt, R.B., Swanson, D.A., Byerly, G.R., Booth, D.B., Hetherington, M.J., and Zartman, R.E., 1987, Geologic map of the Chelan 30-minute by 60-minute quadrangle, Washington: U.S. Geological Survey Miscellaneous Investigations Series Map I-1661, 1 sheet, scale 1:100,000, with 29 p. text.

Tabor, R.W., Waitt, R.B., Frizzell, V.A., Jr., Swanson, D.A., Byerly, G.R., and Bentley, R.D., 1982, Geologic map of the Wenatchee 1:100,000 quadrangle, central Washington: U.S. Geological Survey Miscellaneous Investigations Series Map I-1311, 26 p.,1 plate, scale 1:100,000.

Tabor, R. W., and Cady, W. M., 1978, Geologic map of the Olympic Peninsula, Washington: U.S. Geological Survey Miscellaneous Investigations Series Map I-994, 2 sheets, scale 1:125,000.

Takeuchi, A., and Larson, P.B., 2005, Oxygen isotope evidence for the last Cenozoic development of an orographic rain shadow in eastern Washington, USA: Geology, v. 33, no. 4, p. 313-316.

Thompson, W.F., 1962. Cascade alp slopes and Gipfelfluren as clima-geomorphic phenomena. Erdkunde 16, 81-94.

Tolan, T.L., Reidel, S.P., Beeson, M.H., Anderson, J.L., Fecht, K.R., and Swanson, D.A., 1989, Revisions to the estimates of the areal extent and volume of the Columbia River Basalt Group, *in* Reidel, S. P.; Hooper, P. R., editors, Volcanism and tectonism in the Columbia River flood-basalt province: Geological Society of America Special Paper 239, p. 1-20.

Tomkin, J.H., and Braun, J., 2002. The influence of alpine glaciation on the relief of tectonically active mountain belts. American Journal of Science 302, 169-190.

Turcotte, D.L., Schubert, G., 1982, Geodynamics: Applications of continuum physics to geological problems: Wiley: New York, 450 p.

Valley, P.M., Whitney, D.L., Paterson, S.R., Miller, R.B., and Alsleben, H., 2003, Metamorphism of the deepest exposed arc rocks in the Cretaceous to Paleogene Cascades belt, Washington: evidence for large-scale vertical motion in a continental arc: Journal of Metamorphic Geology, v. 21, p. 203-220.

Vance, J.A., 2002, Age and provenance of Eocene nonmarine sandstones in the central and Northwest Washington Cascades: fission track evidence from detrital zircons: Geological Society of America Abstracts with Programs, v. 34, no. 5.

Wager, L.R., 1933, The rise of the Himalaya, Nature, v. 132, p. 28.

Waitt, R. B., Jr., 1975. Late Pleistocene alpine glaciers and the Cordilleran Ice Sheet at Washington Pass, north Cascade Range, Washington. Arctic and Alpine Research 7, 25-32.

Waitt, R. B., Jr., and Thorson, R. M., 1983. The Cordilleran ice sheet in Washington, Idaho and Montana. In Porter, S.C. (Ed.), Late Quaternary Environments of the United States, University of Minnesota Press, Minneapolis. 53-70.

Walsh, T.J., 1987a, Geologic map of the south half of the Tacoma quadrangle, Washington: Washington Division of Geology and Earth Resources Open File Report 87-3, 10 p., 1 plate, scale 1:100,000.

Walsh, T.J., 1987b, Geologic map of the Astoria and Ilwaco quadrangles, Washington and Oregon: Washington Division of Geology and Earth Resources Open File Report 87-2, 28 p., 1 plate, scale 1:100,000.

Walsh, T.J., Korosec, M.A., Phillips, W.M., Logan, R.L., and Schasse, H.W., 1987, Geologic map of Washington--Southwest quadrant: Washington Division of

Geology and Earth Resources Geologic Map GM-34, 2 sheets, scale 1:250,000, with 28 p. text.

Walsh, T.J., 1986a, Geologic map of the west half of the Toppenish quadrangle, Washington: Washington Division of Geology and Earth Resources Open File Report 86-3, 1 sheet, scale 1:100,000, with 7 p. text.

Walsh, T J., 1986b, Geologic map of the west half of the Yakima quadrangle, Washington: Washington Division of Geology and Earth Resources Open File Report 86-4, 1 sheet, scale 1:100,000, with 9 p. text.

Walters, K.L., and Kimmel, G.E., 1968, Ground-water occurrence and stratigraphy of unconsolidated deposits, central Pierce County, Washington: Washington Department of Water Resources Water-Supply Bulletin 22, 428 p.

Watts, A.B. and Burov, E.B., 2003, Lithospheric strength and its relationship to the elastic and seismogenic layer thickness: Earth and Planetary Science Letters, v. 213, p. 113-131.

Weissenborn, A.E., 1969. Geologic Map of Washington. USGS Miscellaneous Geologic Investigations Map I-583.

Wells, R.E., Weaver, C.S., and Blakely, R.J., 1998, Fore-arc migration in Cascadia and its neotectonic significance: Geology, v. 26, no. 8, p. 759-762.

Wells, R.E., 1990, Paleomagnetic rotations and the Cenozoic tectonics of the Cascade arc, Washington, Oregon, and California: Journal of Geophysical Research B, v. 95, no. 12, p. 19,409-19,417.

Whetten, J. T., Carroll, P.I., Gower, H.D., Brown, E.H., and Pessl, F., Jr., 1988, Bedrock geologic map of the Port Townsend 30- by 60- minute quadrangle, Puget Sound region, Washington: U.S. Geological Survey Miscellaneous Investigations Series Map I-1198-G, 1 sheet, scale 1:100,000.

Whipple, K.X., Kirby, E., and Brocklehurst, S.H., 1999. Geomorphic limits to climate-induced increases in topographic relief. Nature 401, 39-43.

Willis, B., 1903, Physiography and deformation of the Wenatchee-Chelan district, Cascade Range, *in* Contributions to the geology of Washington: U.S. Geological Survey Professional Paper 19, p. 41-97.

Yount, J.C., and Gower, H.D., 1991, Bedrock geologic map of the Seattle 30' by 60' quadrangle, Washington: U.S. Geological Survey Open-File Report 91-147, 37 p., 4 pl.

VITA

Sara Gran Mitchell was born Sara Elizabeth Gran in 1974. She earned her Bachelor of Arts degree in geology in 1996 from Carleton College in Northfield, Minnesota. She then worked as a field geologist and geographic information system specialist at the Minnesota Geological Survey before starting graduate work at the University of Vermont, Burlington, in the fall of 1997. In 2000, she earned a Master of Science degree in geology. Her M. Sc. thesis, entitled, "The paleoseismic history of the Nahef East Fault, Northern Israel, using cosmogenic ^{36}Cl," was advised by Dr. Paul R. Bierman. Results of this M. Sc. research were published in the *Journal of Geophysical Research* (Mitchell et al., 2001). She worked briefly for John Shomaker and Associates, Inc., a hydrogeology consulting firm in Albuquerque, New Mexico, before starting her Ph. D. program at the University of Washington in the fall of 2000. During the 2003-2004 academic year, she took a leave of absence to teach Geomorphology and Introduction to Geology as a visiting instructor at Carleton College. She earned her Ph. D. in 2006 from the Department of Earth and Space Sciences at the University of Washington with this study on the topographic history and evolution of the Cascade Range in Washington State. Results of this research have been published in *Quaternary Research* (Mitchell and Montgomery, 2006), are accepted pending revisions at the *American Journal of Science,* and will soon be submitted to *Earth Surface Processes and Landforms*. The author will begin a tenure-track faculty position at The College of the Holy Cross in Worcester, Massachusetts, in the fall of 2006.